

**UNIVERSITÉ DU QUÉBEC À CHICOUTIMI**

**MÉMOIRE PRÉSENTÉ À  
L'UNIVERSITÉ DU QUÉBEC À CHICOUTIMI  
COMME EXIGENCE PARTIELLE  
DE LA MAÎTRISE EN INGÉNIERIE**

**BY**

**JUNFENG GUO**

**USE OF THE ULTRASONIC TECHNIQUE  
IN MEASURING INCLUSIONS IN Al-Si ALLOY MELTS**

**JUILLET 2007**



### **Mise en garde/Advice**

Afin de rendre accessible au plus grand nombre le résultat des travaux de recherche menés par ses étudiants gradués et dans l'esprit des règles qui régissent le dépôt et la diffusion des mémoires et thèses produits dans cette Institution, **l'Université du Québec à Chicoutimi (UQAC)** est fière de rendre accessible une version complète et gratuite de cette œuvre.

Motivated by a desire to make the results of its graduate students' research accessible to all, and in accordance with the rules governing the acceptance and diffusion of dissertations and theses in this Institution, the **Université du Québec à Chicoutimi (UQAC)** is proud to make a complete version of this work available at no cost to the reader.

L'auteur conserve néanmoins la propriété du droit d'auteur qui protège ce mémoire ou cette thèse. Ni le mémoire ou la thèse ni des extraits substantiels de ceux-ci ne peuvent être imprimés ou autrement reproduits sans son autorisation.

The author retains ownership of the copyright of this dissertation or thesis. Neither the dissertation or thesis, nor substantial extracts from it, may be printed or otherwise reproduced without the author's permission.

## RÉSUMÉ

La présence d'inclusions dans les alliages d'aluminium est l'un des problèmes les plus sérieux rencontrés lors du moulage de ces alliages. Les inclusions réduisent les propriétés mécaniques et augmentent la porosité; elles sont nuisibles à la finition de la surface et elles ont tendance à augmenter la corrosion. Quelques inclusions non métalliques fragiles agissent en tant que concentrations de contraintes et peuvent causer des bris prématurés des composantes. Avec la demande croissante de pièces coulées en aluminium de plus haute qualité, particulièrement dans les industries de l'automobile et de l'aérospatiale, beaucoup d'attention a été prêtée à la propreté du métal liquide.

L'amélioration de la propreté de la fonte d'aluminium peut être effectuée par des techniques d'enlèvement ou par la surveillance des inclusions. Du point de vue de contrôle ou de surveillance, un certain nombre de techniques, telles que PoDFA (Porous Disc Filtration Analysis), LAIS (Liquid Aluminum Inclusion Sampler), Prefil (Pressure Filtration), et Qualiflash ont été développées pour mesurer les inclusions dans les fontes d'aluminium. Cependant, ces techniques prennent du temps et peuvent seulement fournir des résultats en dehors de la ligne de coulée; par conséquent, l'information est souvent obtenue trop tard pour faire les ajustements nécessaires dans le processus de coulée. Actuellement, bien qu'il y ait une technique de mesure en ligne disponible, à savoir LiMCA II, celle-ci est trop chère et par conséquent n'est généralement pas accessible.

La technique de détection à ultrasons semble être une méthode prometteuse pour résoudre le problème des inclusions en raison de sa capacité à sonder l'intérieur des matériaux. La présente étude a été entreprise pour étudier la capacité de la technique ultrasonique pour mesurer diverses inclusions dans l'aluminium et dans l'alliage commercial de type 356 à deux températures différentes.

Des inclusions de  $\text{TiB}_2$ , d' $\text{AlSr}$ , d' $\text{Al}_3\text{Ti}$ , et d' $\text{Al}_2\text{O}_3$  ont été ajoutées aux alliages d'aluminium utilisés pour être étudiées à l'aide d'une machine "Metalvision MV20/20 ultrasonic". Les données obtenues ont fourni des informations sur (i) la valeur de propreté de l'aluminium, (ii) la dimension moyenne des particules, et (iii) le nombre total de particules pour chaque gamme de dimension particulière, en fonction du temps d'essai. Un examen de la microstructure des échantillons solidifiés obtenus à partir des prélèvements de

la fonte a été également effectué en utilisant une microsonde électronique de type Jeol JXA-8900L.

La comparaison entre les résultats obtenus par la technique ultrasonique et les mesures effectuées par microsonde sur les microstructures correspondantes a montré que la machine ultrasonique peut être utilisée comme dispositif en ligne pour déterminer la propreté de la fonte pendant une longue période (5 h dans la présente étude). Les courbes de propreté du métal liquide obtenues par la machine ultrasonique sont fiables et peuvent être employées comme guide pour les coulées à condition que la température du bain liquide et les conditions d'agitation soient correctement ajustées.

L'augmentation de la concentration des inclusions réduit le niveau de propreté de la fonte et est reflétée par une diminution correspondante de la courbe de propreté de la fonte illustrée par la machine ultrasonique, indiquant ainsi sa réponse relative au changement du niveau d'inclusions. L'augmentation de la température de coulée du métal liquide accélère cependant la décomposition de l'alliage mère, augmentant le nombre de particules d'inclusions dans la fonte et réduisant de ce fait la valeur de propreté de fonte.

Normalement, quand les inclusions  $\text{TiB}_2$  sont ajoutées à la fonte d'aluminium, la fluidité de la fonte diminue de manière significative. Les autres techniques d'analyse des inclusions (LiMCA et toutes les autres techniques de filtration) peuvent seulement détecter les inclusions  $\text{TiB}_2$  quand leur concentration est très basse (moins de 10 ppm). En appliquant la technique à ultrasons, des mesures peuvent être conduites correctement pour des concentrations aussi hautes que 90 ppm. Ceci indique que la technique ultrasonique fournit une alternative améliorée pour la mesure des inclusions  $\text{TiB}_2$  dans l'aluminium liquide. Ce fait est d'importance, puisque les inclusions sont invariablement présentes en raison de l'addition de  $\text{TiB}_2$  qui est essentielle aux processus d'affinage de grain utilisés pour l'aluminium.

## ABSTRACT

The presence of inclusions in aluminum alloys is one of the most serious problems encountered in the production of aluminum castings. Inclusions may reduce mechanical properties, are detrimental to surface finish, increase porosity, and display a tendency to increase corrosion. Some brittle non-metallic inclusions act as stress raisers, and can cause premature failure of a component. With the increasing demand for higher quality aluminum cast products, especially in the automotive and aerospace industries, much attention has been paid to the cleanliness of molten aluminum.

The control of melt cleanliness may be carried out through inclusion-removal and inclusion-monitoring techniques. From the monitoring point of view, a number of techniques, such as PoDFA (Porous Disc Filtration Analysis), LAIS (Liquid Aluminum Inclusion Sampler), Prefil (Pressure Filtration), and Qualiflash have been developed for the measurement of inclusions in aluminum melts. These techniques however are time-consuming and can only provide off-line results; consequently, the information is often obtained too late to make timely adjustments in the casting process. Currently, although there is also an on-line inclusion-measuring technique available, namely LiMCA II, it is too expensive and hence not generally accessible.

The Ultrasonic detection technique appears to be a promising method to resolve this problem because of its capacity for probing the interior of materials. The present study was undertaken to investigate the capacity of the ultrasonic technique for measuring various inclusions in liquid aluminum and commercial 356 alloy at two different temperatures each.

Inclusions of  $\text{TiB}_2$ ,  $\text{AlSr}$ ,  $\text{Al}_3\text{Ti}$ , and  $\text{Al}_2\text{O}_3$  were studied using a Metalvision MV20/20 ultrasonic machine. The data provided plots of (i) the cleanliness value, (ii) average particle size, and (iii) particle count for each particle size range, as a function of testing time. An examination of the microstructure of solidified samples obtained from samplings of the melt was also carried out using Jeol JXA-8900L electron probe microanalyzer.

Analysis of the ultrasonic data and their corresponding microstructures showed that the ultrasonic machine may be used as an on-line device for determining the melt

cleanliness for a long period of time, 5 h in the present study. The melt cleanliness curves obtained by the ultrasonic machine are reliable and may be used as a guide for casting provided that the melt temperature and stirring conditions are properly adjusted.

Increasing the concentration of inclusions reduces the cleanliness level of the melt, and is reflected by a corresponding decrease in the melt cleanliness curve of the ultrasonic machine, indicating its response to the change in inclusion level. Increasing the melt superheat, however, accelerates the decomposition of the master alloy, thereby increasing the number of inclusion particles in the melt and reducing the melt cleanliness value.

Normally, when  $\text{TiB}_2$  inclusions are added to aluminum melt, the fluidity of the melt will decrease significantly. Other techniques, including LiMCA and all the filtration techniques, can only detect  $\text{TiB}_2$  inclusions when the concentration is very low (less than 10 ppm B). By applying the ultrasonic technique, measurements may be conducted properly for concentrations as high as 90 ppm B; thus the ultrasonic technique provides an improved alternative for the measurement of  $\text{TiB}_2$  inclusions in liquid aluminum. This fact is of significance, since inclusions are invariably present because the addition of  $\text{TiB}_2$  is essential to the grain refining processes used for aluminum.

## **ACKNOWLEDGEMENTS**

It is such a great pleasure to finally have the opportunity to convey my gratitude to all those who were involved directly or indirectly in making this work a success, particularly to my supervisors, Professors F. H. Samuel and A.M. Samuel, for their invaluable guidance and help at each stage of the process. I would also like to express my appreciation to my colleagues Alain Bérubé and Mathieu Paradis for their help and for creating an enjoyable working atmosphere.

Grateful acknowledgement is hereby tendered to the Natural Sciences and Engineering Research Council of Canada (NSERC), General Motors Powertrain Group (U.S.A.), Corporativo Nemak (Mexico), the Fondation de l'Université du Québec à Chicoutimi (FUQAC), and the Centre québécois de recherche et développement de l'aluminium (CQRDA), for assistance (in the form of scholarships) and in-kind support received.

Finally, I would like to declare my deep gratitude to the members of my family, especially my parents. Without their continuous encouragement and support, I would not have been able to complete my Master's Degree successfully.

## TABLE OF CONTENTS

<b>ABSTRACT .....</b>	<b>iii</b>
<b>ACKNOWLEDGEMENTS .....</b>	<b>v</b>
<b>TABLE OF CONTENTS .....</b>	<b>vi</b>
<b>LIST OF FIGURES .....</b>	<b>viii</b>
<b>LIST OF TABLES.....</b>	<b>xii</b>
<b>CHAPTER 1    DEFINING OF THE PROBLEM.....</b>	<b>2</b>
1.1      INTRODUCTION .....	2
1.2      OBJECTIVES .....	5
<b>CHAPTER 2    SURVEY OF THE LITERATURE .....</b>	<b>7</b>
2.1      INTRODUCTION OF ALUMINUM ALLOYS .....	7
2.2      ALUMINUM CASTING ALLOYS .....	8
2.3      INCLUSIONS IN ALUMINUM ALLOY MELT.....	10
2.3.1    Deleteriousness of Inclusions .....	10
2.3.2    Sources of Inclusions .....	12
2.3.3    Classification of Inclusions.....	12
2.4      HYDROGEN IN ALUMINUM MELTS .....	15
2.4.1    Precipitation of Hydrogen.....	15
2.4.2    Effects of Porosity.....	17
2.4.3    Sources of Hydrogen .....	17
2.5      INCLUSION REMOVAL METHODS .....	18
2.5.1    Gravity Sedimentation .....	19
2.5.2    Degassing and Flotation.....	20



2.5.3	Filtration.....	22
2.5.4	Electromagnetic Separation .....	23
2.5.5	Fluxing.....	24
2.6	VARIOUS INCLUSION MEASUREMENT TECHNIQUES .....	25
2.6.1	PoDFA.....	28
2.6.2	LAIS.....	29
2.6.3	Prefil (Pressure Filtration) Technique.....	31
2.6.4	Qualiflash Technique .....	33
2.6.5	Reduced Pressure Test .....	35
2.6.6	LiMCA Technique .....	37
2.6.7	Ultrasonic Technique .....	39
2.6.8	Other Detection Techniques.....	43
<b>CHAPTER 3 EXPERIMENTAL PROCEDURES .....</b>		<b>45</b>
3.1	MATERIALS .....	45
3.2	METALVISION MV20/20 MACHINE.....	46
3.3	MELT PREPARATION AND ULTRASONIC TESTS .....	49
3.4	METALLOGRAPHY .....	52
<b>CHAPTER 4 RESULTS AND DISCUSSION .....</b>		<b>56</b>
4.1	INTRODUCTION OF PREVIOUS WORK .....	56
4.2	MEASUREMENTS OF MELT CLEANLINESS .....	59
4.2.1	Melt Cleanliness Curves (Short Testing Periods) .....	60
4.2.2	Metallographic Examination.....	72
4.2.3	Particle Size and Its Distribution .....	81
4.2.4	Melt Cleanliness Curves (Long Periods).....	91
<b>CHAPTER 5 CONCLUSIONS.....</b>		<b>96</b>
<b>RECOMMENDATIONS.....</b>		<b>99</b>
<b>REFERENCES.....</b>		<b>101</b>

## LIST OF FIGURES

<b>Figure 1</b>	The solubility of hydrogen at one atmosphere pressure in pure aluminum. ....	16
<b>Figure 2</b>	Morphology of (a) gas pores, and (b) gas-shrinkage pores observed in aluminum castings. ....	17
<b>Figure 3</b>	Schematic representation of inclusion removal by gas bubbles. ....	21
<b>Figure 4</b>	Schematic diagram illustrating electromagnetic separation. ....	24
<b>Figure 5</b>	Schematic diagram of the elements of the flux injection process. ....	25
<b>Figure 6</b>	Principle of the PoDFA Method of Measuring Metal Cleanliness. ....	29
<b>Figure 7</b>	Schematic diagram of the LAIS technique. ....	30
<b>Figure 8</b>	Prefil technique Apparatus. ....	32
<b>Figure 9</b>	The Qualiflash apparatus. ....	34
<b>Figure 10</b>	Schematic representation of the RPT apparatus. ....	36
<b>Figure 11</b>	Schematic of the LiMCA operation. ....	38
<b>Figure 12</b>	A schematic view of the configuration of inclusion detection in molten metals using the pitch-catch mode. ....	41
<b>Figure 13</b>	The sensor assembly used in the ultrasonic technique measurement of melt cleanliness: (1) mechanical stirrer, (2) air-cooled guide rods, and (3) electric furnace. ....	48
<b>Figure 14</b>	A photo of the oscilloscope screen captured during the measurement of inclusions in the melt. ....	48
<b>Figure 15</b>	Screen capture of MV20/20 software showing the results from an aluminum melt sample. ....	49
<b>Figure 16</b>	Close-up of the sensor assembly used in ultrasonic measurements. ....	51
<b>Figure 17</b>	Close-up of the solidified sample. ....	52

<b>Figure 18</b>	Schematic diagram of the sample dimensions .....	53
<b>Figure 19</b>	JEOL JXA-8900L Electron Probe Microanalyzer. ....	54
<b>Figure 20</b>	Cleanliness values displayed by commercial 356 alloy melts containing $\text{TiB}_2$ inclusions as a function of time (melt temperature $640^\circ\text{C}$ ).....	62
<b>Figure 21</b>	Cleanliness values displayed by commercial 356 alloy melts containing $\text{TiB}_2$ inclusions as a function of time (melt temperature $680^\circ\text{C}$ ).....	62
<b>Figure 22</b>	Cleanliness values displayed by commercial 356 alloy melts containing $\text{AlSr}$ inclusions as a function of time (melt temperature $640^\circ\text{C}$ ).....	63
<b>Figure 23</b>	Cleanliness values displayed by commercial 356 alloy melts containing $\text{AlSr}$ inclusions as a function of time (melt temperature $680^\circ\text{C}$ ).....	63
<b>Figure 24</b>	Cleanliness values displayed by commercial 356 alloy melts containing $\text{Al}_3\text{Ti}$ inclusions as a function of time (melt temperature $640^\circ\text{C}$ ).....	65
<b>Figure 25</b>	Cleanliness values displayed by commercial 356 alloy melts containing $\text{Al}_3\text{Ti}$ inclusions as a function of time (melt temperature $680^\circ\text{C}$ ).....	65
<b>Figure 26</b>	Cleanliness values displayed by commercial 356 alloy melts containing $\text{Al}_2\text{O}_3$ inclusions as a function of time (melt temperature $640^\circ\text{C}$ ).....	66
<b>Figure 27</b>	Cleanliness values displayed by commercial 356 alloy melts containing $\text{Al}_2\text{O}_3$ inclusions as a function of time (melt temperature $680^\circ\text{C}$ ).....	66
<b>Figure 28</b>	Cleanliness values displayed by commercial pure aluminum melts containing $\text{TiB}_2$ inclusions as a function of time (melt temperature $680^\circ\text{C}$ ).....	68
<b>Figure 29</b>	Cleanliness values displayed by commercial pure aluminum melts containing $\text{TiB}_2$ inclusions as a function of time (melt temperature $720^\circ\text{C}$ ).....	68
<b>Figure 30</b>	Cleanliness values displayed by commercial pure aluminum melts containing $\text{AlSr}$ inclusions as a function of time	

	(melt temperature 680°C).....	69
<b>Figure 31</b>	Cleanliness values displayed by commercial pure aluminum melts containing AlSr inclusions as a function of time (melt temperature 720°C).....	69
<b>Figure 32</b>	Cleanliness values displayed by commercial pure aluminum melts containing Al <sub>3</sub> Ti inclusions as a function of time (melt temperature 680°C).....	70
<b>Figure 33</b>	Cleanliness values displayed by commercial pure aluminum melts containing Al <sub>3</sub> Ti inclusions as a function of time (melt temperature 720°C).....	70
<b>Figure 34</b>	Cleanliness values displayed by commercial pure aluminum melts containing Al <sub>2</sub> O <sub>3</sub> inclusions as a function of time (melt temperature 680°C).....	71
<b>Figure 35</b>	Cleanliness values displayed by commercial pure aluminum melts containing Al <sub>2</sub> O <sub>3</sub> inclusions as a function of time (melt temperature 720°C).....	71
<b>Figure 36</b>	Backscattered images of TiB <sub>2</sub> inclusions in 356 alloy after the (a) first and (b) last additions.....	76
<b>Figure 37</b>	Backscattered images of Al <sub>3</sub> Ti in 356 alloy after the (a) first and (b) last additions.....	77
<b>Figure 38</b>	Backscattered images of Al <sub>2</sub> O <sub>3</sub> in 356 alloy after the (a) first and (b) last additions.....	78
<b>Figure 39</b>	Backscattered images of TiB <sub>2</sub> inclusions in pure aluminum after the (a) first and (b) last additions.....	79
<b>Figure 40</b>	Backscattered images showing the distribution of Al <sub>2</sub> O <sub>3</sub> inclusions in pure aluminum after the (a) first and (b) last additions. The images were taken over the entire sample surface in this case.....	80
<b>Figure 41</b>	Particle sizes of TiB <sub>2</sub> inclusions in pure aluminum as a function of time (melt temperature 680°C).....	82
<b>Figure 42</b>	Particle size distribution of TiB <sub>2</sub> inclusions in pure aluminum as a function of time (melt temperature 680°C).....	83
<b>Figure 43</b>	Particle sizes of Al <sub>3</sub> Ti inclusions in 356 alloy as a function	

	of time (melt temperature 640°C). ....	83
<b>Figure 44</b>	Particle size distribution of $\text{Al}_3\text{Ti}$ inclusions in 356 alloy as a function of time (melt temperature 640°C). ....	84
<b>Figure 45</b>	Backscattered images of $\text{TiB}_2$ inclusions in pure aluminum after the last addition and corresponding X-ray image of Ti. ....	85
<b>Figure 46</b>	Backscattered images of strontium oxide films in 356 alloy after the last addition of $\text{AlSr}$ inclusion. ....	86
<b>Figure 47</b>	X-ray images of oxygen corresponding to the strontium oxides shown in Figure 47. ....	87
<b>Figure 48</b>	X-ray images of strontium corresponding to the strontium oxides shown in Figure 47. ....	88
<b>Figure 49</b>	Backscattered images of $\text{Al}_3\text{Ti}$ inclusions in pure aluminum after the last addition. ....	89
<b>Figure 50</b>	Backscattered images of $\text{Al}_3\text{Ti}$ inclusions in 356 alloy after the last addition and corresponding X-ray image of titanium. ....	90
<b>Figure 51</b>	Cleanliness values of $\text{Al}_3\text{Ti}$ inclusions in commercial 356 alloy as a function of time (melt temperature 680°C). ....	92
<b>Figure 52</b>	Particle sizes of $\text{Al}_3\text{Ti}$ inclusions in commercial 356 alloy as a function of time (melt temperature 680°C). ....	92
<b>Figure 53</b>	Particle size distribution of $\text{Al}_3\text{Ti}$ inclusions in commercial 356 alloy as a function of time (melt temperature 680°C). ....	93
<b>Figure 54</b>	The real condition of $\text{Al}_3\text{Ti}$ inclusion in solidified sample obtained before the test (melt temperature 680°C). ....	93
<b>Figure 55</b>	The real condition of $\text{Al}_3\text{Ti}$ inclusion in solidified sample obtained 0.5h after starting the test (melt temperature 680°C). ....	94
<b>Figure 56</b>	The real condition of $\text{Al}_3\text{Ti}$ inclusion in solidified sample obtained 5h after starting the test (melt temperature 680°C). ....	94

## LIST OF TABLES

<b>Table 1</b>	Different types of inclusions observed in molten aluminum.....	14
<b>Table 2</b>	Inclusion detection methods.....	27
<b>Table 3</b>	Inclusion types and their sources used in this study.....	46
<b>Table 4</b>	Details of melts prepared for ultrasonic tests .....	50

## **CHAPTER 1**

### **DEFINING OF THE PROBLEM**

## **CHAPTER 1**

### **DEFINING OF THE PROBLEM**

#### **1.1 INTRODUCTION**

The quality of aluminum casting alloys involves three interrelated steps: (i) control of trace elements (alkali elements), (ii) removal of non-metallic inclusions, and (iii) reduction of dissolved gas content (hydrogen).<sup>1, 2</sup> The presence of inclusions in aluminum alloys is one of the most serious problems encountered in the production of aluminum castings. Inclusions may reduce mechanical properties, are detrimental to surface finish, increase porosity, and show a tendency to increase corrosion. Some brittle non-metallic inclusions act as stress raisers, and can cause premature failure of a component. As a result, the size, shape, type and distribution of non-metallic inclusions in the final product are often considered the performance fingerprints of the foundry.

In recent decades, with the increasing demand for higher quality aluminum cast products, especially in the automotive and aerospace industries, much attention has been paid to the cleanliness of molten aluminum. The control of melt cleanliness can be carried out by means of inclusion-removal and inclusion monitoring techniques. From



the monitoring point of view, various techniques, such as PoDFA (Porous Disc Filtration Analysis), LAIS (Liquid Aluminum Inclusion Sampler), Prefil (Pressure Filtration), and Qualiflash have been developed for the measurement of inclusions in aluminum melts. These techniques, however, are time consuming and can only provide off-line results; consequently, the information is often obtained too late to make timely adjustments in the casting process.<sup>3, 4, 5</sup> Currently, although there is also an on-line inclusion measuring technique known as LiMCA II, it is very expensive and hence not generally accessible.<sup>4</sup> Another technique is thus required to accomplish the intended purpose.

The Ultrasonic detection technique, because of its capacity to probe the interior of materials, appears to be a promising method for resolving this problem. The technique has numerous advantages compared with various techniques based on the extraction of a metal sample followed by analysis in the laboratory. First, it provides on-line information which allows the operator enough time to make a number of essential adjustments to the process. In addition, all the other methods are more expensive, either in terms of the capital cost of the equipment or in terms of the manual labor required to obtain and interpret the results; they also require much more sample preparation and analysis time. Furthermore, the ultrasonic technique is capable of monitoring significantly large proportions of the total metal volume, and hence its results are much more representative than those observed with other methods. In certain cases of flowing metal in a launder, it is possible to achieve analysis of at least 25% of

the entire metal melt. Moreover, this technique is capable of detecting different locations along the product line. Multiple-probe assemblies can even monitor different locations simultaneously.

Although the ultrasonic technique has some difficulty in discriminating the types and shapes of inclusions, when used together with the PoDFA technique (which provides a qualitative assessment of inclusions), it is able to provide researchers with an in-depth understanding of the nature and behavior of the melt treatment process. A study was undertaken to investigate the capacity of this technique for measuring various inclusions in liquid aluminum and commercial 356 alloy at two different temperatures. The characteristics of these inclusions were investigated using the sampling cup from RPT technique to obtain solidified samples of the alloy melts. These samples were examined using a Jeol JXA-8900L electron probe microanalyzer.

## **1.2 OBJECTIVES**

A series of melt cleanliness measurements were carried out using the ultrasonic technique. The objectives of this study were as follows:

1. Determine the capacity of the ultrasonic technique for detecting different types of inclusions in liquid aluminum and 356 alloy.
2. Investigate the characteristics of various inclusions in liquid aluminum and the 356 alloy.
3. Investigate the effect of temperature on the inclusion measurements made by the ultrasonic technique for different types of inclusions.

**CHAPTER 2**

**SURVEY OF THE LITERATURE**

## **CHAPTER 2**

### **SURVEY OF THE LITERATURE**

#### **2.1 INTRODUCTION OF ALUMINUM ALLOYS**

Researchers have made tremendous progress in the aluminum industry since the electrolysis process of producing aluminum was discovered by Charles Martin Hall and Paul T. Héroult in 1888. Various aluminum alloys and industrial components were subsequently developed for diversified purposes.

Generally, aluminum alloys may be classified into two categories: wrought alloys and casting alloys. Each country has developed its own nomenclature and designation, and so far no internationally accepted system has been adopted for identification. In the United States, a four-digit numerical system is being used for wrought alloys, ranging from the 1xxx series representing the controlled pure composition to the 9xxx series reserved for future use. With respect to casting alloys, such was also the case for a series range from 1xx.x to 9xx.x.<sup>6</sup>

Many of these alloys, which are based on phase solubility, are heat-treatable. These treatments include solution treatment, quenching and age-hardening or

precipitation.<sup>7</sup> A large number of other wrought alloys, which rely instead on work-hardening in combination with various annealing procedures, are designated work-hardening alloys. Certain other cast alloys are non-heat-treatable and may only be used in as-cast conditions.<sup>8</sup>

Due to their high strength-to-weight ratio, high wear resistance, good corrosion resistance, high reflectivity and excellent conductivity of heat and electricity, aluminum alloys have been widely used in many areas, especially in the automobile and aerospace industries.

## **2.2 ALUMINUM CASTING ALLOYS**

Aluminum casting alloys constitute a group of cast materials which, in tonnage terms, is second only to ferrous castings,<sup>9</sup> mainly because aluminum casting alloys are the most versatile of foundry alloys. They have many characteristics in common with other foundry alloys and generally have the highest castability ratings. As casting materials, they display favourable performance including good fluidity for filling thin sections, chemical stability and low melting points as compared to a number of metals. The capacity for rapid heat transfer from the molten aluminum to the mold produces much shorter casting cycles. In addition, many aluminum alloys are relatively free from hot shock cracking and tearing tendencies, and yield a good as-cast surface finish with few or no blemishes.<sup>6</sup>

The quality of aluminum casting alloy involves three interrelated steps: the

control of trace elements (alkali elements), removal of non-metallic inclusions, and reduction of dissolved gas content (hydrogen). As a general rule, the level of second phase inclusions in aluminum alloys can be substantial. Thus, if the melt is not adequately processed, the cast product is more of a composite than an aluminum alloy.<sup>10</sup>

The presence of inclusions in aluminum alloys is one of the most serious problems encountered in the production of aluminum castings. Inclusions may reduce mechanical properties, are detrimental to surface finish, increase porosity, and tend to increase corrosion. Some brittle non-metallic inclusions act as stress raisers, and can cause premature failure of a component. As a result, the size, shape, type and distribution of non-metallic inclusions in the final product are often considered the performance fingerprints of the foundry.

The level of melt cleanliness ultimately determines the quality rank of the part being cast. In order to acquire the highest quality aluminum castings, inclusions should be removed completely from their melts, a condition which can never be achieved in practice. It is possible, however, to remove inclusions in compliance with the specific requirement of customers. In order to do so, it is necessary to have a sound understanding of the source, the removal techniques and subsequent detection techniques of these inclusions.

## **2.3 INCLUSIONS IN ALUMINUM ALLOY MELT**

The term “inclusion” was defined as any exogenous solid or liquid phase particle or agglomerate of different phases present in an aluminum alloy above the liquidus temperature. Inclusion size may vary from less than one micron to a hundred microns or even larger. Inclusions may be observed in the form of gases, elements and particles, including oxides, carbides, nitrides, borides and hydrogen.

Generally, any inclusion over 10-20 microns in diameter is considered to be deleterious to aluminum applications, although even smaller inclusions may also cause problems if present in substantial quantity.<sup>11</sup> The inclusion concentration in unprocessed aluminum melts ranges from 0.005 to 0.02 (volume fraction) and has been observed in a variety of morphologies.<sup>1</sup> It is important to note that the analysis of inclusions is, in most cases, a trace analysis in view of the relatively low concentration of inclusions. Inclusion particle sizes vary from one micron to several millimeters in some extreme cases. A further significant aspect is inclusion-size distribution, although this has not yet been investigated thoroughly for the sole reason that reliable methodologies to assess the presence of inclusions are still being perfected.

### **2.3.1 Deleteriousness of Inclusions**

Inclusions in aluminum take a range of forms including films, clusters and discrete particles of kinds of compounds. They are very often causes for the rejection of a casting part by the customer, since the presence of inclusions may lead to various



problems in the subsequent manufacture of castings. Inclusions in the aluminum melt would increase the fluidity of the liquid metal and cause an obvious loss of fluidity, leading to difficulties in feeding ultra-thin casting parts. Filtration of the metal to remove the inclusions increases the fluidity by more than 5 to 10 percent. Some of the non-metallic inclusions are very brittle and act as stress raisers causing the premature failure of a component. Both tensile strength and elongation are reduced drastically because of the presence of inclusions. The yield strength, however, remains relatively unaffected.

The hardness of some inclusions has been observed to reach about 9.5 on the Mohs scale as compared to 10 for diamonds. Small amounts of these extremely hard inclusions in the casting can lead to extensive tool wear during machining and cause castings to display poor machinability. Various kinds of inclusions act as nucleation sites for the formation of porosity, resulting in poor surface finish and an increased tendency to corrosion. They may also bring about a lack of pressure-tightness in a casting and make the surface finish unsuitable for anodizing, painting or varnishing purposes.<sup>12</sup>

There is no general agreement, however, on the question of what size and which type of inclusions are the most harmful, and which are to be tolerated in aluminum alloys. In some cases, inclusions in the size range of 10-20  $\mu\text{m}$  effective diameter at a concentration of a few parts per million, can be harmful in rolled aluminum products used for manufacturing beverage containers, while in other cases,

inclusions as small as 5  $\mu\text{m}$  can be harmful in the manufacturing of foil products.

### **2.3.2 Sources of Inclusions**

Inclusions in aluminum alloy melts may be identified as exogenous or endogenous.<sup>9</sup> Exogenous inclusions are imported to the molten metal from external sources, such as refractory degradation, potroom metal, lining of the crucible wall, coating materials, stirrer erosion and refractory/metal reactions; such inclusions are usually present in form of discrete particles:  $\text{Al}_4\text{C}_3$  is a typical inclusion of this kind. Endogenous inclusions, however, which are more common in aluminum alloy melts, may be non-metallic compounds, intermetallic compounds and kinds of salts; they are produced either from chemical reactions within the melt itself or from deliberate melt treatments such as alloying, grain refinement or fluxing. In addition, an excessive temperature or any transfer turbulence during melting would accelerate the oxidation of aluminum,<sup>12</sup> while poor separation of fluxing reaction products can also produce some inclusions.

### **2.3.3 Classification of Inclusions**

Inclusions in aluminum alloy melts can be classified according to their morphology, size, phase and composition. From the point of view of morphology, they can be assigned to two groups. The first group contains massive inclusions with an irregular distribution. Such inclusions result in casting leaks and a reduction in density

and ductility. The second group contains dispersed inclusions with a uniform distribution. This kind of inclusion increases the fluidity of the aluminum melt, reducing its fluidity and ability to fill the mold space during solidification.<sup>13</sup>

According to the phases present in aluminum melts, the inclusions may be categorized as solid or liquid. Solid inclusions are isolated, rigid particles or agglomerates of different phases, textures and morphologies which may be introduced into the melt through extraneous sources or during processing; oxides, nitrides, carbides and borides constitute this group of inclusions. Liquid inclusions on the other hand, are particles which are deformable and may coalesce into globules; chlorides, fluorides, and many kinds of salts are part of this class.

With respect to composition, the common types of inclusion in aluminum are oxides, nitrides, carbides, chlorides, fluorides and borides. A summary of the different types of inclusions observed in molten aluminum is provided in Table 1.<sup>14, 15</sup>

**Table 1** Different types of inclusions observed in molten aluminum.<sup>16</sup>

Type	Morphology	Density, g/cm <sup>3</sup>	Dimensions, μm
OXIDES MgAl <sub>2</sub> O <sub>4</sub> (Spinel) Al <sub>2</sub> O <sub>3</sub> (Corundum) MgO SiO <sub>2</sub> CaO	Particles, skins, flakes Particles, skins Particles, skins Particles Particles	3.60 3.97 3.58 2.66 3.37	0.1-100, 10-5000 0.2-30, 10-5000 0.1-5, 10-5000 0.5-30 <5
CARBIDES Al <sub>4</sub> C <sub>3</sub> SiC	Particles, clusters Particles	2.36 3.22	0.5-25 0.5-5
BORIDES TiB <sub>2</sub> AlB <sub>2</sub>	Particles, clusters Particles	4.5 3.19	1-30 0.1-3
NITRIDES AlN	Particles, skins	3.26	10-50
OTHER Chlorides and salts (CaCl <sub>2</sub> , NaCl, MgCl <sub>2</sub> ) Fluorides (cryolite) Sludge Al(FeMnCr)Si	Liquid droplets	1.9-2.2 2.9-3.0 >4.0	0.5-1
ULTRAFINE GAS BUBBLES Argon bubbles N <sub>2</sub> bubbles	-	-	10-30
INTERMETALLICS (TiAl <sub>3</sub> , TiAl, NiAl, Ni <sub>3</sub> Al)	Particles, clusters	-	10-100

## **2.4 HYDROGEN IN ALUMINUM MELTS**

Although hydrogen is the only gas with any significant solubility in molten aluminum, it is easily dissolved and occurs in abundance. As a result, all molten aluminum contains some level of dissolved hydrogen. This gas plays a major role in the development of unsoundness resulting from porosity in castings.

### **2.4.1 Precipitation of Hydrogen**

Hydrogen solubility has such a strong dependence on temperature in the liquid aluminum that it doubles for each 110°C increase in superheat.<sup>9</sup> As can be seen in Figure 1, there is also a considerable change in solubility at the melting point, and the solubility in solid aluminum is too low, relatively speaking. These dissolution natures cause the large amount of hydrogen in the liquid to be unable to dissolve in the solid during the process of solidification. Therefore, a large quantity of hydrogen accumulates in the liquid at the solidifying interface and eventually causes the formation of porosity. John E. Gruzleski made a simple calculation based on Figure 1, proving that only about 5% of the hydrogen dissolved in the liquid can remain in the solid after solidification.<sup>9</sup>

Accumulated hydrogen can lead to the presence of gas porosity and gas-shrinkage porosity in the final castings. Figure 2 shows examples of both kinds of porosity. Gas porosity, which is generally fairly spherical in shape, results either from the precipitation of hydrogen during solidification or from the occlusion of gas bubbles during the high velocity injection of molten metal in die casting operations.

Gas-shrinkage porosity is a combination of gas and shrinkage. These pores typically occur in the interdendritic regions which are the last parts of the structure to freeze. Moreover, both shrinkage and dissolved hydrogen are necessary for the formation of this kind of porosity. The formation of porosity during solidification may also be affected by several other factors such as cooling rate, alloying elements, modification and melt cleanliness. Also, in aluminum casting, the formation of porosity can be accelerated in dirty metal compared to its formation in clean metal.<sup>6, 8, 9</sup>

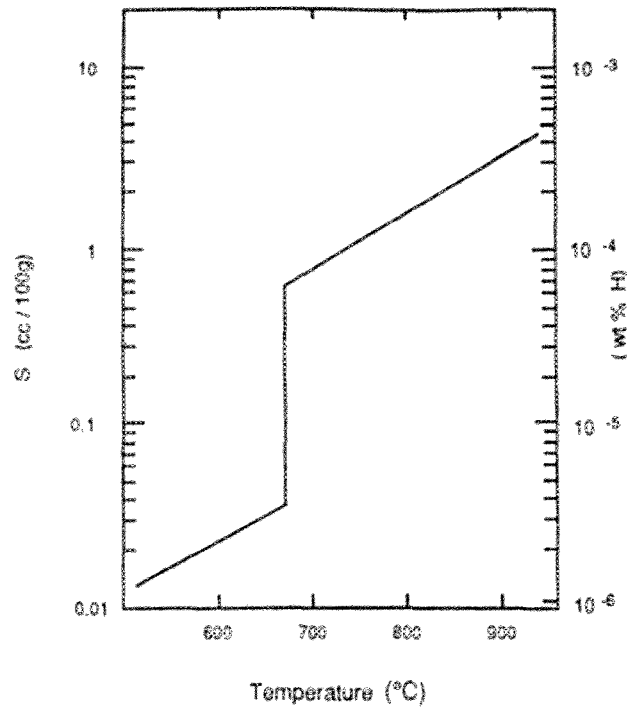


**Figure 1** The solubility of hydrogen at one atmosphere pressure in pure aluminum.<sup>9</sup>

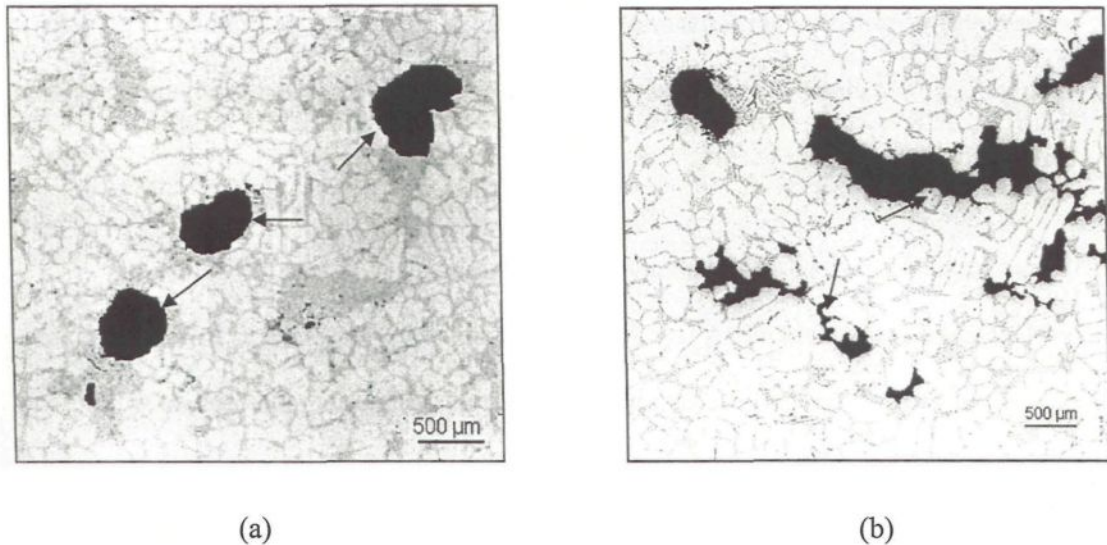


**Figure 2** Morphology of (a) gas pores, and (b) gas-shrinkage pores observed in aluminum castings.<sup>8</sup>

#### 2.4.2 Effects of Porosity

Unfortunately, porosity is an undesirable feature of the cast structure. It would degrade certain important properties of aluminum castings and lead to reduced mechanical properties, poor surface appearance, and some loss of pressure tightness. On the other hand, the generation of porosity may contribute to improving the resistance to hot-tearing.

#### 2.4.3 Sources of Hydrogen

The most important source of hydrogen is the reaction between the liquid metal and water which is usually present as moisture in the atmosphere. Even with a well-defined flame, most fuels contain 10-20 percent water vapor as the product of combustion.<sup>17</sup> Either the direct impingement of flame on the metal surface or poor

crucible wall condition could lead to the introduction of hydrogen into the metal. The amount of hydrogen introduced into the liquid metal is observably proportional to the atmospheric moisture.

Certain kinds of foundry tools, such as plungers, ladles or crucibles, which have been insufficiently preheated, are likely to be significant sources of hydrogen. Furthermore, the surface of charged materials may contain moisture, or become oxidized, thereby contributing to the generation of aluminum hydroxides when melted. Also, charge ingots may contain an initial amount of gas, which subsequently becomes trapped within the melt, while many grain refiners, fluxes, and degassing pills used during melt treatment, are all potential sources of hydrogen.<sup>8,9,17</sup> These materials will tend to absorb some moisture and introduce it below the surface of the metal, if not stored under sufficiently dry conditions.

## **2.5 INCLUSION REMOVAL METHODS**

Inclusion removal has been recognized as a critical phase in the processing of aluminum alloys since the presence of inclusions can lead to various problems in the manufacture of castings including reduced mechanical properties, poor surface finish, increased porosity or a tendency to increased corrosion.

Early attempts at inclusion control often focused on the molding process, in particular the incorporation of pouring basins and runner extensions whose function was to trap dirt particles before they entered the mold cavity. None of these trial runs to



remove inclusions was particularly effective however, and at best will only remove the largest particles. With the increasing use of aluminum alloy castings for structural applications in the aerospace industry, and for mass produced automotive parts, researchers and manufacturers have devoted a significant amount of attention to this field. Hence, a wide variety of inclusion removal methods were developed, including sedimentation, flotation, filtration, degassing, and fluxing. Each of these methods is briefly reviewed below to establish a general idea for the discussion of inclusion detection which follows.

It is clear that each technique has its own advantages within a certain range of inclusion diameter, and there is a widespread tendency to apply a combination of these techniques in order to obtain greater efficiency of inclusion removal.

### **2.5.1 Gravity Sedimentation**

Inclusions which sink into the gravitational field as a result of a difference in density between inclusions and melt are said to be removed by gravity sedimentation. Theoretically, inclusions which are heavier than the base melt have the capacity to settle towards the bottom of the container. Due to inordinately low particle terminal velocities and high drag forces, however, gravity sedimentation methods are limited to inclusion sizes greater than 90  $\mu\text{m}$ .<sup>16, 18</sup> In addition, sedimentation buildup reduces furnace capacity and virtually all pouring or transfer operations have the possibility of carrying over some of this loosely sedimentated particulate into the casting operation itself.

Gravity sedimentation, which involves no great capital cost, is a rough and ready method to apply when necessary. In practice however, stirring and moderate turbulence may be employed to stimulate particle agglomeration and to enhance sedimentation efficiency.<sup>19, 20, 21</sup>

### **2.5.2 Degassing and Flotation**

Degassing is carried out in order to remove dissolved hydrogen from molten aluminum. Since gas-purging is the only widespread method used in foundry applications, this discussion will be confined to a specific family of techniques. The treatment gas can be introduced into the melt in several ways. The simplest, but least effective, is to use a straight graphite lance which produces large bubbles 2-3 cm in diameter. A much finer dispersion of gas bubbles may be obtained using a porous graphite head. The most sophisticated and most efficient degasser available for foundry use is an amalgamation of these technologies. A rotary impeller-degasser introduces treatment gas into the melt through a special impeller head which rotates rapidly and then disperses it gas throughout the melt.<sup>9</sup>

As it turns out, the single most important factor in determining degassing efficiency is the bubble size. The final hydrogen levels obtained depend on initial hydrogen content, purge gas flows, impeller rotation speed, size of vessel, temperature of melt and treatment time applied.

It is a well-established fact in the field that the bubbles produced during

degassing may also act to float out undesirable inclusions which are lighter than the base melt. These inclusions are swept to the melt surface by flotation where they can be removed by skimming. Figure 3 shows a schematic illustration of inclusion removal by flotation.

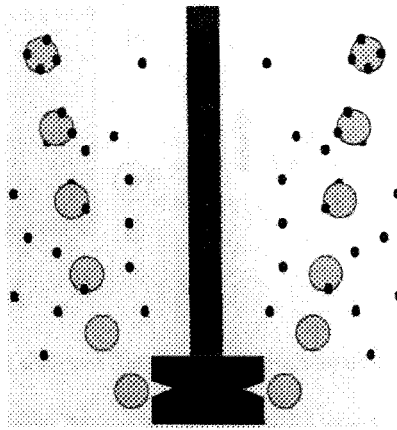


**Figure 3** Schematic representation of inclusion removal by gas bubbles.<sup>16</sup>

In general, inclusions greater than 30-40  $\mu\text{m}$  may be reliably separated from the melt by flotation. The efficiency of flotation depends on the interaction between the bubbles and the inclusions.<sup>22</sup> More gas bubbles in a finer form would be of help in the flotation of small inclusions, although there is no incentive to obtain bubbles of less than about 5mm in diameter, since these already degas at close to 100% efficiency.<sup>23</sup> Inclusion-removal also depends on inclusion-size, inclusion-velocity, inclusion-density, and interfacial tensions in the bubble, melt and inclusion system.<sup>18</sup> The addition of chlorine or other halogens is believed to affect the surface tension of the bubbles and to make inclusions stick to the bubbles more rapidly.<sup>24</sup>

In addition, stirring, which is produced by the movement of bubbles as well as by a paddle-stirrer, may also facilitate inclusion removal. Ultrasonic vibration applied to aluminum melts has also shown a positive effect, since it can affect the wettability of the inclusions.<sup>25</sup>

### **2.5.3 Filtration**

Most of the inclusions in foundry aluminum alloys are smaller than 30  $\mu\text{m}$ . Removal of these inclusions may be accomplished by filtration. Traditionally, two fundamental types of filtration have been identified: deep-bed filtration and cake filtration. The deep-bed filter consists of a packed bed of refractory particles through which the molten aluminum flows. The inclusions then deposit themselves onto the grains of the filter medium as a result of diffusion, direct interception, gravity, and surface forces. In cake filtration, on the other hand, the inclusions are deposited on the upper surface of the filter. The aggregate of inclusions here acts as a second filter above the original medium, which creates an additional resistance to flow thereby causing the separation of inclusions from the melt.<sup>1, 26</sup> In the natural course of events, the filter cake will eventually become so thick that it will unduly impede liquid flow.

Ceramic foam is widely used to filter aluminum used to manufacture a wide range of products, including critical materials such as computer memory discs, packaging materials, aerospace materials, bright finish trim and automotive extrusions.<sup>27, 28</sup> The rapid proliferation of this technology may be attributed to the fact

that these disposable filters provide a flexible, inexpensive, safe and effective means of removing inclusions from aluminum alloy melts.<sup>27, 28, 29</sup> Both deep-bed and cake filtration occur in modern ceramic foam filters. The most effective filtration proceeds during the deep-bed period. Eventually, the filter becomes so clogged with inclusions that cake filtration predominates. When this stage is reached, the filter is, to all intents and purposes clogged up.

#### **2.5.4 Electromagnetic Separation**

An externally applied electromagnetic force acts upon the melt in the application of this technique. In view of the fact that the inclusion does not have the same conductivity as the melt, an inclusion in the melt will feel the effect of the pressure gradient or volume force. As a result of Newton's third law, the inclusions will move in the opposite direction and thus become separated. As will be seen in Figure 4, the inclusions present in the melt experience a force opposite to the direction of the applied Lorentz force – called Archimedes' electromagnetic force.

The force may be created either by sending a current through the melt thereby inducing a magnetic field, or by letting the magnetic field induce a current in the melt. The use of an applied electric field in conjunction with a magnetic field can also produce an Archimedes' electromagnetic force.<sup>18</sup>

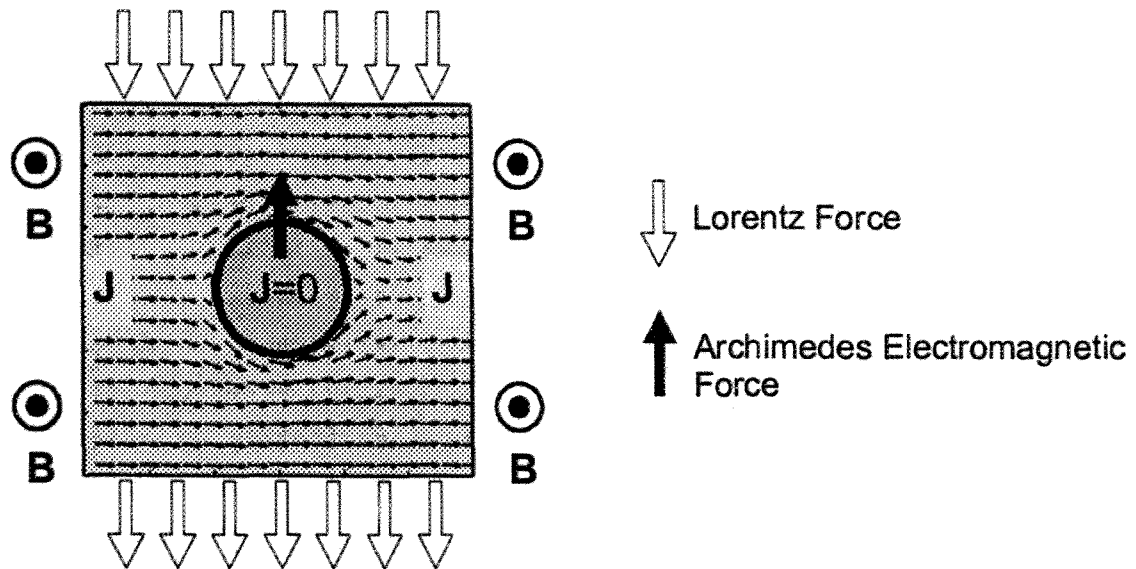


**Figure 4** Schematic diagram illustrating electromagnetic separation.<sup>16</sup>

It would be possible for larger force densities to allow the sedimentation of smaller particles to take place and hence separate the inclusions from the bulk melt. Correspondingly, because of the complexity of producing strong and highly homogeneous magnetic fields, large force densities in large volumes are difficult to achieve.<sup>30</sup> If the force field is not uniform, strong electromagnetically driven fluid motion and turbulence may appear thus creating an uncontrollable situation. Consequently, electromagnetic separation has not yet come into widespread use.

### 2.5.5 Fluxing

Fluxing by injection is another technique that is widely used in the aluminum industry to improve molten metal cleanliness. Fluxes may be applied manually or by means of injection equipment. Figure 5 shows the elements of the flux injection process.

These fluxes may be classified into two categories. The first group is called passive fluxes and will protect only the surface of the molten metal aluminum from oxidation while more or less preventing the pick-up of hydrogen by the melt. The second group of fluxes, named active fluxes, will react with aluminum oxide chemically and thus clean the melt effectively.<sup>31</sup>

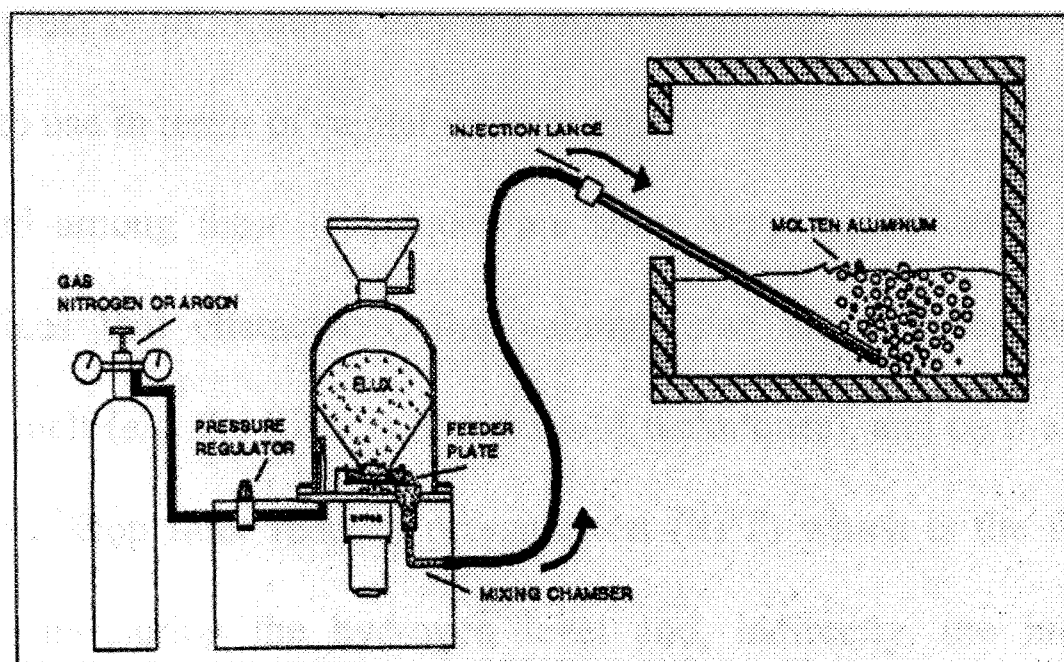


**Figure 5** Schematic diagram of the elements of the flux injection process.<sup>32</sup>

## 2.6 VARIOUS INCLUSION MEASUREMENT TECHNIQUES

A stable and predictable quality is of great importance to the manufacturer of aluminum castings. Compared with other parallel procedures, however, the measurement of melt cleanliness is the weakest step in the chain of events constituting molten metal processing. This fact has imposed limitations on the development of the

aluminum industry.

Nevertheless, a variety of inclusion detection techniques were also developed over the past few decades. These techniques include qualitative, quantitative and analytical laboratory procedures as well as on-line and off-line techniques, such as PoDFA (Porous Disc Filtration Analysis), LAIS (Liquid Aluminum Inclusion Sampler), Prefil, LiMCA and ultrasonic detection techniques.

The above assessment techniques may be classified into five categories based on their principle of operation: chemical analysis, quantitative metallography, volumetric tests, nondestructive techniques and shop floor tests.<sup>1</sup> Table 2 summarizes all kinds of inclusion detection methods in current use and applied in research. Their details will be provided in subsequent sections.



**Table 2** Inclusion detection methods.<sup>16</sup>

Detection methods	Sample Weight, g	Particle Size Affected, $\mu\text{m}$	Operation Type
<b>Pressure Filter Tests</b> PoDFA LAIS Prefil Qualiflash	$\leq 2000$ $\leq 1000$	All sizes	Off-line Off-line Off-line
<b>Electrical Resistivity Test</b> LiMCA II	$\leq 100$ per min	$> 15$	On-line
<b>Acoustic Detection</b> Signal-noise technique Pulse-echo technique		$> 10$	On-line
<b>Electrochemical Dissolution</b>	$\leq 100$	All sizes	Off-line
<b>Chemical Analysis</b> Emission spectroscopy : Hot extraction; Combustion analysis; Neutron activation; Gas chromatography	0.5-30	All sizes	Off-line
<b>Eddy Current Method</b>	-	-	On-line
<b>Capacitance Probe</b>	-	-	On-line
<b>X-Ray Detection</b>	-	-	Off-line
<b>Electromagnetic Detection</b>	$\leq 200$ per min	$> 10$	On-line

### 2.6.1 PoDFA

The porous disc filtration apparatus (PoDFA) technique was introduced as a method for assessing metal cleanliness by Alcan.<sup>33</sup> This technique is able to distinguish between dirty metal and relatively clean samples. It has also been used to evaluate the performance of on-line melt treatment devices. Moreover, it can even distinguish inclusion type and differentiate between the levels of boride, carbide and spinel present within an individual sample. This qualitative aspect of the technique has proved invaluable in establishing the cause of the problem in unsatisfactory metal.<sup>34</sup>

In this technique, a certain volume of metal is passed through a fairly impermeable filter thus concentrating the inclusions present in the melt in the form of the cake on the filter. The filters with the residue are then sectioned vertically along the central plane and prepared for metallographic examination. Figure 6 shows the principle of the technique. A balance located below the filter crucible enables the operator to weigh, precisely, the right amount of metal that filters through. The concentration of the inclusion is reported in  $\text{mm}^2/\text{kg}$  indicating the area of inclusions in the sectioned part.<sup>16,34</sup>

However, this technique is not sensitive at inclusion concentrations of less than  $1 \text{ mm}^2/\text{kg}$ . The results may also be influenced by the presence of inclusion particles of less than  $10 \text{ }\mu\text{m}$  in size. The main disadvantage in practice is that it is an off-line test, and is too time-consuming and labor intensive.<sup>34</sup> Nevertheless, this technique is

considered to be effective and has been used successfully to assess inclusion levels in cast shops.

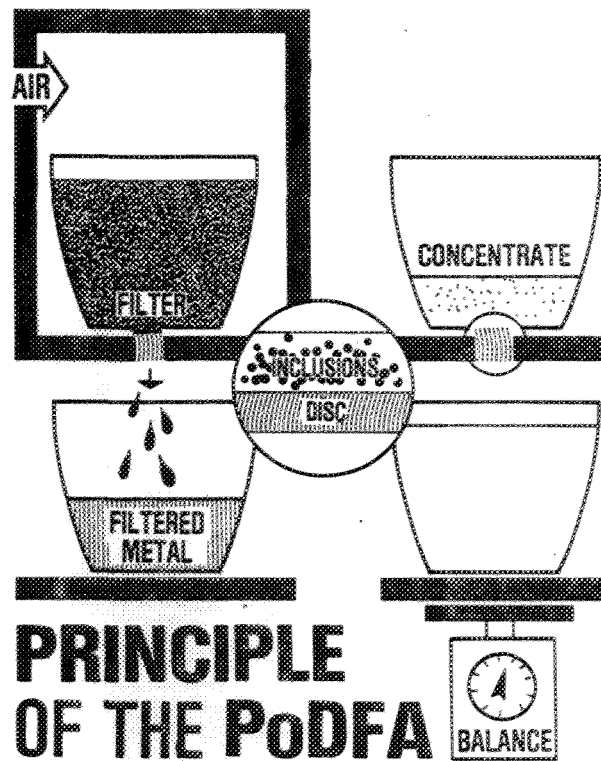


**Figure 6** Principle of the PoDFA Method of Measuring Metal Cleanliness.<sup>34</sup>

### 2.6.2 LAIS

The LAIS (Liquid Aluminum Inclusion Sampling) technique, also termed the Union Carbide Particulate Tester, is one of the most widely accepted tests for the cleanliness of liquid aluminum and its alloys. It is based on the vacuum-filtration technique and is similar to PoDFA except that the sample is obtained from inside the melt. The liquid metal is pulled through a filter in which the inclusions become trapped and can be examined metallographically and analyzed chemically.<sup>35</sup>

As seen in Figure 7, this system consists of a filter, a filter cup, a tapered plug and a vacuum container. After preheating the sampling device, molten metal is sucked through a filter and into a reservoir by means of either low pressure or a vacuum behind the filter. The entire sampler-assembly is immersed in the bulk melt, so that the filter cup inlet is about 25 cm below the melt surface, thus completely eliminating the need for ladling or remelting. After sampling a certain amount of melt, the assembly is removed from the bath to cool. Next, the filter is cut off from the filter cup, then sectioned, polished and examined for inclusion content.<sup>36, 37</sup>

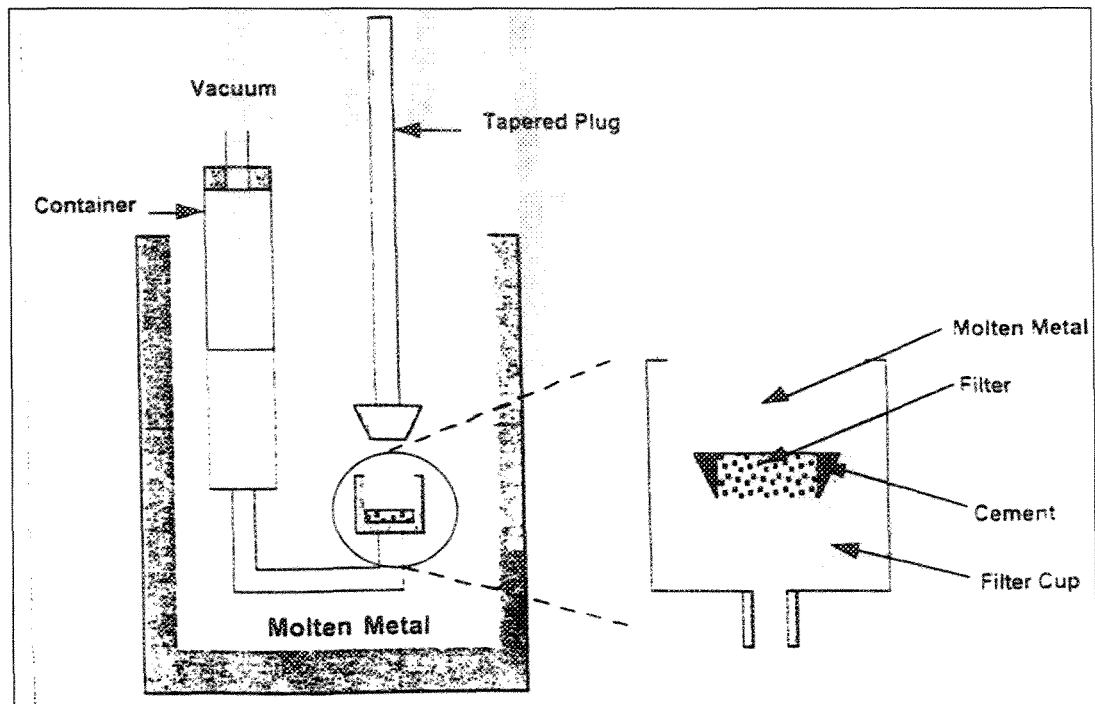


**Figure 7** Schematic diagram of the LAIS technique.<sup>36</sup>

It should be noted that this technique can provide information on the chemical

nature of the inclusions, an asset which other techniques, depending on physical detection, do not possess. The technique is capable of detecting a wide variety of inclusions in aluminum melts.<sup>36</sup> Its metal sampling volume, however, is fairly small. Vacuum leakage problems can occasionally cause back-flow of molten metal. Also, due to differences in the amount of metal collected, the technique is often criticized as not having reproducible results.

### **2.6.3 Prefil (Pressure Filtration) Technique**

The Prefil technique is a derivation of the LAIS test. It can produce in-situ results in the form of flow-rate charts. These charts minimize the need for time-consuming metallographic examinations for inclusion analysis as are required by other pressure filtration techniques such as PoDFA. Thus Prefil is a powerful tool for any world-class aluminum-casting organization in providing comparative cleanliness information on the foundry process.

As will be seen in Figure 8, a photograph of the Prefil apparatus is provided. The machine consists of a two-stage pressure cell, a refractory crucible containing the filter, and a digital balance to record the weight of filtrate as a function of time. The crucible is made of a low-heat capacity, high-insulating, fibrous material. Thus, no preheating is required prior to testing. The machine is equipped with on-board data-logging and software for footprint characterization; it can yield curves of the filtration weight versus time.

Molten aluminum is filtered under pressure through an ultra-fine filter, resulting in a build-up of solid inclusions on the filter surface. The buildup of the cake is then metallographically examined and identified. The inclusion levels are also expressed in the form of units of inclusion area per kilogram of filtered melt ( $\text{mm}^2/\text{kg}$ ). Based on such quantitative analysis of inclusions, the corresponding filtration curve can be established as the relevant Prefil footprint, which enables the researchers to obtain immediate information on the quality of molten metal on a day-to-day basis without the need for continuous metallographic analysis.<sup>12, 38, 39</sup>

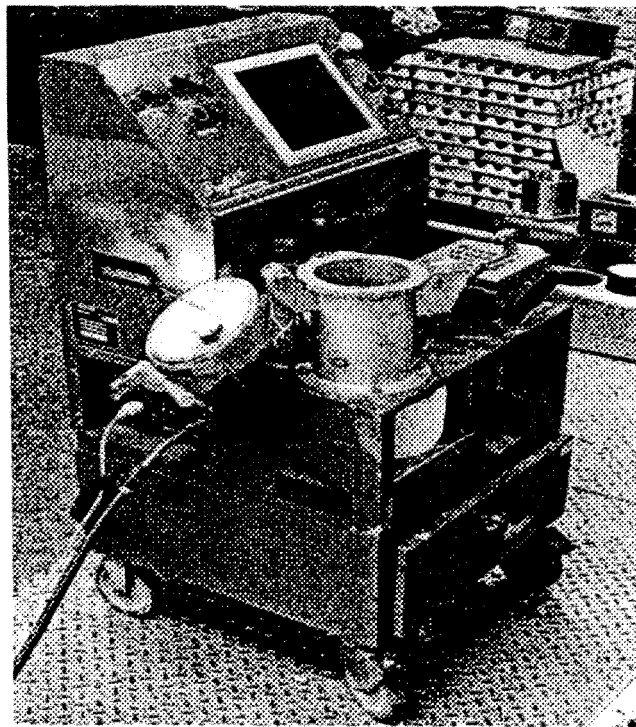


**Figure 8** Prefil technique apparatus.<sup>8</sup>

It is interesting to note that the filtration involved in the Prefil technique and its subsequent permeability is a dynamic process which is critically dependent on the type,

size, shape, and mixture of inclusions present in relation to the filter itself. In the case of liquid metals, temperature, fluidity and the surface of the fluid also influence the characteristic behavior of the system.<sup>40, 41</sup>

#### **2.6.4 Qualiflash Technique**

Qualiflash is a shop apparatus which may be used to evaluate the quantity of inclusion in molten aluminum before casting. This device is patented and its name, “Qualiflash”, is a registered trade mark. It, too, is based on filtration, and more particularly on the clogging of a filter by oxides. It has the capacity to provide immediate and reproducible results which allow the foundryman to decide quickly and easily whether a bath is ready to be poured, or must undergo further treatment. Thus, this technique makes it possible to control the quality of the alloy from the earliest stages of casting.<sup>42, 43</sup>

The simplicity of this system recommends its use since only a small quantity of metal is required for sampling. As is shown in Figure 9, the apparatus is mounted on a trolley so that it can be moved around easily in the foundry. A funnel-shaped shell is used to cast the sample of metal, which is often heated to a regular temperature by means of a resistance collar. A fresh extruded ceramic filter is held against the bottom of the shell by a spring plug. A step-like ingot mold is placed underneath the shell to recover the metal which flows through the filter.<sup>42, 44</sup> Melt cleanliness is gauged by the number of steps covered by the liquid metal which filters through into the step mould,

with 10 indicating the highest quality.<sup>45</sup> The system also includes a thermocouple with the apparatus to measure, exactly, the temperature of the metal in the spoon before it is poured into the shell. The temperature may be read conveniently on the electric control box. A temperature range appropriate to the alloy to be tested is specified in order to optimize the sensitivity of the system to differences in oxide levels.<sup>43, 44</sup>

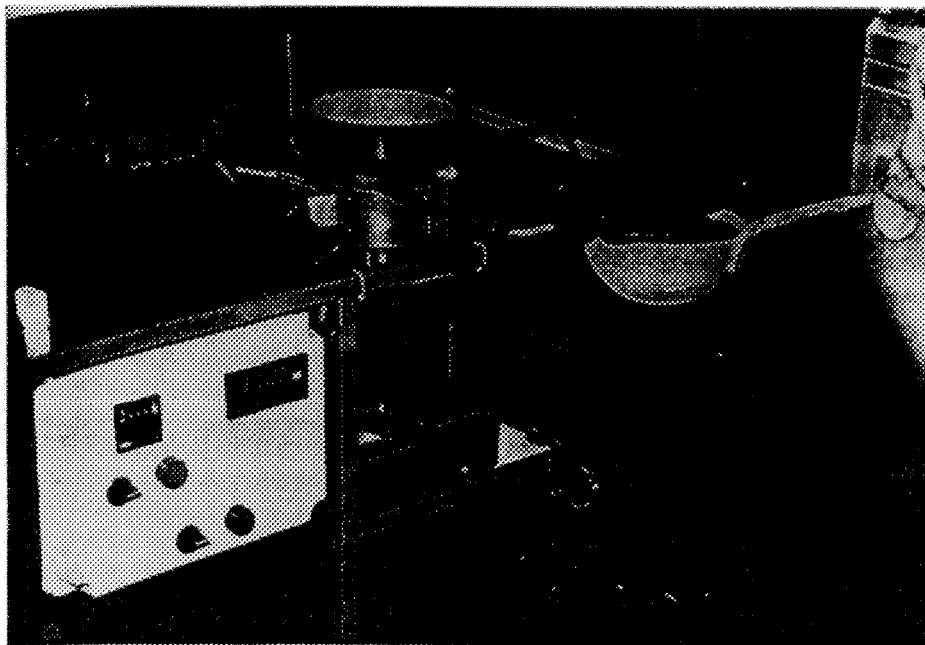


**Figure 9** The Qualiflash apparatus.

The metal flows through the filter for about 20 seconds, at most, after which the result can be read instantaneously, simply by counting the number of steps covered in the ingot mold. The main advantage of this technique is the greater speed of the procedure by contrast with other filtration methods. The only item requiring expenditure is the filter which must be replaced after each measurement. The process of measuring is so simple that even unskilled personnel may operate this shop equipment with ease.



### 2.6.5 Reduced Pressure Test

The reduced pressure test (RPT), sometimes referred to as the vacuum solidification test (VST), is the most widely used foundry procedure for determining excessive hydrogen present in the melt. The test uses a sample of molten alloy solidifying under reduced pressure (usually 1 to 100 mm Hg). This reduced pressure encourages pore and gas bubble formation, so that the sample solidified from gassy metal will display exaggerated porosity.<sup>46, 47, 48</sup>

As may be seen in Figure 10, the RPT apparatus includes a vacuum chamber, crucible or sample cup, chamber base, vacuum gauge, vacuum regulator release valve and vacuum pump. The sample crucible is preheated to melt temperature by immersing it into the melt itself. The crucible is filled carefully to limit the possibility of turbulence since any turbulence will increase the hydrogen and result in an artificial test. The sample is then rapidly transferred to the vacuum chamber in order to minimize temperature loss prior to the test. A vacuum is drawn in a short time and the sample is allowed to solidify.<sup>46</sup> A qualitative assessment of the hydrogen content of the liquid may be obtained by visual examination of the reduced pressure specimen. A puffy or convex top surface corresponds to high gas content, while a smooth or concave surface represents low content. At times, samples may be sectioned and polished in order to obtain an improved porosity profile through the application of such sophisticated means of investigation as image analysis.<sup>47, 48</sup>

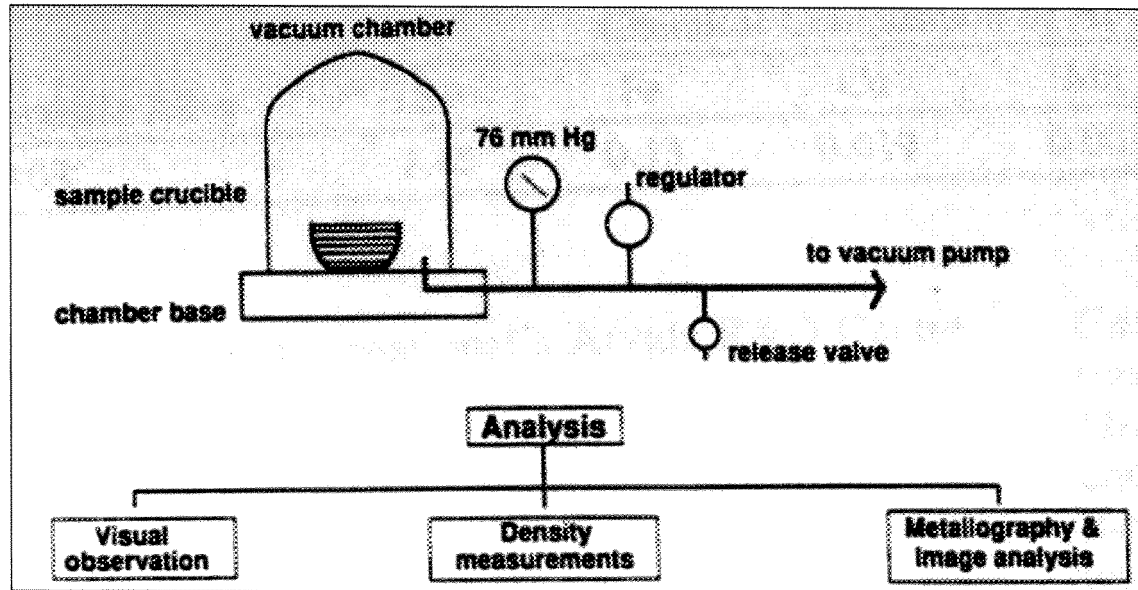


Figure 10 Schematic representation of the RPT apparatus.<sup>47</sup>

The popularity of the reduced pressure test stems from its simplicity. Over the years, it has been proven to be quick, inexpensive and effective. Operators require little training and the test is rapidly performed. One major disadvantage, however, is that this test is not quantitative; nor is it sensitive to the very low hydrogen contents obtained/required in ingots prepared from properly filtered and degassed melts for manufacturing purposes. In addition, the results are influenced by other factors such as inclusions present in the melts, reduced pressure, and solidification rate. A serious problem for many foundry men is the failure to establish sampling and apparatus testing procedures adequately together with the lack of proper auditing procedures to ensure compliance with the norm.<sup>46</sup>

### 2.6.6 LiMCA Technique

The Liquid Metal Cleanliness Analyzer (LiMCA) is the most fully-developed measuring system for inclusions in liquid metals to date. It is a real-time device initially created by Alcan. Compared with other techniques, such as sedimentation, filtration and metallography, which require considerable amounts of labor and are time-consuming, the LiMCA method has the advantage of providing not only information on the volume concentration of inclusions, but also on the size distribution of inclusions immediately and quantitatively. To date, this technique has been successfully applied in quality and process control operations by leading aluminum companies, such as Alcan, Alusuisse, Alcoa, Reynolds and Pechiney.<sup>49, 50, 51, 52</sup>

The LiMCA technique is based on the electric sensing zone (ESZ) principle. Figure 11 shows a schematic diagram of this measuring system. The probe head consists of an electrically insulating sampling tube and two electrodes connected to a battery with an electromotive force maintaining a constant current through the orifice (typically 300  $\mu\text{m}$ ). A slight change in the orifice resistance is produced every time a nonconductive particle is carried through it by the metal flow. This resistance change causes a microvolt pulse of a duration approximately equal to the transit time of the particle across the same orifice. The amplitude of the voltage change is proportional to the electric current and the volume of the particle. Thus the number concentration and size distribution of inclusions within the melt may be deduced by counting the number

of pulses and measuring their respective amplitudes.<sup>50, 52</sup>

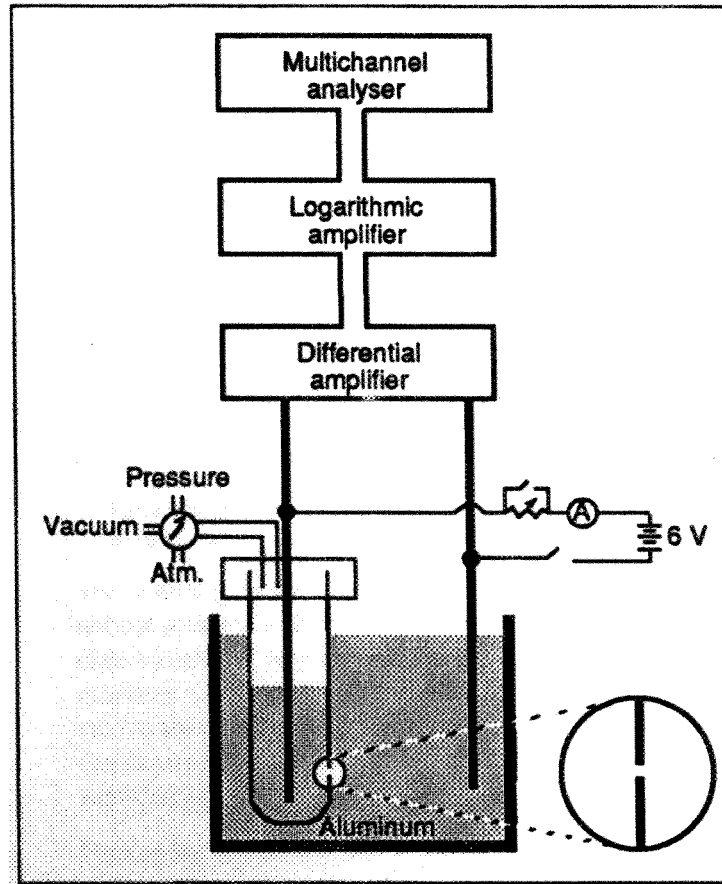


**Figure 11** Schematic of the LiMCA operation.<sup>51</sup>

The LiMCA technique is considered to be a reliable tool for the on-line detection of small particles in liquid metals. It can be used either alone or in conjunction with PoDFA or LAIS for larger inclusions. Over the last several decades, the LiMCA system has been successfully applied in the aluminum industry in terms of process understanding, control, and optimization; it has also generated numerous results that were previously unattainable.<sup>16,53</sup>

According to the ESZ principle, however, every particle generates a voltage

pulse when passing through the orifice; nonconducting particles of the same size but of different type give rise to voltage pulses of the same magnitude. This implies that any microbubbles and micro droplets of salt generated by proprietary degassing units in molten aluminum will be counted by the LiMCA system as inclusions, thus leading to an overestimation in the number of potentially harmful solid inclusions within a melt. In addition, the LiMCA is not capable of effectively detecting conductive inclusions such as intermetallic particles which are often present in molten aluminum. If the particle is larger than the diameter of the orifice, the orifice will become blocked and requires to be replaced. Moreover, the cost of the LiMCA technique is relatively high; hence it is clear that this method is not likely to be widely used by the foundry industry.

#### **2.6.7 Ultrasonic Technique**

Various techniques, which are currently available for evaluating melt quality, are normally based on extraction of a metal sample followed by analysis in a laboratory. Although these approaches are often capable of providing useful information regarding inclusion content, they require considerable sample preparation and analysis time to reveal possible molten metal processing problems; consequently, the information is often obtained too late to make timely adjustments in the casting process.<sup>3, 4</sup>

Thus, for a long time, the aluminum industry has been in search of a technique which takes online measurements of inclusions to provide feedback information for process optimization. This result can only be obtained by analyzing the metal while it is

still in the molten state. As regards aluminum processes, there is a commercial device available to measure the cleanliness; it is the Liquid Metal Cleanliness Analyzer (LiMCA). The LiMCA technique however suffers from too many limitations.<sup>3,4</sup> As is known to researchers in this field, LiMCA uses an orifice with a diameter of 0.5mm or less through which molten Al is pumped in order to measure the size and count the number of the particles. If the particle is larger than the diameter of the orifice, the orifice will become blocked and will require to be replaced. This means that LiMCA has little ability to detect particles larger than 100 $\mu$ m. Furthermore, due to fact that the volume of the molten Al sampled through the small orifice is rather small, such analysis may not be representative. Moreover, the LiMCA machine is very expensive and hence not accessible, in general.<sup>4</sup> Consequently, another technique is required to accomplish universal purpose of the research.

The Ultrasonic detection technique, because of its capacity for probing the interior of materials, is a promising method for the resolution of the problem. This technique is based on the principle of sound pulse dissipation. A transmitter sends a signal from a piezoelectric crystal through the molten metal. If there is no inclusion, ultrasound will propagate in molten metals without much attenuation. When inclusions are present however, ultrasonic signatures such as velocity and attenuation of the liquid and ultrasonic energy scattered by inclusions will change. All changes in these signals are collected by a receiver and displayed on an oscilloscope. Figure 12 provides a schematic illustration of this system.

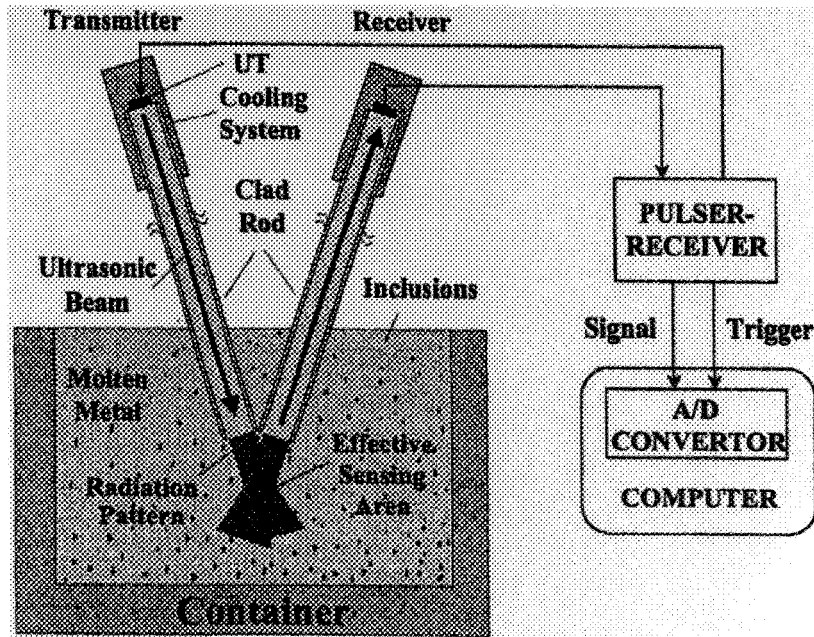


**Figure 12** A schematic view of the configuration of inclusion detection in molten metals using the pitch-catch mode.<sup>3</sup>

#### (i) The Principle of Ultrasonic Technique

In the ultrasonic technique, a transmitter sends pulse signals from a piezoelectric crystal; these high frequency sound pulses are then delivered into the liquid metal. Since the nonmetallic particles have different ultrasonic properties from the liquid metal they interact with the sound energy pulses. Any inclusions suspended in the melt would reveal their presence in two ways: firstly, because these inclusions scatter some of the sound and cause attenuation, the peak height of the reflected signal is less than that of the initial pulse. This difference in the peak heights provides a measure of the attenuation, namely, the general level of cleanliness of the melt.<sup>54</sup> Additionally, larger particles cause discrete reflections. The peak height of these reflections is proportional to the size of the particle causing the reflection. Thus various

threshold values can be introduced when the relationship between the amplitude of the reflection and the inclusion size is obtained using standard particles whose sizes are already known. The number of reflections crossing each of these threshold values can then be counted so as to yield a particle size distribution.

## **(ii) Advantages of Ultrasonic Technique**

Compared with various techniques based on the extraction of a metal sample followed by analysis in the laboratory, the ultrasonic technique is possessed of a number of advantages. First, it is able to provide on-line information which allows the operator sufficient time to make any required adjustments to the process. In addition, all the other methods available are more expensive, either in terms of the capital cost of the equipment or in terms of the manual labor required to obtain and interpret the results, while they also require much more sample preparation and analysis time. Furthermore, the ultrasonic technique is capable of monitoring significantly large proportions of the total metal volume and hence its results are much more representative than those of other methods. In some cases of flowing metal in a launder, it is possible to achieve analysis of at least 25% of the entire metal melt. Moreover, this technique can detect different locations along the product line. Multiple-probe assemblies can even monitor different locations simultaneously.

Although the ultrasonic technique is unable to discriminate between the types and shapes of inclusions, the technique used together with the PoDFA technique (which



provides a qualitative assessment of inclusions) can provide us with an in-depth understanding of the nature and behavior of the melt treatment process.

#### **2.6.8 Other Detection Techniques**

Many other inclusion detection techniques, including Chemical Analysis, Electrochemical Dissolution, X-Ray Detection, Eddy Current Method, Capacitance Probe and Electromagnetic Detection, also exist for molten metals. However, because of their lack of advanced improvement, imprecision, cumbersome operation, or their costliness, they did not find substantive application in commercial production.<sup>16</sup>

**CHAPTER 3**

**EXPERIMENTAL PROCEDURES**

## **CHAPTER 3**

### **EXPERIMENTAL PROCEDURES**

In order to fulfill the objectives of this study, various inclusions were added to both pure aluminum and commercial 356 alloy melts by plunging master alloys into the melt. Three additions of each inclusion type were added to the base alloy. For each melt condition, Ultrasonic measurements were taken at two temperatures using a Metalvision MV20/20 machine. Solidified samples were also obtained for each melt condition by pouring a small amount of the melt into a metallic cup. The microstructures of these samples were then examined, using a Jeol JXA-8900L electron probe microanalyzer, to analyze and support the results obtained by applying the ultrasonic technique. Backscattered images showing the inclusion distribution over the entire sample surface and details of the different inclusion types were obtained. X-ray images of the constituent elements were also obtained to verify the inclusion types. Details of the experimental procedures are as follows.

#### **3.1 MATERIALS**

Pure aluminum and commercial 356 alloy were used for preparing the melts.

Inclusion additions of titanium diboride, strontium aluminide, titanium aluminide and aluminum oxide were made to the melt using master alloys for the first three items, and an Al-Al<sub>2</sub>O<sub>3</sub> composite alloy for the alumina addition, as shown in Table 3. The additions were made so as to obtain specified levels of B, Sr, Ti (in ppm), and Al<sub>2</sub>O<sub>3</sub> (in vol. percent) in the melt.

**Table 3** Inclusion types and their sources used in this study

Inclusion Type	TiB <sub>2</sub>	AlSr	Al <sub>3</sub> Ti	Al <sub>2</sub> O <sub>3</sub>
Inclusion source	Al-5%Ti-1%B master alloy	Al-10%Sr master alloy	Al-10%Ti master alloy	Al-20%Al <sub>2</sub> O <sub>3</sub> composite alloy containing 20 vol. percent Al <sub>2</sub> O <sub>3</sub>

### 3.2 METALVISION MV20/20 MACHINE

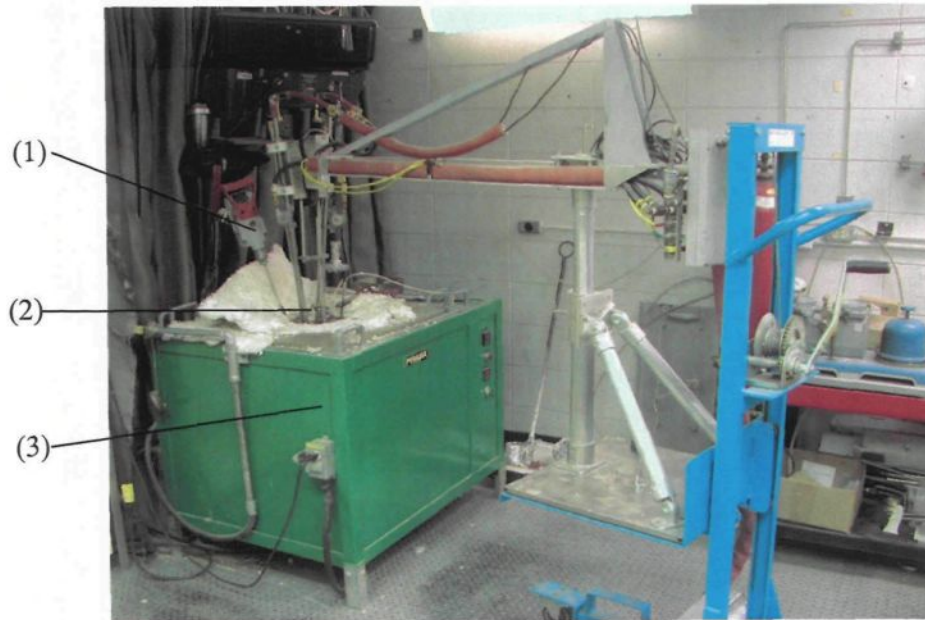
The MV20/20 machine consists of a sensor assembly, a pulser/receiver unit, and a computer. Figure 13 shows the sensor assembly used in the ultrasonic machine. It consists of two transducers, two air-cooled guide rods, a reflector plate and an adjustable support stand. Mechanical stirring was conducted using an impeller mounted on an electric drill, also shown in the picture.

Figure 14 shows a photograph of the oscilloscope screen captured during the measurement of inclusions which indicates the presence of any suspended inclusion. The peak height of these reflections is proportional to the size of the particle causing the reflection, therefore, according to the relationship between the amplitude and size of

inclusion obtained from standard particles, whose sizes are already known, the number of reflections crossing each of these can be counted by our program on the computer to yield a particle size distribution.

A computer connected to the machine provides plots of (i) *cleanliness value*, (ii) *particle size*, and (iii) *particle count* for each particle size as a function of testing time. Figure 15 depicts a screen capture of the MV20/20 software showing the results obtained from an aluminum melt. From this, it is possible to see that the system measures particle size 100 times per second and records and displays how frequently particles are detected.

The data is updated every twelve seconds. Over the first ten seconds, the system measures the particle size and then calculates the average size. Following this, a two-second period is required to measure the cleanliness value. A cleanliness value of around ten indicates a melt containing a relatively small number of inclusions, while a value of around zero indicates a melt containing a relatively large number of inclusions. The cleanliness value is an indicator of overall concentration of inclusions in the melt, including those too small to produce discrete reflections (i.e. inclusions  $< 20\mu\text{m}$ ).<sup>55</sup>



**Figure 13** The sensor assembly used in the ultrasonic technique for measurement of melt cleanliness: (1) mechanical stirrer, (2) air-cooled guide rods, and (3) electric furnace.

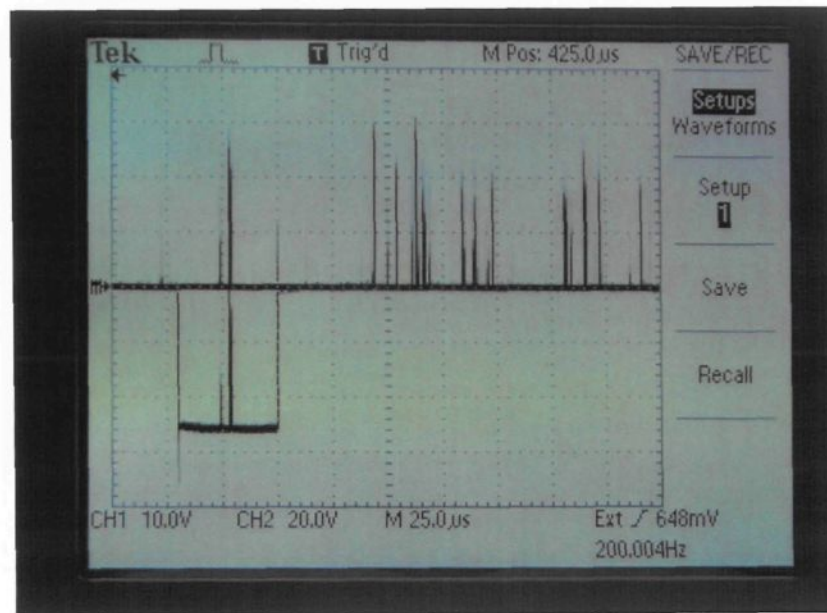


**Figure 14** A photograph of the oscilloscope screen captured during the measurement of inclusions in the melt.



**Figure 15** Screen capture of MV20/20 software showing the results from an aluminum melt sample.

### 3.3 MELT PREPARATION AND ULTRASONIC TESTS

About 20 kg of pure aluminum (or 356 alloy) ingots were melted in a 30 kg-capacity SiC crucible in which the ultrasonic tests were conducted. The temperature of the melt was maintained at a specified temperature. Degassing was carried out for about 15 minutes using pure dry argon before any inclusions were added.

Following degassing, a specified inclusion-type was added to the melt. As soon as the melt reached the required temperature, the ultrasonic test was started. The melt was stirred throughout the entire period of measurement using a rotary impeller. Table 4 provides the details of the melts which were prepared for carrying out the ultrasonic

tests.

**Table 4** Details of melts prepared for ultrasonic tests

Inclusion type added	Addition level *	Alloy and Melt Temperature			
		Pure Al		356 alloy	
		680 °C	720 °C	640 °C	680 °C
TiB <sub>2</sub>	In terms of ppm B	15	15	15	15
		30	30	30	30
		38	38	60	60
		--	--	90	90
AlSr	In terms of ppm Sr	40	40	40	40
		100	100	100	100
		250	250	250	250
Al <sub>3</sub> Ti	In terms of ppm Ti	600	600	600	600
		1000	1000	1000	1000
		3000	3000	3000	3000
		5000	5000	--	--
Al <sub>2</sub> O <sub>3</sub>	In terms of vol. percent Al <sub>2</sub> O <sub>3</sub>	2%	2%	2%	2%
		6%	6%	6%	6%

\* Additions of inclusions are made using master alloys and Al-Al<sub>2</sub>O<sub>3</sub> composite alloy to achieve the specified levels of B, Sr and Ti in ppm and Al<sub>2</sub>O<sub>3</sub> in vol. percent in the melt.

For each melt condition, a sampling of the melt was taken before and after the ultrasonic test to obtain a solidified sample so as to monitor the actual condition of the changes in inclusion levels taking place during the ultrasonic test. In the same manner, ultrasonic tests were carried out for each addition (three additions were made for each



powder) of  $\text{TiB}_2$ ,  $\text{AlSr}$ ,  $\text{Al}_3\text{Ti}$  and  $\text{Al}_2\text{O}_3$  in liquid pure aluminum and commercial 356 alloy at two different temperatures.

Figure 16 shows a close-up of the sensor assembly used in ultrasonic measurements during operation. It is recommended that the sleeves on the guide rods should be changed daily. After two days' testing, all the guide rods and the reflector should be replaced, otherwise, the guide rods dissolve slowly and get shorter. This eventuality would make scraping the rods more difficult since the ends of the guide rods would no longer be flush with the ends of the ceramic fiber sleeves and would thus become slightly recessed inside the sleeves.



**Figure 16** Close-up of the sensor assembly used in ultrasonic measurements

It should be mentioned that after a series of measurements for each inclusion type, the crucible was washed thoroughly using pure aluminum to ensure that no

inclusions from the preceding tests be introduced to the next series of measurements. This step was one of the procedures of major importance which were followed for this study.

### 3.4 METALLOGRAPHY

As mentioned earlier, in order to obtain a qualitative analysis of the inclusion types and levels corresponding to each melt condition, a sampling of the melt was taken before and after the ultrasonic test to obtain a solidified sample. Solidified samples, as shown in Figure 17, were then sectioned, mounted in bakelite and polished to a fine finish ( $1\mu\text{m}$ ). Figure 18 provides a schematic diagram of the sample dimensions.



**Figure 17** Close-up of the solidified sample.

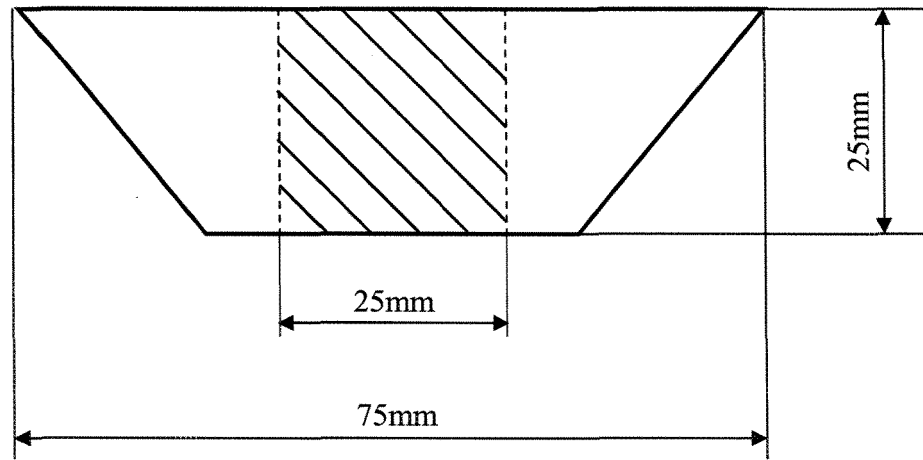


**Figure 18** Schematic diagram of the sample dimensions

The polished samples were used to examine the microstructure of the various inclusion types studied. Backscattered images showing the distribution of inclusions over the entire sample surface and details of the different inclusion types were obtained using a Jeol JXA-8900L electron probe microanalyzer, as shown in Figure 19. X-ray images of the constituent elements were also obtained to verify the inclusion types.

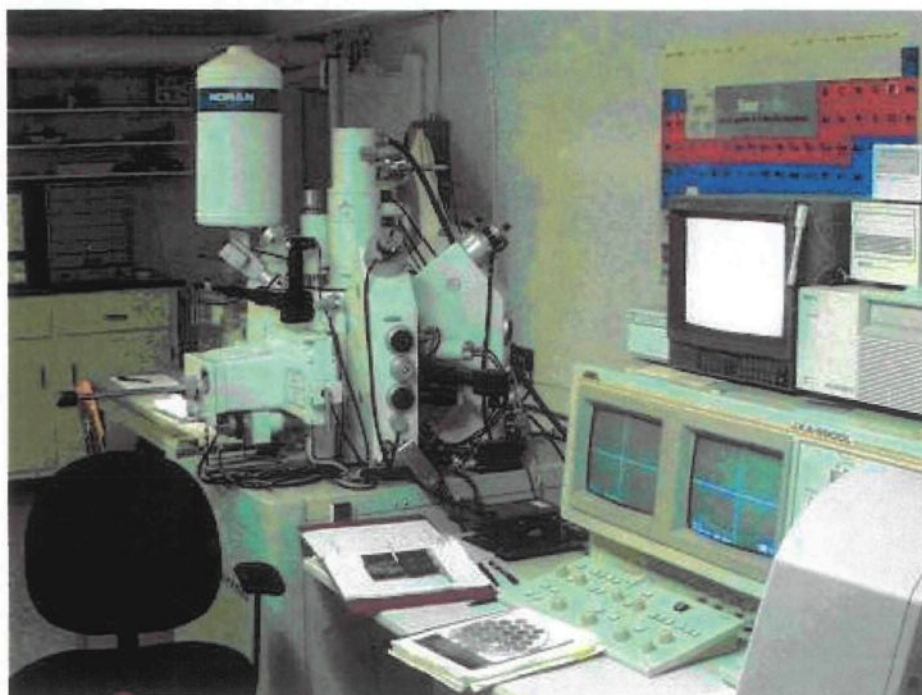


**Figure 19** JEOL JXA-8900L Electron Probe Microanalyzer.

## **CHAPTER 4**

### **RESULTS AND DISCUSSION**

## **CHAPTER 4**

### **RESULTS AND DISCUSSION**

#### **4.1 INTRODUCTION OF PREVIOUS WORK**

The quality of aluminum products is frequently and critically associated with the presence of inclusions of nonmetallic materials within the molten aluminum during manufacturing steps. Various techniques for the evaluation of aluminum melt cleanliness have been developed over the past decades. In order to investigate the capacity and sensitivity of these techniques, a series of studies was previously carried out by our group. The Prefil (Pressure Filtration) and LiMCA techniques were employed to investigate their reliability in measuring different types of inclusions in commercial aluminum melts, and to study the role of the major melt treatment parameters commonly used in aluminum foundries; these parameters include grain refining and morphology modification, as well as the effect of inclusions on the formation of porosity.

In evaluating the Prefil technique, three primary alloys: 356, 319 and 4104 were used in a succession of experiments. Prefil curves indicate demonstrable

sensitivities to variations in the melt treatment conditions. There is a clear difference between the Prefil curves produced before and after melt treatments. The reproducibility of Prefil curves was empirically demonstrated using statistical methods. Satisfactory correlation was obtained between the results produced by LiMCA technique and the metallographic analysis of the Prefil residues.<sup>40</sup>

The unfiltered part of the metal in contact with the filter were then sectioned, mounted in bakelite and polished for metallographic examination. Inclusions of  $\text{Al}_4\text{C}_3$ ,  $\text{MgO}$ ,  $\text{MgAl}_2\text{O}_4$  and a number of other oxides were observed in the solidified Prefil samples. It was noted that mechanical stirring plays a significant role in increasing the amount of inclusions in the melt. Degassing by means of pure dry argon injected into the melt through a rotary impeller (speed~160 rpm) appears to be the best technique for the purpose of inclusion removal.

In the case of the LiMCA technique, intensive studies on aluminum melt cleanliness were undertaken to investigate the capacity and the sensitivity of the LiMCA technique in measuring different types of inclusions regularly present in commercial pure aluminum and Al-6%Si casting alloys at two different temperatures.

Additions of typical inclusions present in aluminum casting alloys, such as  $\text{Al}_2\text{O}_3$ ,  $\text{Al}_4\text{C}_3$ ,  $\text{MgO}$ ,  $\text{CaO}$ ,  $\text{TiB}_2$  and  $\text{Al}_3\text{Ti}$ , were made to the melt. LiMCA data were obtained in the form of plots which provided the total concentration number and volume concentration of inclusions, as a function of time and particle size. An examination of

the microstructure of the solidified samples obtained from the LiMCA probe tube and from samplings of the melt was also carried out using an electron probe microanalyzer (EPMA).

Analysis of LiMCA data and with the corresponding microscopy examination show that the LiMCA technique is an entirely reliable one for the measurement of different types of inclusions present in aluminum melts. The sensitivity of this technique tends to increase with a decrease in melt temperature. It should be noted that more satisfactory results were found in the tests conducted at 680°C.

Microstructural evidence for the agglomeration of a vast amount of  $\text{TiB}_2$  inclusions, as captured by the LiMCA probe tube, shows that LiMCA is the only technique which is able to capture such agglomerates on-line, in view of the fact that other techniques such as the PoDFA and Prefil based on the filtration principle cannot measure such  $\text{TiB}_2$  agglomerates without clogging their filter systems and interrupting the measurement process. This finding is significant, and demonstrates an important aspect of the LiMCA technique, considering that Al-Ti-B master alloys are regularly employed for grain-refining in the aluminum industry.<sup>8</sup>

In order to complete the systematic work of the measurement of aluminum melt cleanliness, the evaluation of different inclusion types by the ultrasonic technique was undertaken for the present study. Details of the results from the Metalvision MV20/20 machine are discussed in the following subsections.



## 4.2 MEASUREMENTS OF MELT CLEANLINESS

The ultrasonic technique has been reported over the last few years as an on-line method for monitoring melt properties. Earlier studies usually focused on the principle of this technique and the perfecting of the assembly configuration. Simulation systems using water were often used to investigate the optimal system configurations and to evaluate sensitivity, accuracy, inspection volume and speed for the detection of inclusions.<sup>3, 4, 5</sup> Unfortunately, few of the projects were conducted in molten aluminum.

Thus, the capacity and the sensitivity of the ultrasonic technique as applied in molten aluminum are still incomplete in this area. Evaluation of various inclusion types by the ultrasonic technique was undertaken for the present study. Two types of material were used: commercial 356 alloy and pure aluminum. The first represents the base alloy corresponding to the popular commercial 3xx series of aluminum foundry alloys used for automotive applications, while the second may be used as a reference for aluminum wrought alloys.

Specified amounts of each inclusion type were added to the melt in the form of master alloys or a composite alloy in the case of alumina inclusions. The details of all the additions are listed in Table 2. Ultrasonic tests were carried out for each addition of  $\text{TiB}_2$ ,  $\text{AlSr}$ ,  $\text{Al}_3\text{Ti}$  and  $\text{Al}_2\text{O}_3$  in liquid 356 alloy and pure aluminum at two different temperatures corresponding to conditions of low and high superheat. The capacity of the ultrasonic technique for measuring the inclusions under the superheat conditions was

then investigated. The effect of superheat on the fluidity of the molten metal and hence the influence on sedimentation of the inclusion particles and any consequent changes in melt cleanliness measurements were also studied.

#### **4.2.1 Melt Cleanliness Curves (Short Testing Periods)**

Figures 20-21 show the cleanliness values obtained as a function of time with  $\text{TiB}_2$  inclusion addition to commercial 356 alloy at melt temperatures of  $640^\circ\text{C}$  and  $680^\circ\text{C}$ . As shown in these figures, the cleanliness decreases with an increase in the concentration of  $\text{TiB}_2$  inclusions. Thus, the presence of more inclusions suspended in the melt will increase the attenuation caused by them and lower the cleanliness values read by the machine. A comparison of these two figures shows that the cleanliness values at  $680^\circ\text{C}$  are slightly higher than those at  $640^\circ\text{C}$  for the same addition. This disparity may be attributed to the lower fluidity of the melt at the higher temperature, leading to much easier sedimentation in the melt. In this case, it is especially important to ensure that the melt is mechanically stirred while taking the measurements of inclusions.

The fact that  $\text{TiB}_2$  particles in the melt are exceedingly small and always clustered together will be discussed in the next part of this chapter. Normally, when  $\text{TiB}_2$  inclusions are added to aluminum melt, the fluidity of the melt will decrease significantly. Other techniques including LiMCA and all the available filtration techniques may only detect  $\text{TiB}_2$  inclusions when the concentration is very low (less

than 10 ppm B), since all these techniques are not able to measure such agglomerates without their systems getting clogged, and hence interrupting the measurements.<sup>8, 40</sup> With the ultrasonic technique, however, as shown in Figures 20-21, measurements may be conducted properly for concentrations as high as 90 ppm B, after which the cleanliness value will become zero, indicating that most of the ultrasonic signals are absorbed by these clusters. Nevertheless, 90 ppm B is high enough when considering the process of aluminum grain refining. This is a significant finding and indicates that the ultrasonic technique offers the best alternative for measuring  $\text{TiB}_2$  inclusions in liquid aluminum since such inclusions are invariably present due to the inevitable application of grain refining processes in the aluminum industry.

Figures 22-23 show the melt cleanliness values obtained as a function of time, with the addition of AlSr inclusions to commercial 356 alloy at melt temperatures of 640°C and 680°C. As will have been observed, with the increase in the concentration of AlSr inclusions, the melt cleanliness also decreases significantly, while the melt cleanliness of AlSr inclusions at 680°C is much lower than it is at 640°C for the corresponding addition levels. This fact was then analyzed, based on the corresponding microstructural evidence, and may be ascribed to the presence of strontium oxide films in the melt which increased the inclusion level detected by the machine. Strontium, with its high chemical affinity for oxygen, would be more easily oxidized at the higher melt temperature.

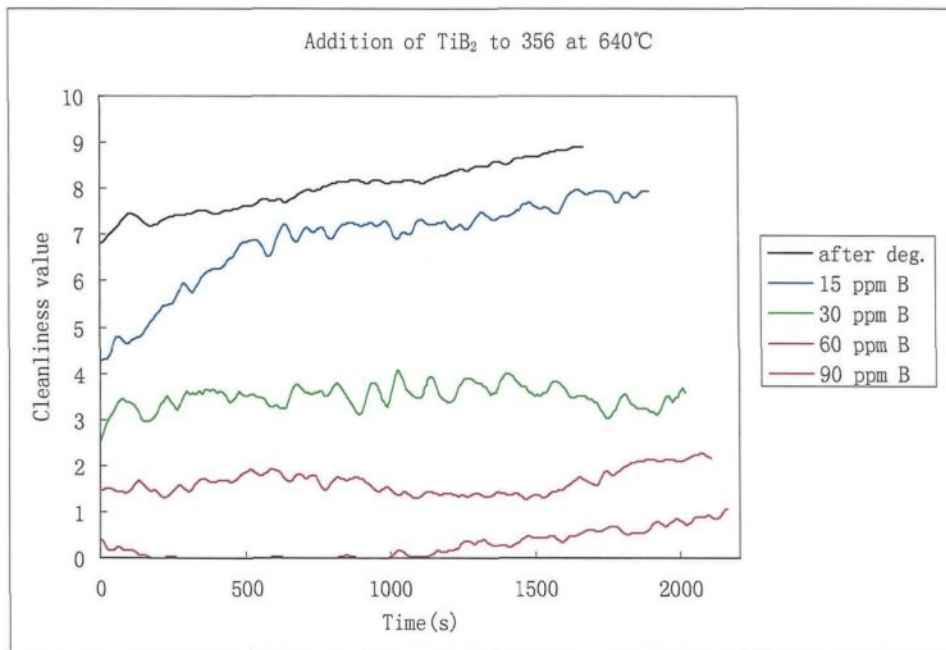


**Figure 20** Cleanliness values displayed by commercial 356 alloy melts containing TiB<sub>2</sub> inclusions as a function of time (melt temperature 640°C).

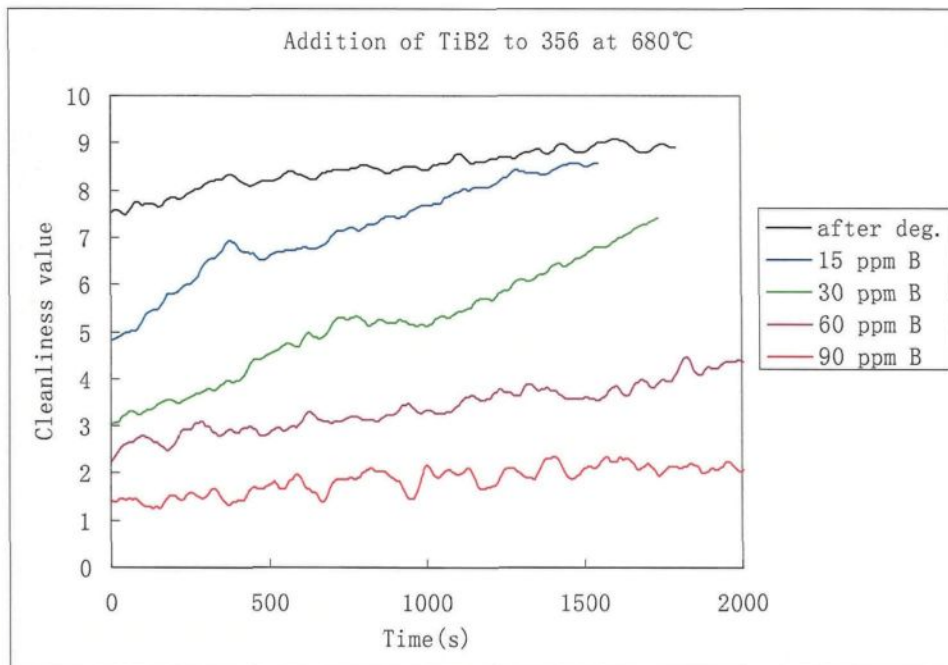


**Figure 21** Cleanliness values displayed by commercial 356 alloy melts containing TiB<sub>2</sub> inclusions as a function of time (melt temperature 680°C).

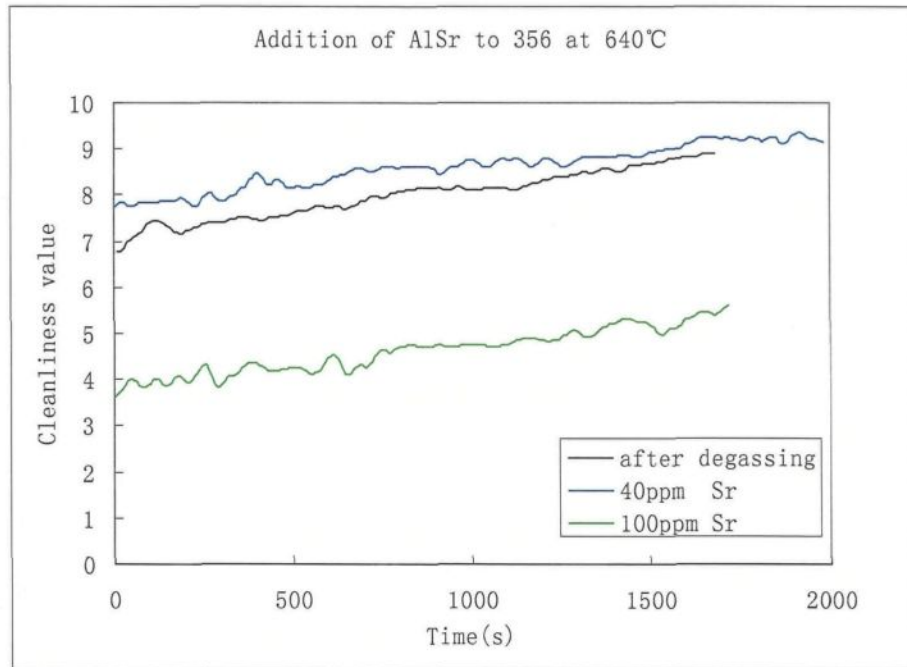


**Figure 22** Cleanliness values displayed by commercial 356 alloy melts containing AlSr inclusions as a function of time (melt temperature 640°C).

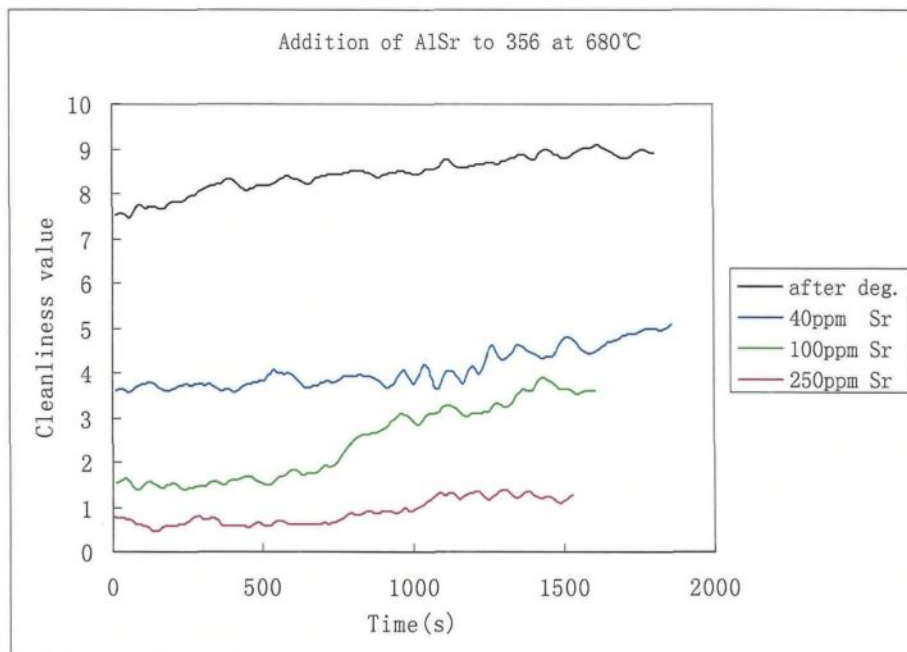


**Figure 23** Cleanliness values displayed by commercial 356 alloy melts containing AlSr inclusions as a function of time (melt temperature 680°C).

Figures 24-25 provide the cleanliness values obtained as a function of time, with the addition of  $\text{Al}_3\text{Ti}$  inclusions to commercial 356 alloy at melt temperatures of  $640^\circ\text{C}$  and  $680^\circ\text{C}$ . Here too, the cleanliness decreases with the increase in the concentration of inclusions. It will also be seen that the cleanliness values of the melt are slightly lower at the higher melt temperature, as observed in the case of the  $\text{AlSr}$  inclusion additions. This drop in cleanliness values occurs because higher melt temperature accelerates the decomposition of  $\text{Al-10\%Ti}$  master alloy, and hence, the lower melt cleanliness values observed in Figure 25.

Figures 26-27 provide the cleanliness values obtained as a function of time, with the addition of  $\text{Al}_2\text{O}_3$  inclusions to commercial 356 alloy at melt temperatures of  $640^\circ\text{C}$  and  $680^\circ\text{C}$ . A satisfactory consistency is observed in all the curves shown in Figures 20-27. Three important observations may be noted from these curves.

- (i) Increasing the concentration of inclusions gradually reduces the cleanliness level of the melt.
- (ii) Sedimentation may occur during the interval of testing if the mechanical stirring is not properly adjusted (i.e. without causing turbulence which may result in the introduction of surface oxide films into the melt). This phenomenon would provide a false representation of the melt cleanliness observed by an “increase” in the cleanliness value as read by the ultrasonic machine.
- (iii) The kinetics of sedimentation is strongly related to the density of the inclusion

type added, as well as to the melt superheat.

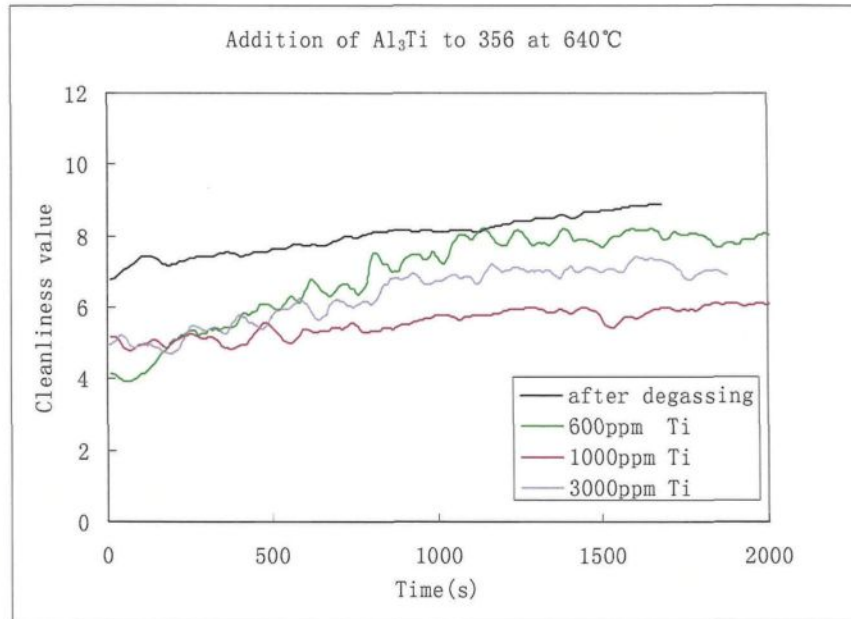


**Figure 24** Cleanliness values displayed by commercial 356 alloy melts containing  $\text{Al}_3\text{Ti}$  inclusions as a function of time (melt temperature 640°C).

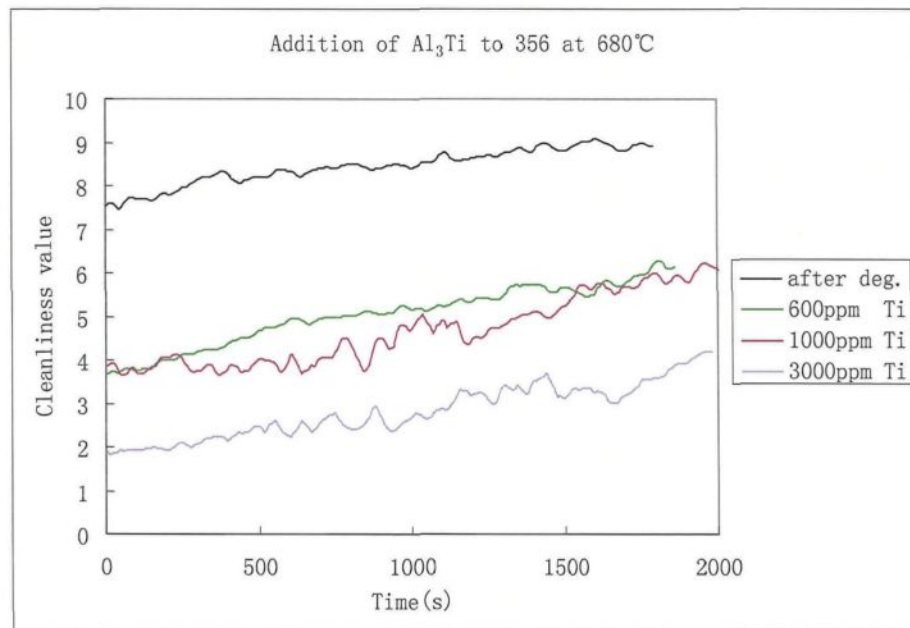


**Figure 25** Cleanliness values displayed by commercial 356 alloy melts containing  $\text{Al}_3\text{Ti}$  inclusions as a function of time (melt temperature 680°C).

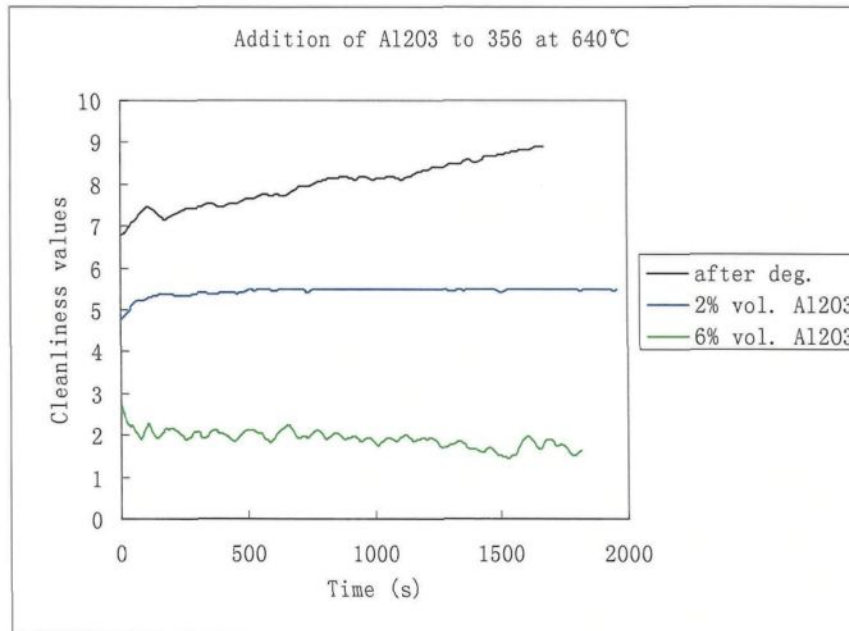


**Figure 26** Cleanliness values displayed by commercial 356 alloy melts containing  $\text{Al}_2\text{O}_3$  inclusions as a function of time (melt temperature  $640^\circ\text{C}$ ).

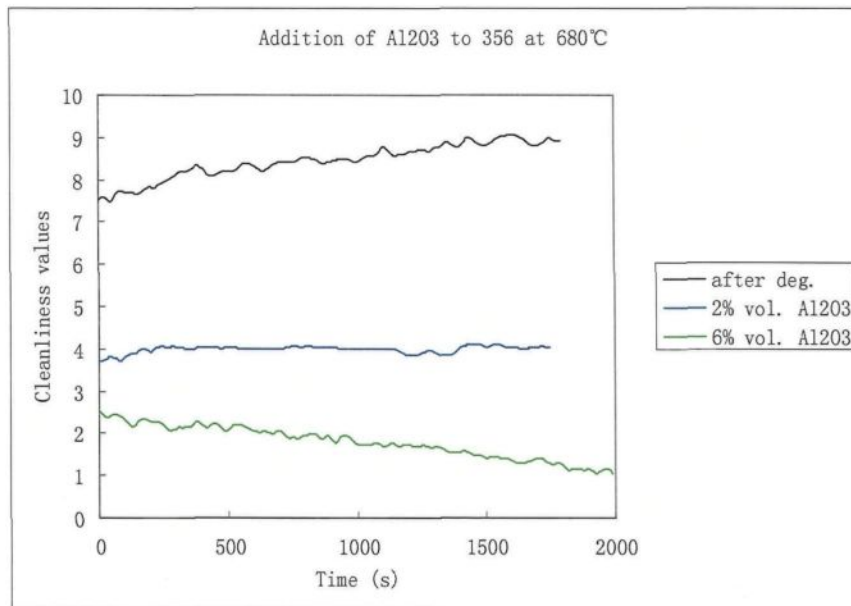


**Figure 27** Cleanliness values displayed by commercial 356 alloy melts containing  $\text{Al}_2\text{O}_3$  inclusions as a function of time (melt temperature  $680^\circ\text{C}$ ).



Also, an initial period of about 2-3 minutes at the beginning of testing should be disregarded when analyzing the cleanliness curves, since this represents the “stabilizing” period of the machine before it accommodates to the melt conditions. Compared to the initial period of 15-20 minutes in the study of the LiMCA technique for measuring Al-6%Si alloy melts at 750°C, the ultrasonic technique is more efficient and would, hence, be much more appropriate to the practices of the aluminum industry.

Figures 28-35 show the results of melt cleanliness curves as a function of time obtained from the corresponding inclusion measurements in pure aluminum. Compared to the results shown in Figures 20 through 27 for 356 alloy, a satisfactory similarity was observed for all these inclusion types. Thus, it is reasonable to say that the ultrasonic technique is entirely capable of measuring the cleanliness of liquid aluminum, and that these results may be used as a guide in the molten metal processing of aluminum casting.

It should be mentioned that throughout the whole period of ultrasonic measurement, mechanical stirring must be maintained at all times since, for some inclusion types such as  $\text{Al}_2\text{O}_3$ , sedimentation occurs rapidly; this topic will be addressed later on in the thesis.

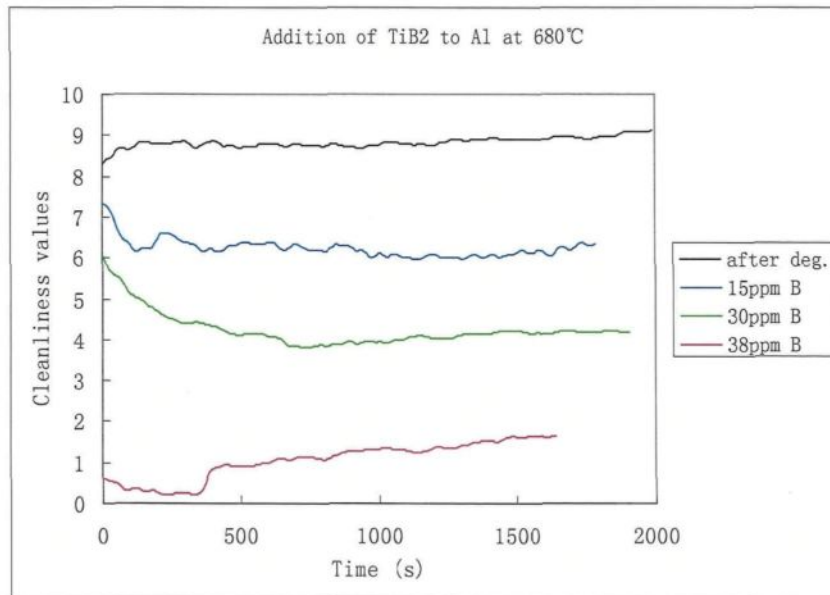


**Figure 28** Cleanliness values displayed by commercial pure aluminum melts containing TiB<sub>2</sub> inclusions as a function of time (melt temperature 680°C).

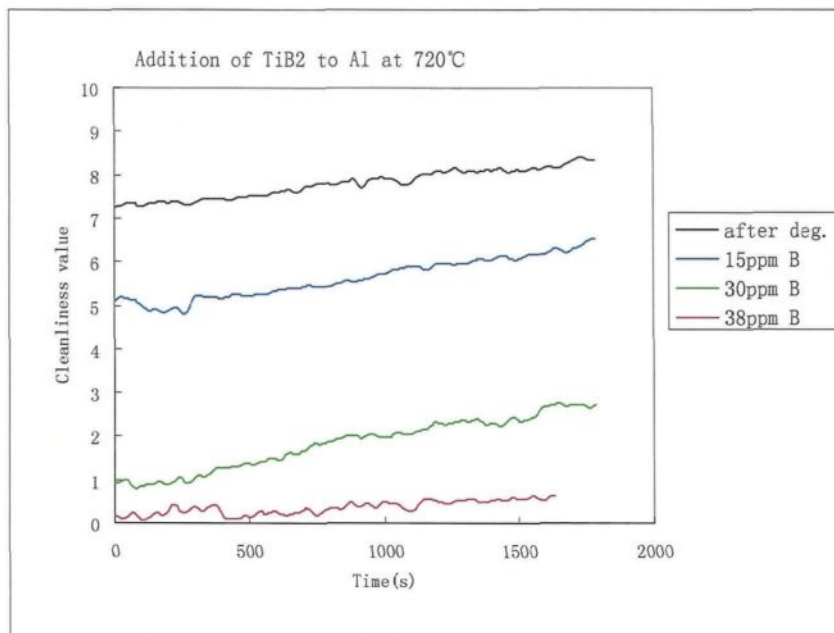


**Figure 29** Cleanliness values displayed by commercial pure aluminum melts containing TiB<sub>2</sub> inclusions as a function of time (melt temperature 720°C).

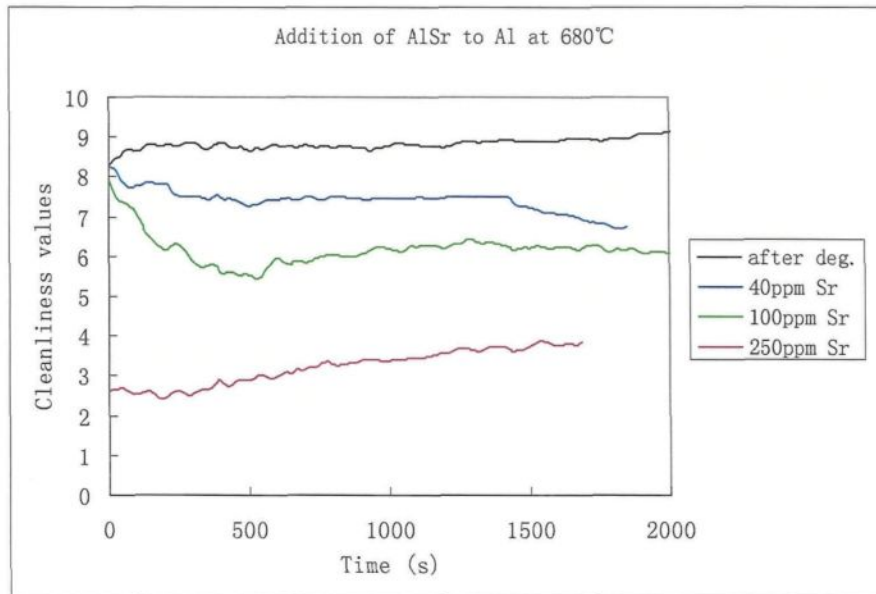


**Figure 30** Cleanliness values displayed by commercial pure aluminum melts containing AlSr inclusions as a function of time (melt temperature 680°C).

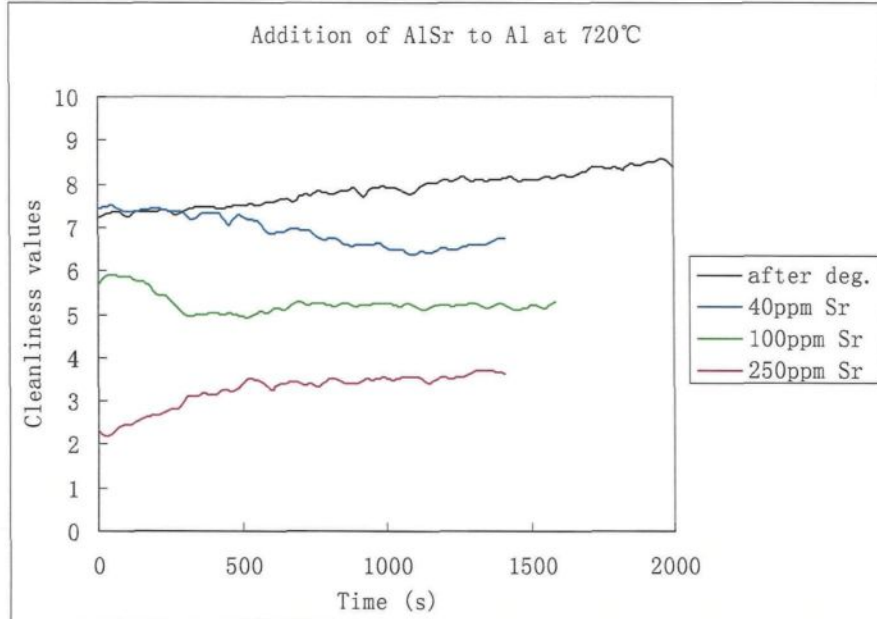


**Figure 31** Cleanliness values displayed by commercial pure aluminum melts containing AlSr inclusions as a function of time (melt temperature 720°C).

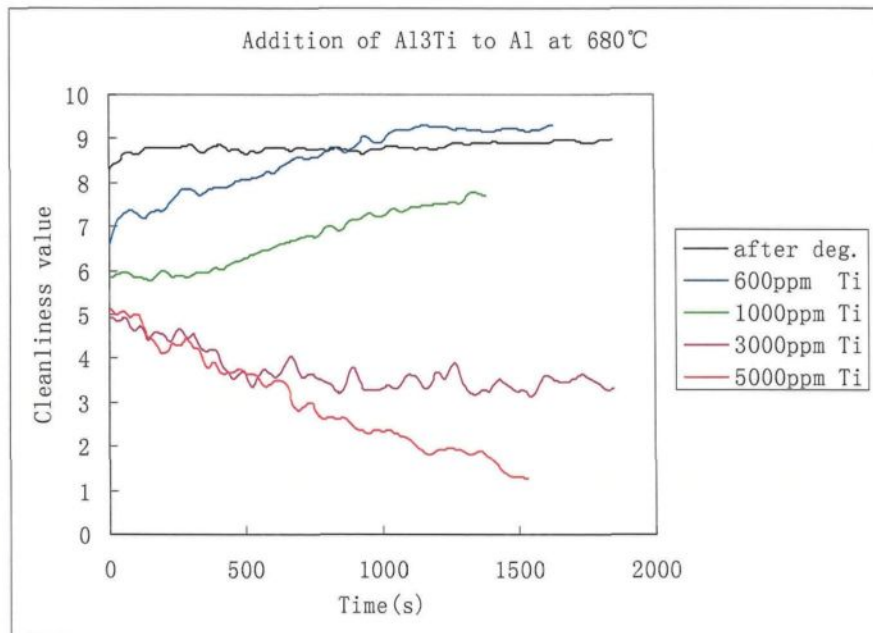


**Figure 32** Cleanliness values displayed by commercial pure aluminum melts containing Al<sub>3</sub>Ti inclusions as a function of time (melt temperature 680°C).

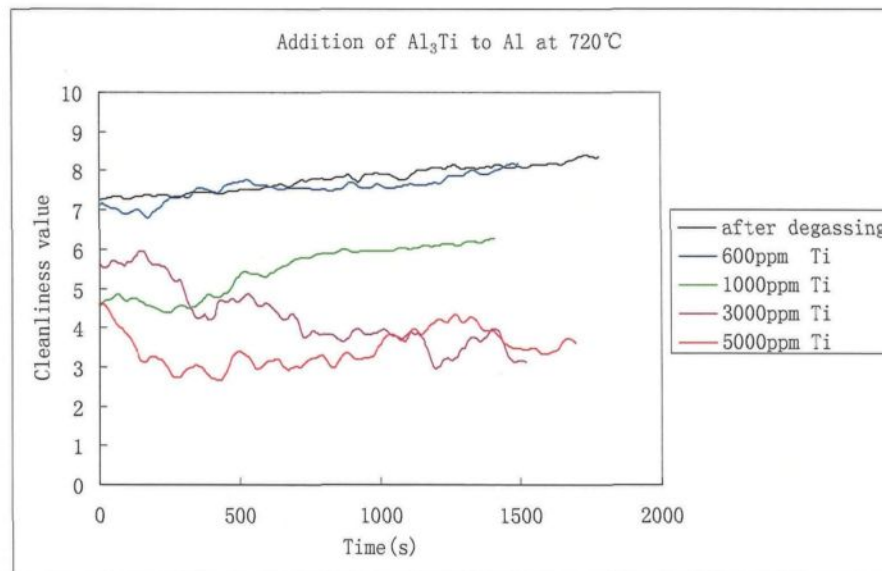


**Figure 33** Cleanliness values displayed by commercial pure aluminum melts containing Al<sub>3</sub>Ti inclusions as a function of time (melt temperature 720°C).

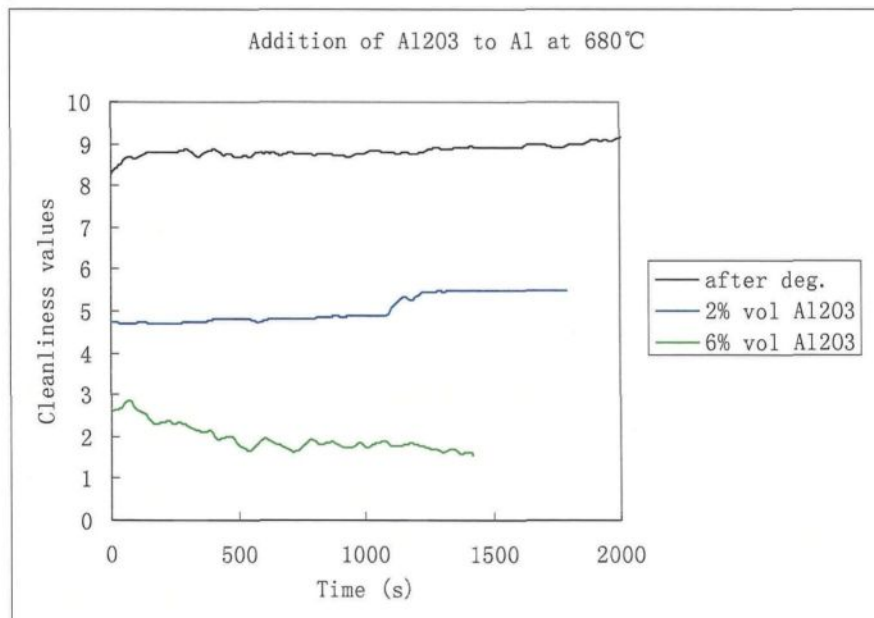


**Figure 34** Cleanliness values displayed by commercial pure aluminum melts containing  $\text{Al}_2\text{O}_3$  inclusions as a function of time (melt temperature  $680^\circ\text{C}$ ).

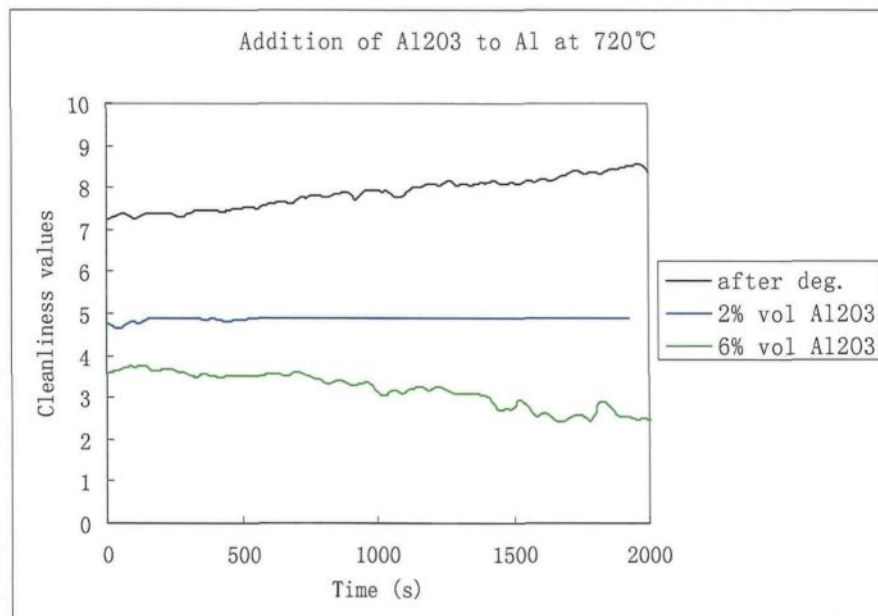


**Figure 35** Cleanliness values displayed by commercial pure aluminum melts containing  $\text{Al}_2\text{O}_3$  inclusions as a function of time (melt temperature  $720^\circ\text{C}$ ).

#### 4.2.2 Metallographic Examination

In order to obtain a qualitative understanding of the measurement results acquired for different inclusion additions to the 356 alloy and pure aluminum melts, samples obtained by metallography for microstructural analysis were prepared from samplings taken from the melt before and after the ultrasonic test for each melt condition. The solidified samples were then sectioned from the central part of the sample. The sections,  $25 \times 25$  mm in area and 5 mm thick, were mounted in bakelite and polished to a fine finish. The polished sections were examined using a Jeol JXA-8900L electron probe microanalyzer. Backscattered images showing the inclusion distribution over the entire sample surface together with details of the different inclusion types were obtained. X-ray images of the constituent elements were also obtained to verify the inclusion types.

Figure 36 shows backscattered images of  $\text{TiB}_2$  inclusions observed in the 356 alloy. It is clear that, the size of these  $\text{TiB}_2$  particles is exceedingly small and they appear in the form of clusters. In actual fact, when  $\text{TiB}_2$  inclusions are added to an aluminum melt, the fluidity of the melt decreases significantly making it difficult to measure their concentration in the melt. While other techniques can only detect this inclusion type when the concentration is less than 10 ppm, with the ultrasonic technique, this limit is raised to 90 ppm, as was observed from our study. This is of significant consideration given that grain refining is a melt treatment process normally applied to

aluminum alloys using Al-Ti-B master alloys leading to the inevitable presence of  $\text{TiB}_2$  inclusions in the melt.

Figure 37 shows backscattered images of  $\text{Al}_3\text{Ti}$  inclusions in 356 alloy after the first and last additions have been made. Compared to the  $\text{TiB}_2$  particles, the  $\text{Al}_3\text{Ti}$  particles are much larger. As was observed in another study carried out by an earlier research group, only small  $\text{Al}_3\text{Ti}$  inclusions are responsible for the grain-refining properties of the Al-10%Ti master alloy used to add these inclusions to the melt. The majority of  $\text{Al}_3\text{Ti}$  particles in the master alloy, however, appear in the form of plates of a considerable length. These particles, being much larger than the grain size of  $\alpha\text{-Al}$ , are not expected to act as nuclei for the solidifying  $\alpha\text{-Al}$  dendrites.

The efficiency of the Al-Ti master alloy would thus vary, depending on the relative amounts of these long plates and the relatively small particles of  $\text{Al}_3\text{Ti}$  present in the master alloy. This point would explain the inconsistent behavior reported for Al-Ti master alloys and why they are less effective as grain refiners than Al-Ti-B master alloys.

Figure 38 shows backscattered images of  $\text{Al}_2\text{O}_3$  inclusions in 356 alloy after the first and last additions. The  $\text{Al}_2\text{O}_3$  inclusions were added in the form of Al-20% $\text{Al}_2\text{O}_3$  composite alloy containing 20 vol. percent  $\text{Al}_2\text{O}_3$  particulate with an average particle size of about 40  $\mu\text{m}$ . As shown, the morphology of  $\text{Al}_2\text{O}_3$  inclusions corresponds exactly to the actual inclusion concentrations.

Figure 39 shows backscattered images of TiB<sub>2</sub> inclusions in pure aluminum after the first and last additions. Again, as in Figure 36, the TiB<sub>2</sub> inclusions are extremely small and clustered together. In this context, F. Gazanion *et al.*<sup>56</sup> have reported that the sedimentation behavior of TiB<sub>2</sub> particles remains the same over holding periods of up to 24 hours. The TiB<sub>2</sub> particles and clusters tend to agglomerate together to reduce the surface energy during sedimentation and further holding. To a certain extent, the microstructures observed in this study reflect these findings.

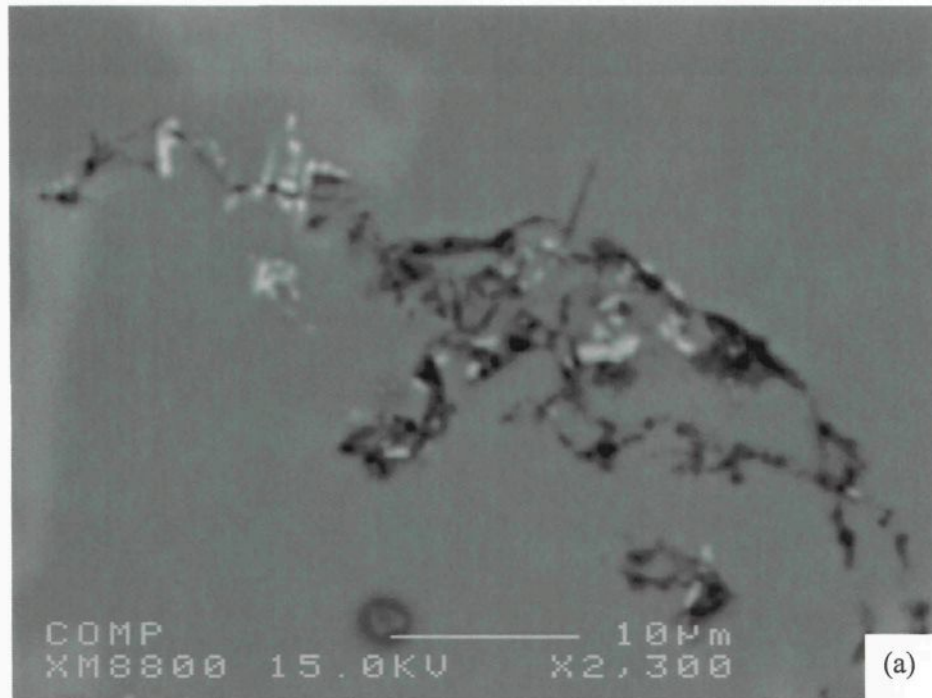
Figure 40 shows backscattered images of Al<sub>2</sub>O<sub>3</sub> inclusions in pure aluminum after the first and last addition, showing the inclusion distribution over the entire sample length. Sedimentation is observed in both cases, due to the higher density of the Al<sub>2</sub>O<sub>3</sub> particles, around 3.97 g/cm<sup>3</sup>, which is much greater than that of pure aluminum. These figures indicate that the sedimentation of Al<sub>2</sub>O<sub>3</sub> particles in pure aluminum takes place rapidly considering that the solidification of this small sample only takes a few seconds.

Due to the fact that all inclusions in aluminum melt have a tendency to sink or to float, mechanical stirring is an essential procedure which should be applied while carrying out inclusion measurement in order to evaluate the actual inclusion condition of the melt. For this reason, a rotary impeller was kept in the furnace at all times in order to stir the melt continuously while using the ultrasonic machine.

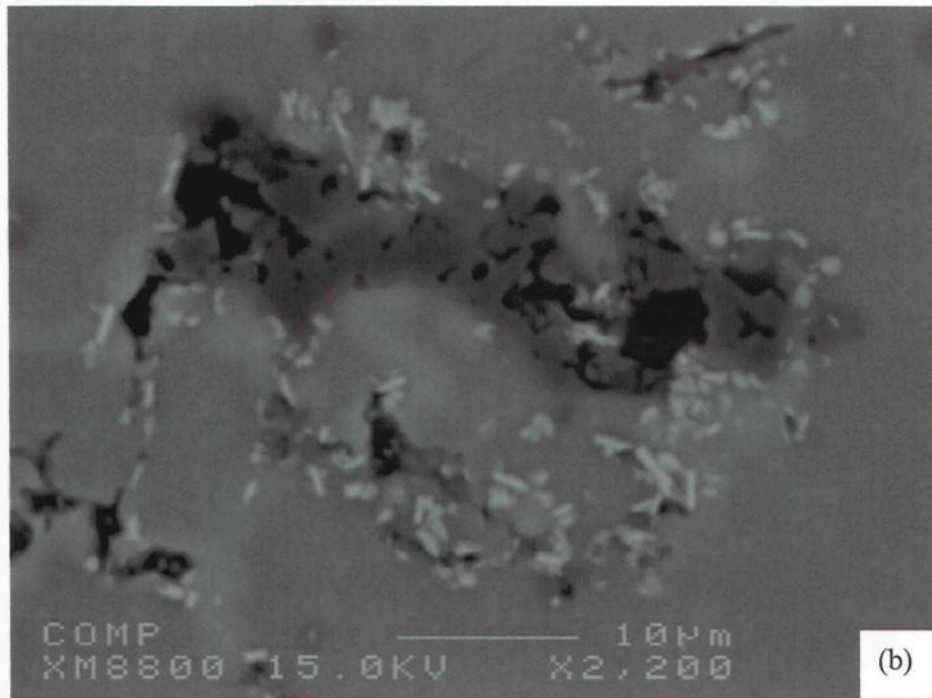
The difference in inclusion concentrations between the first and last additions of the different inclusion types may clearly be observed from Figures 36-40, thereby



indicating that the ultrasonic machine is sensitive to inclusion concentrations and is thus able to distinguish 'clean' and 'dirty' melts. As an on-line technique, this is what is being anticipated in the aluminum industry.



(a)



(b)

**Figure 36** Backscattered images of  $\text{TiB}_2$  inclusions in 356 alloy after the (a) first and (b) last additions.

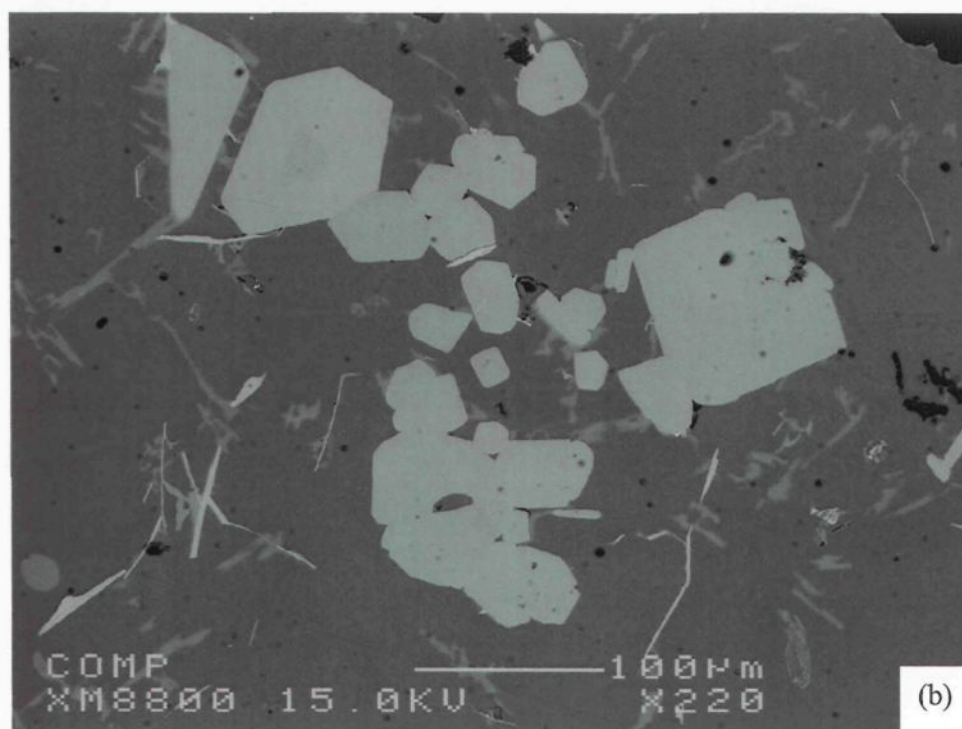
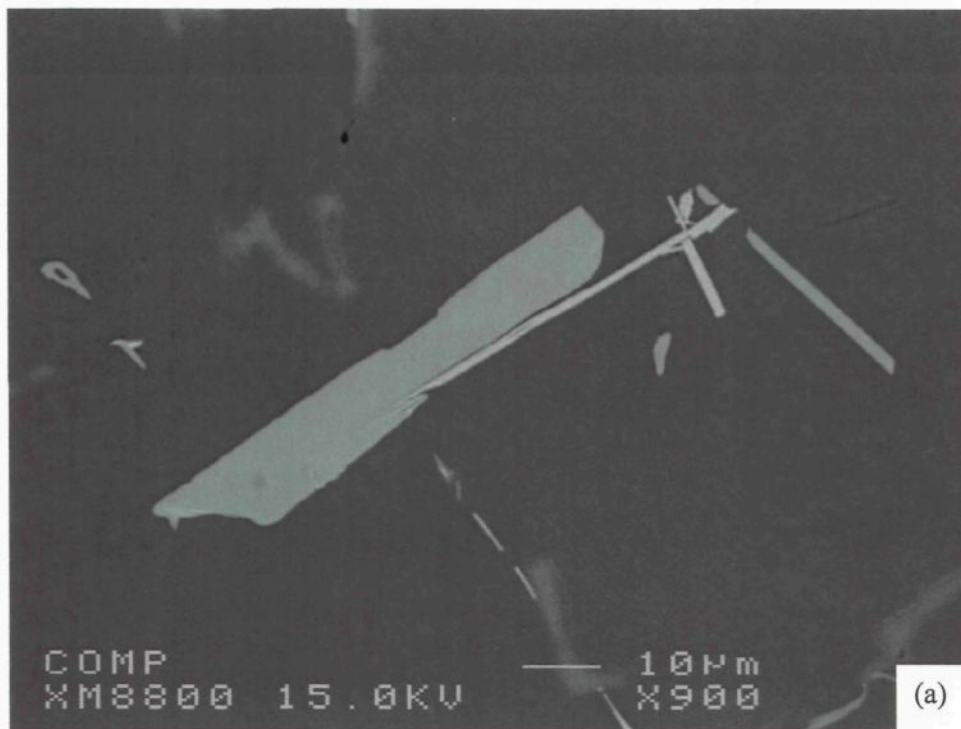


**Figure 37** Backscattered images of  $\text{Al}_3\text{Ti}$  in 356 alloy after the (a) first and (b) last additions.

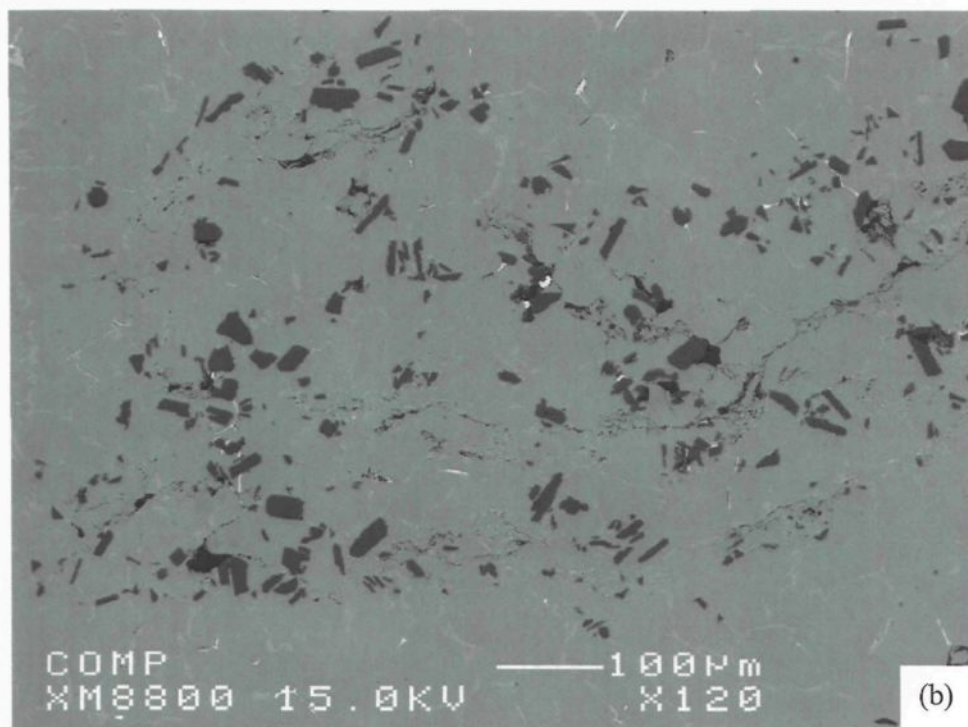
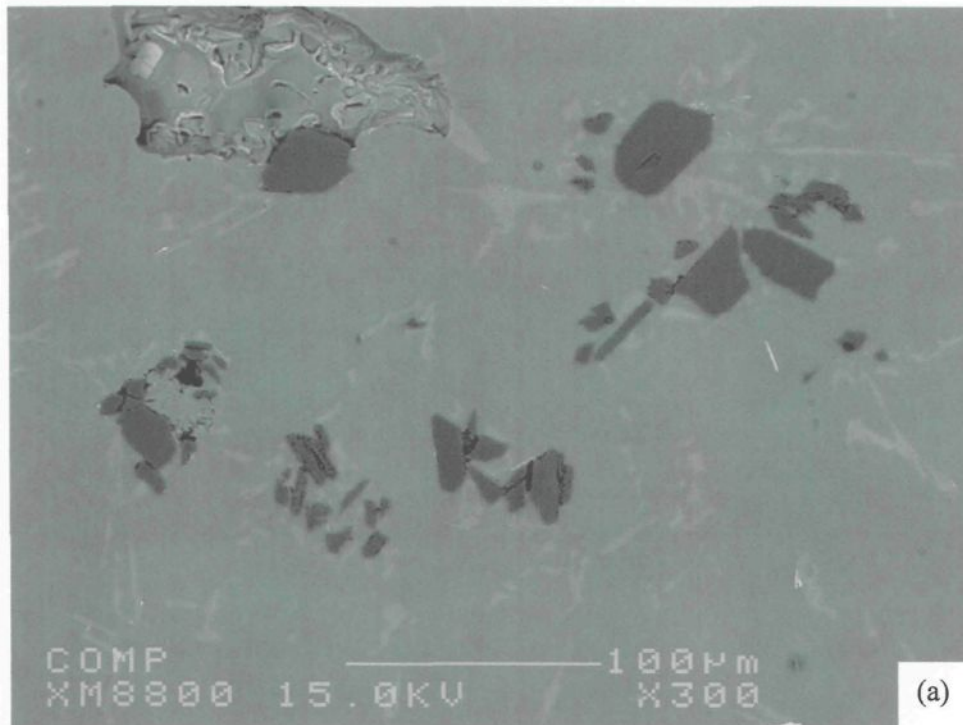


**Figure 38** Backscattered images of  $\text{Al}_2\text{O}_3$  in 356 alloy after the (a) first and (b) last additions.



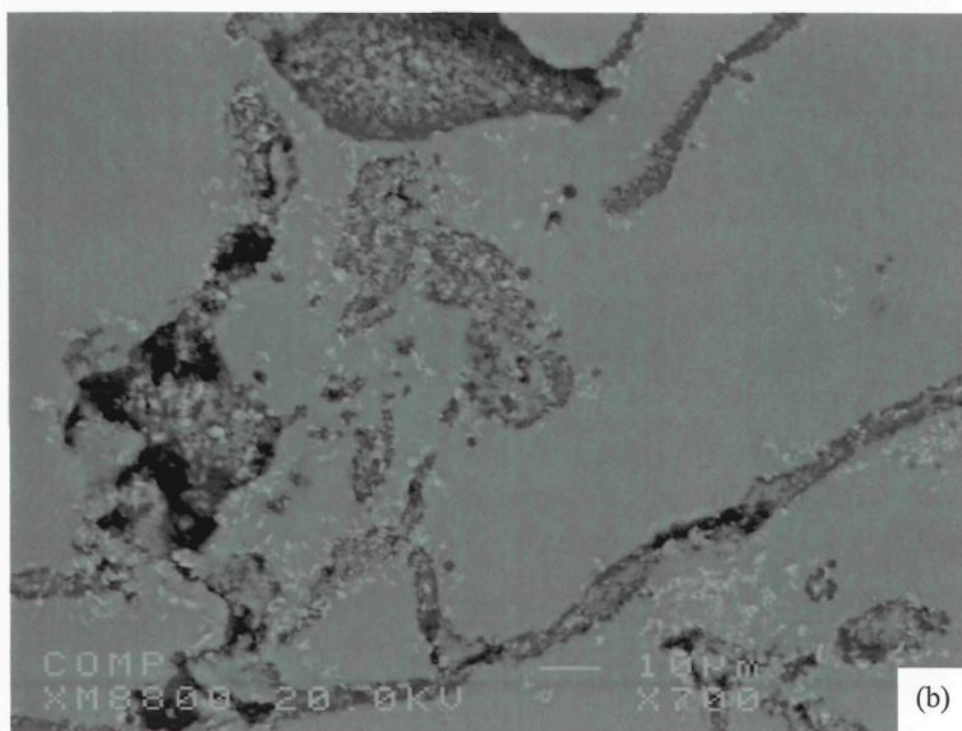
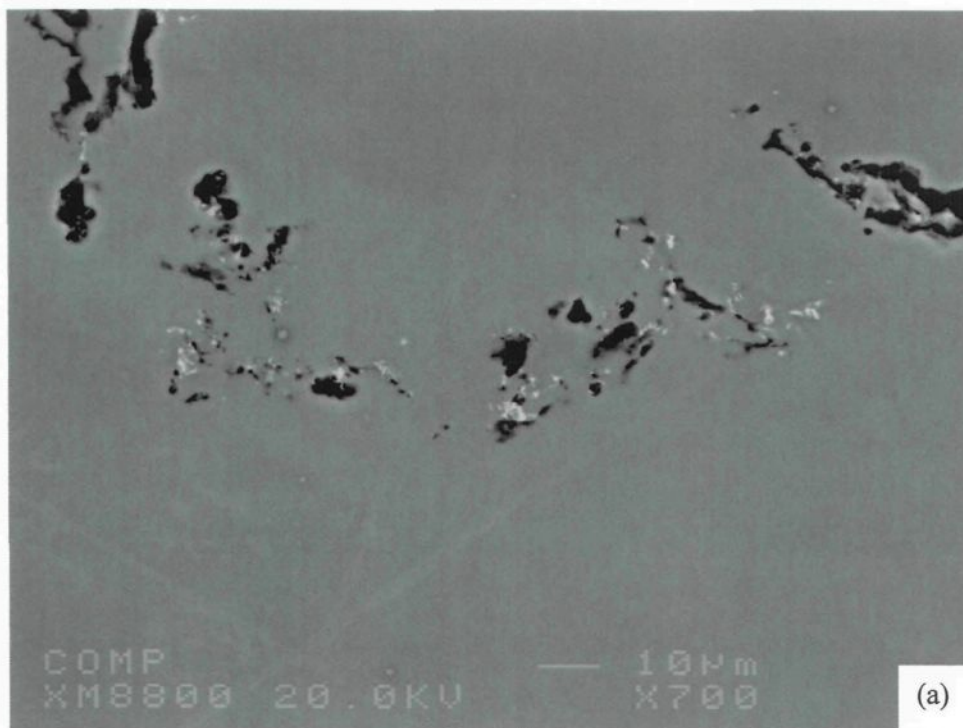


**Figure 39** Backscattered images of  $\text{TiB}_2$  inclusions in pure aluminum after the (a) first and (b) last additions.

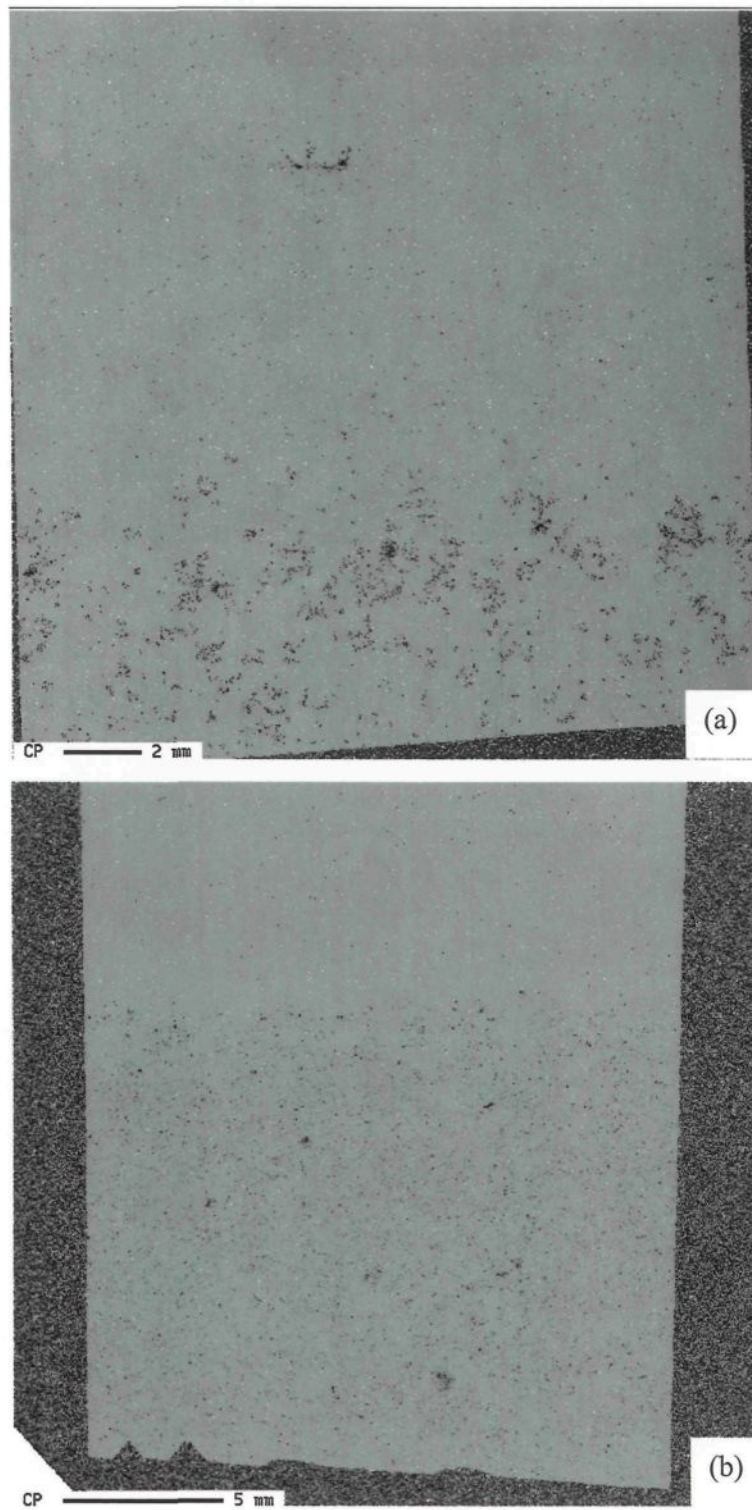


**Figure 40** Backscattered images showing the distribution of  $\text{Al}_2\text{O}_3$  inclusions in pure aluminum after the (a) first and (b) last additions. The images were taken over the entire sample surface in this case.

#### 4.2.3 Particle Size and Its Distribution

As mentioned earlier in the text, the ultrasonic machine provides plots of (i) the cleanliness value, (ii) particle size, and (iii) particle count for each particle size, as a function of testing time. The system measures particle size 100 times per second and records and displays how frequently particles are detected. The data is updated every twelve seconds. Over the first ten seconds, the system measures the particle size and then calculates the average size. Following this, a two-second period is required to measure the cleanliness value. A cleanliness value of around ten indicates a melt containing a relatively small number of inclusions, while a value of around zero indicates a melt containing a relatively large number of inclusions. The results obtained in this study confirmed that the cleanliness value recorded by the ultrasonic machine provides a good representation of the overall concentration of inclusions in the melt, including those too small to produce discrete reflections (i.e. inclusions  $< 20\mu\text{m}$ ).

Figures 41 and 43 show the particle size plots as a function of testing time obtained from the addition of  $\text{TiB}_2$  to pure aluminum, and  $\text{Al}_3\text{Ti}$  to 356 alloy, respectively, while Figure 42 and 44 show the corresponding charts of the particle size distribution in each case. It may appear that the particle size distribution charts provide details of the inclusions which were added to the melt. It must be kept in mind, however, that the ultrasonic machine would record any attenuation to the ultrasonic signal ahead of the probes in the melt. Thus, in addition to the inclusions added to the melt, the

machine would also record some attenuations caused by clusters of small particles, or oxide films entrained within the melt, or even other inclusions resulting from reactions between the added inclusions and the melt. Examples of these inclusions are shown in Figures 45 through 50. In order to confirm these inclusion types, corresponding X-ray images were also taken of their constituent elements, employing the electron probe microanalyzer. The strontium oxide inclusions shown in Figure 46 would more likely correspond to  $\text{Al}_2\text{SrO}_3$ , resulting from the reaction between aluminum, strontium and oxygen in the air.

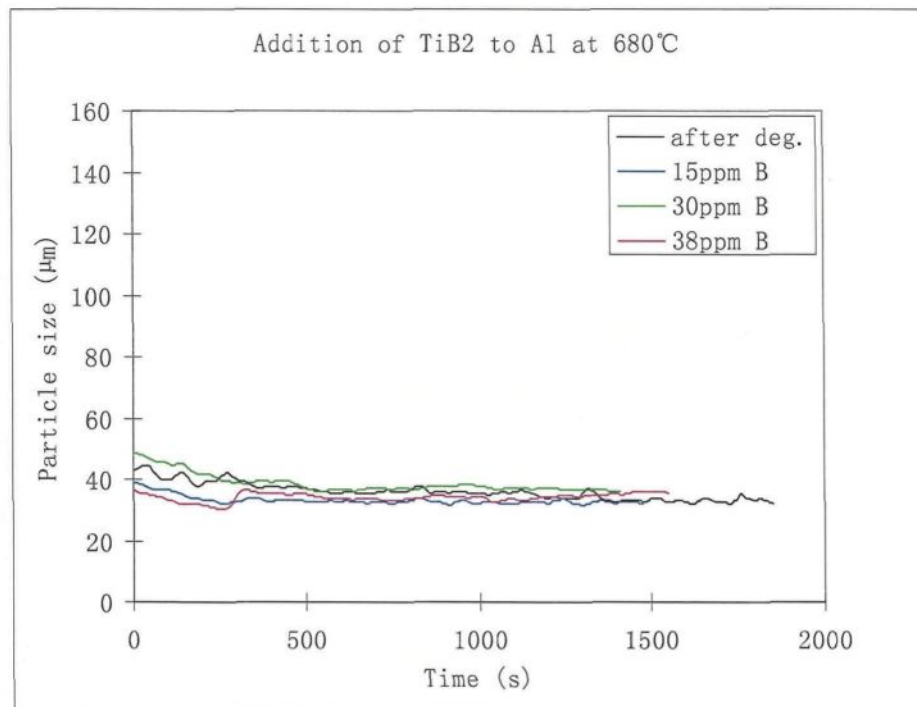


**Figure 41** Particle sizes of  $\text{TiB}_2$  inclusions in pure aluminum as a function of time (melt temperature  $680^\circ\text{C}$ ).



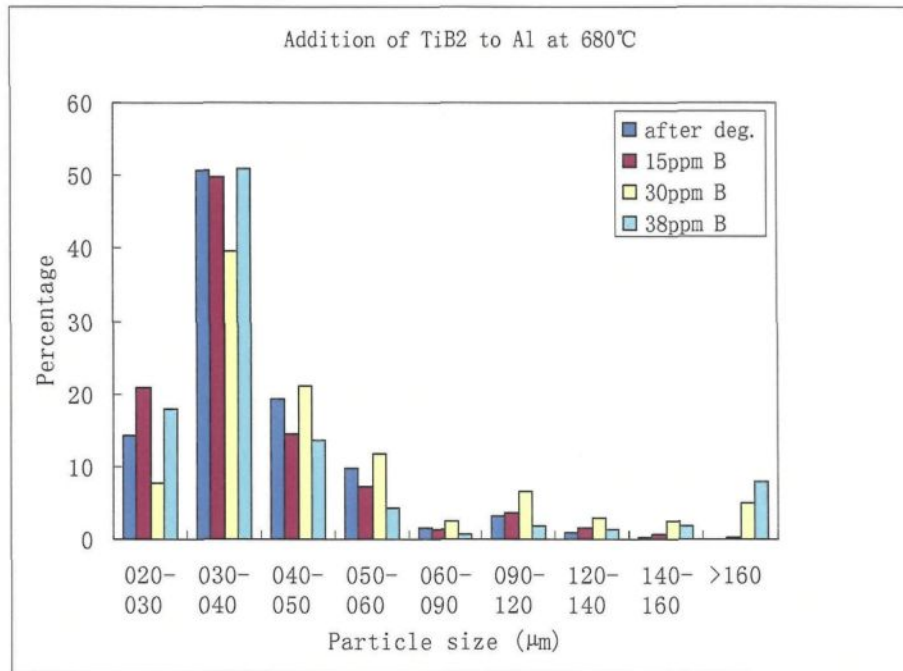


**Figure 42** Particle size distribution of TiB<sub>2</sub> inclusions in pure aluminum as a function of time (melt temperature 680°C).

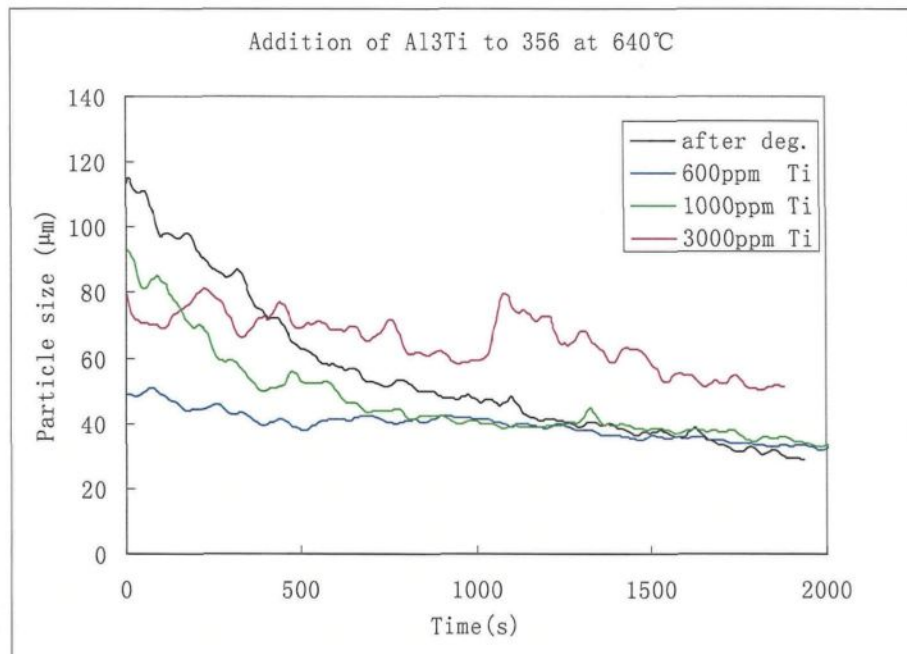


**Figure 43** Particle sizes of Al<sub>3</sub>Ti inclusions in 356 alloy as a function of time (melt temperature 640°C).

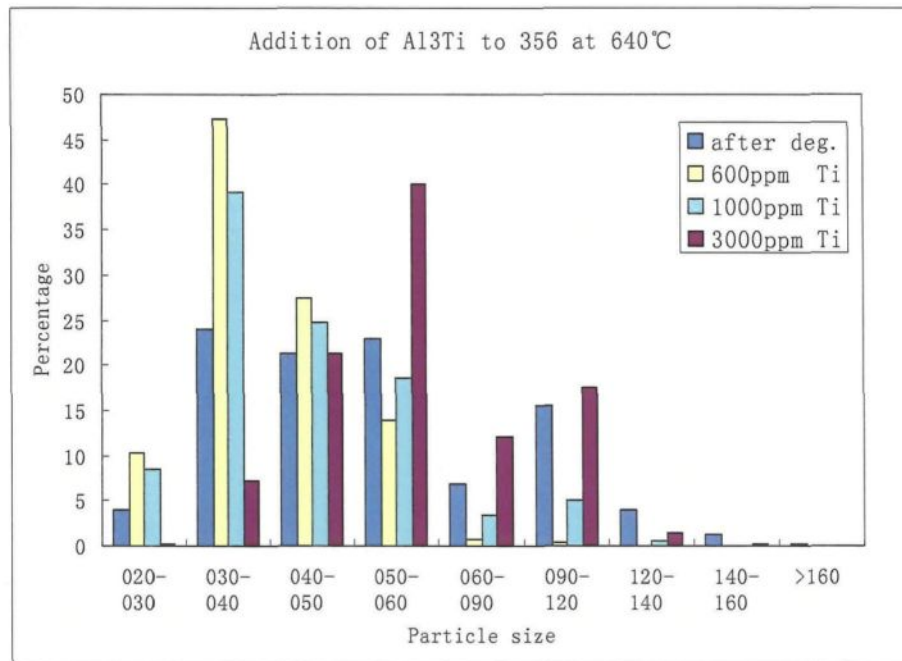


**Figure 44** Particle size distribution of Al<sub>3</sub>Ti inclusions in 356 alloy as a function of time (melt temperature 640°C).

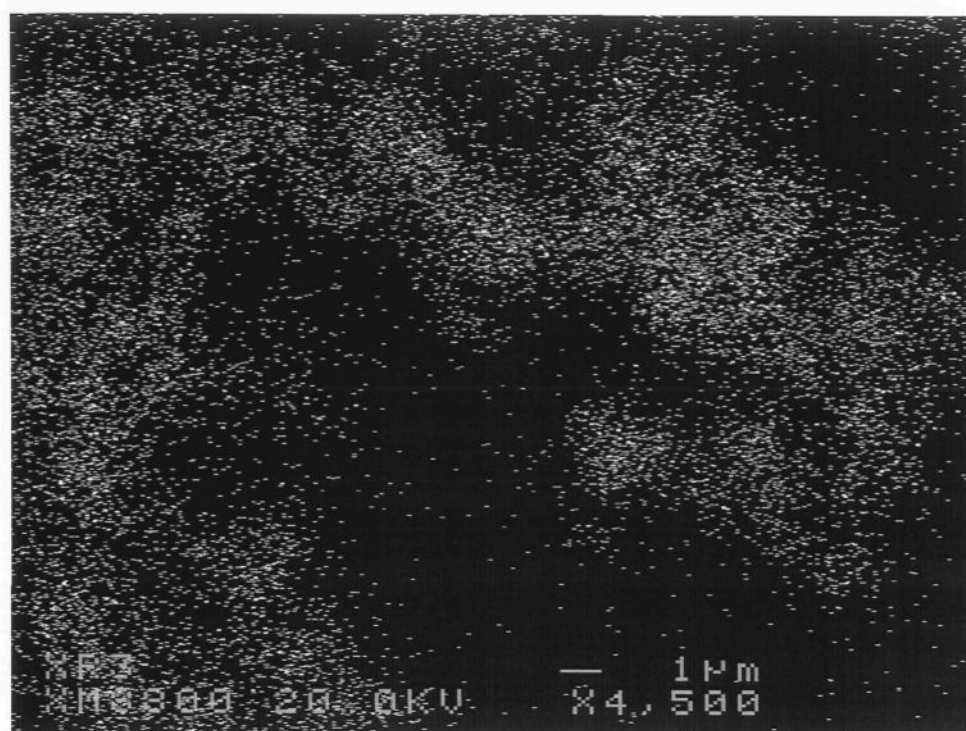
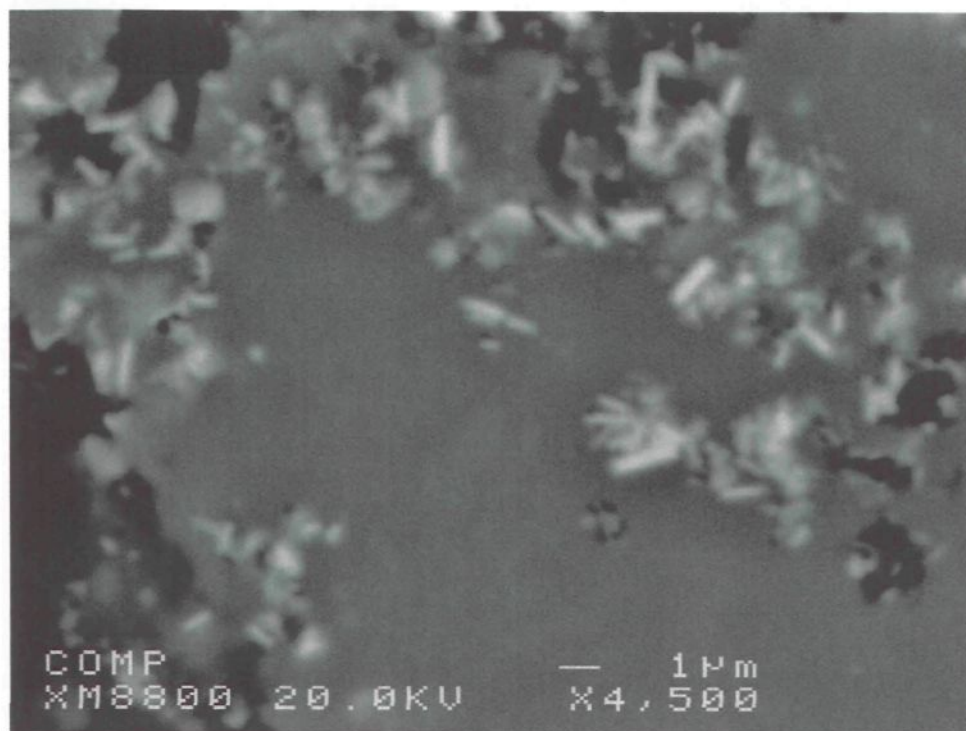


**Figure 45** Backscattered images of  $\text{TiB}_2$  inclusions in pure aluminum after the last addition and corresponding X-ray image of Ti.

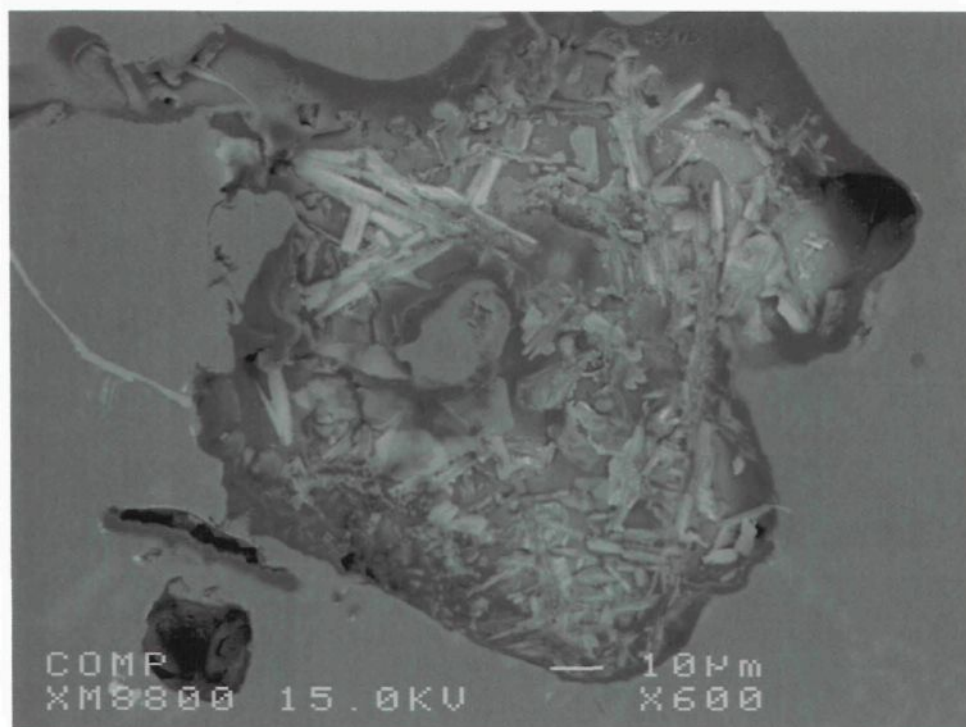
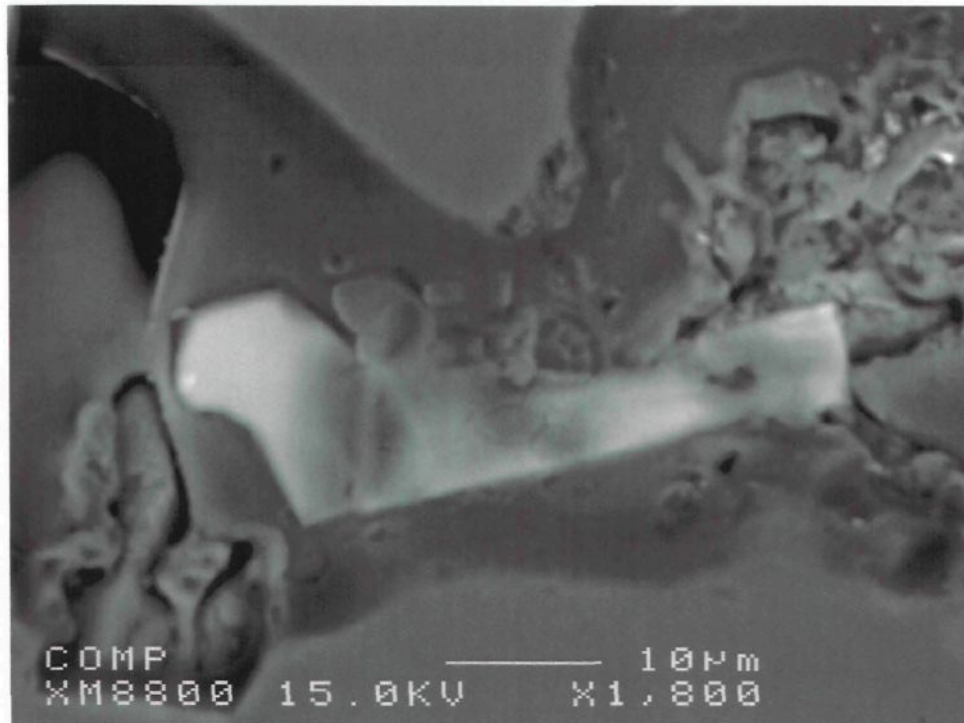


**Figure 46** Backscattered images of strontium oxide films in 356 alloy after the last addition of AlSr inclusion.



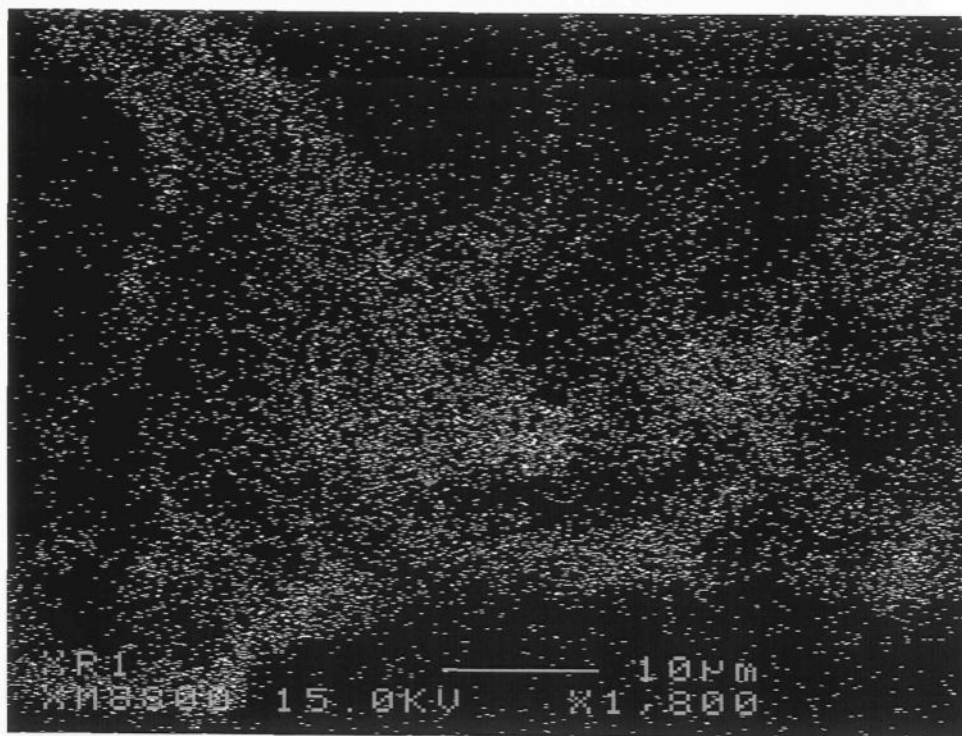


**Figure 47** X-ray images of oxygen corresponding to the strontium oxides shown in Figure 47.

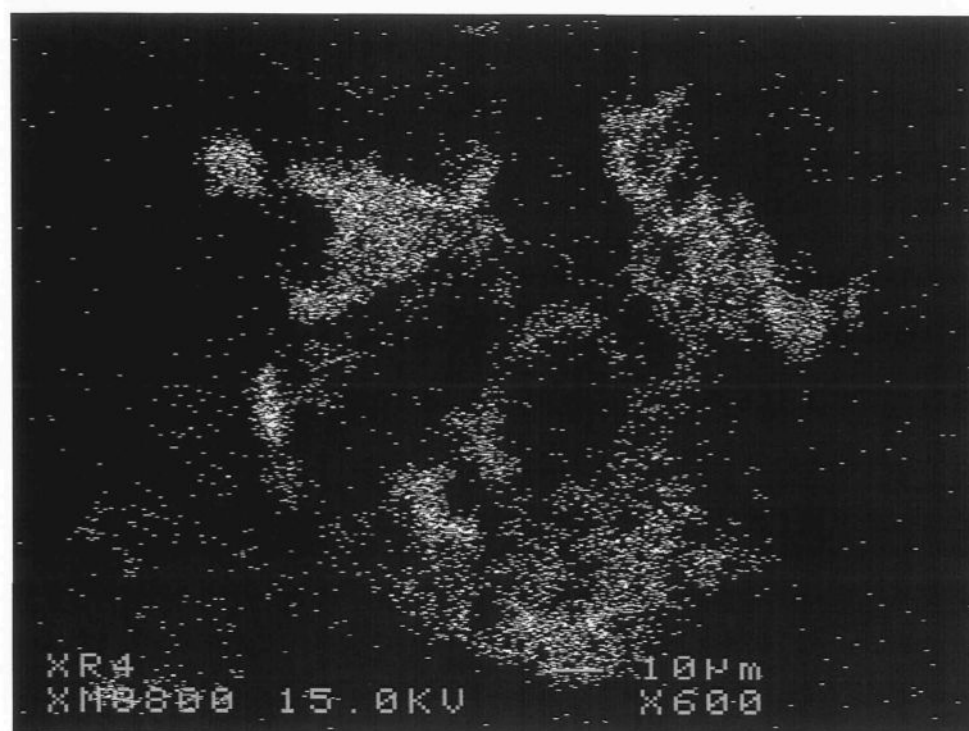
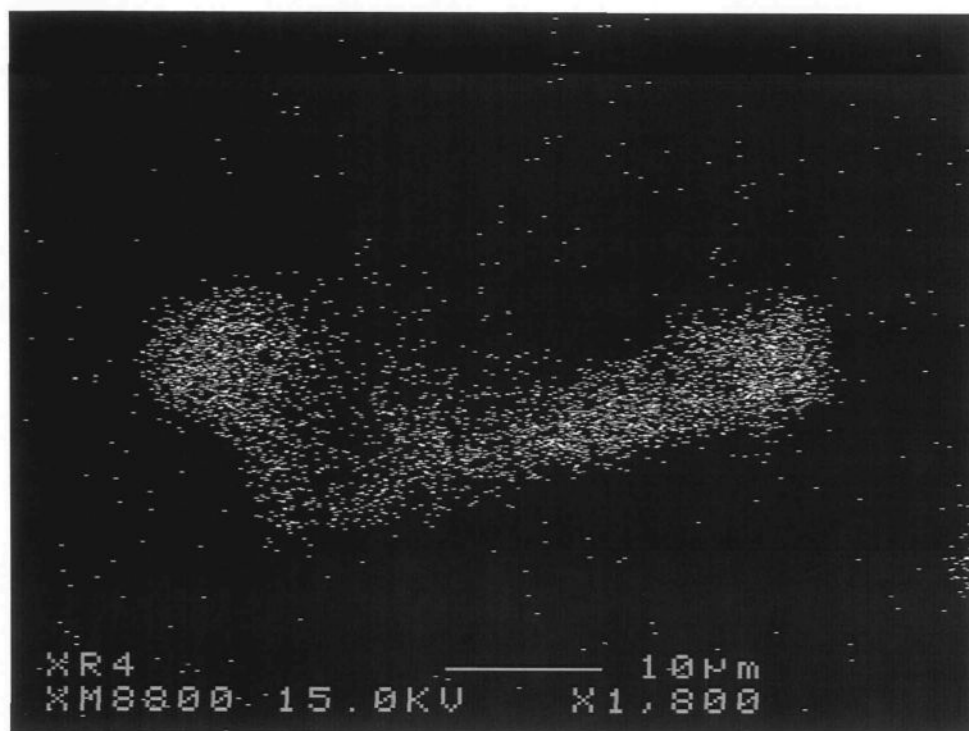


**Figure 48** X-ray images of strontium corresponding to the strontium oxides shown in Figure 47.

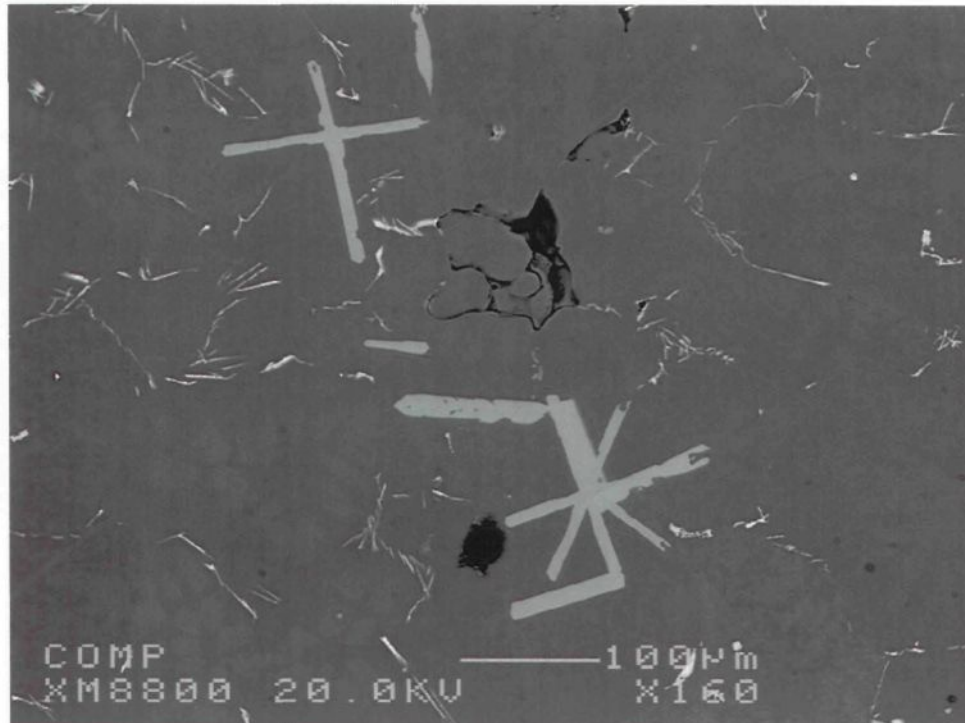


**Figure 49** Backscattered images of Al<sub>3</sub>Ti inclusions in pure aluminum after the last addition.



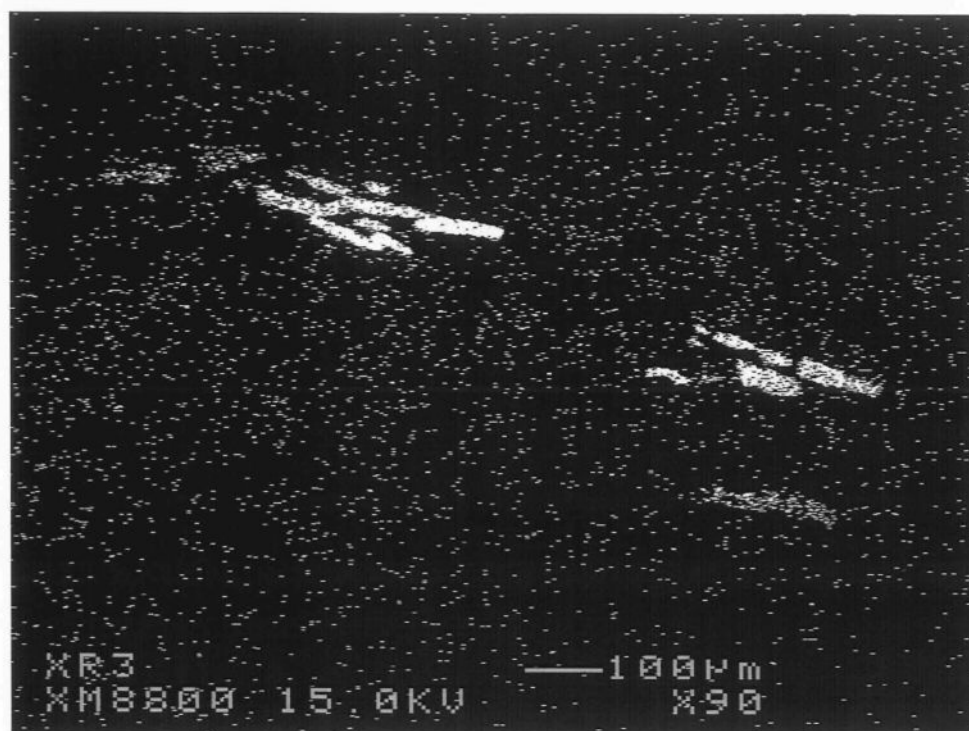
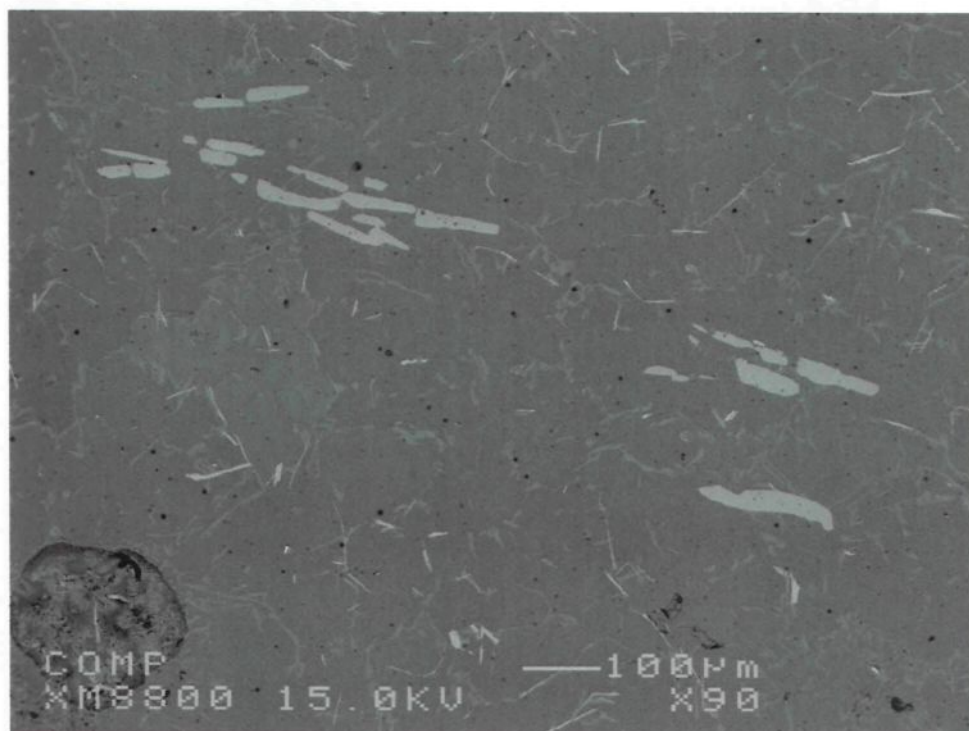


**Figure 50** Backscattered images of  $\text{Al}_3\text{Ti}$  inclusions in 356 alloy after the last addition and corresponding X-ray image of titanium.



#### 4.2.4 Melt Cleanliness Curves (Long Periods)

Compared with various other techniques based on the extraction of a metal sample followed by analysis in the laboratory, the ultrasonic technique can boast of numerous advantages. The most important one of these is that this technique provides real-time information which allows the operator to have enough time to make any necessary adjustments to the process. With proper mechanical stirring, this Metalvision MV20/20 ultrasonic machine can run unattendedly for long periods of time.

In order to prove this point, one measurement of  $\text{Al}_3\text{Ti}$  inclusions in commercial 356 alloy was conducted at  $680^\circ\text{C}$ . Figures 51-52 show the cleanliness values and the particle size of  $\text{Al}_3\text{Ti}$  inclusions as a function of time, respectively. Figure 53 shows the particle size distribution throughout the entire period of measurement.

Metallography samples were taken before the test, 0.5h and 5h after starting the test, and then were examined by microscope. Backscattered images of these samples are presented in Figures 54-56. Satisfactory consistency was observed between these pictures and the results obtained from the ultrasonic machine, thus validating the fact that it is able to provide on-line information and can run unattendedly for a long period of time with the appropriate mechanical stirring. It should be mentioned that, only in the case of  $\text{Al}_3\text{Ti}$ , the average platelet size measured from the backscattered photos shown in Figures 37, is about  $50\mu\text{m}$ , which is very close to the size measured by the ultrasonic machine as displayed in Figure 52.

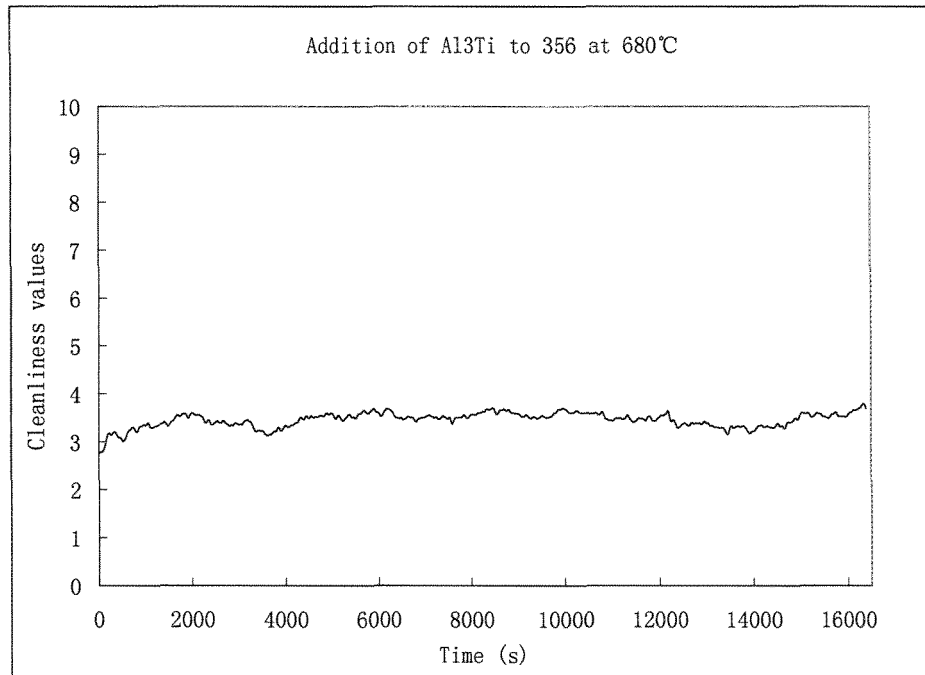


**Figure 51** Cleanliness values of Al<sub>3</sub>Ti inclusions in commercial 356 alloy as a function of time (melt temperature 680°C).

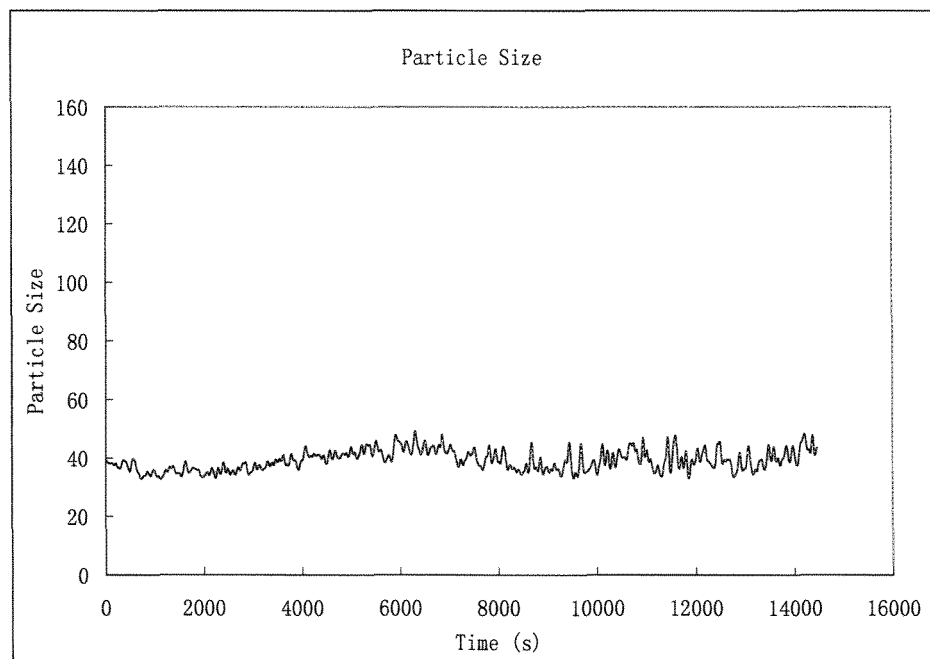


**Figure 52** Particle sizes of Al<sub>3</sub>Ti inclusions in commercial 356 alloy as a function of time (melt temperature 680°C).

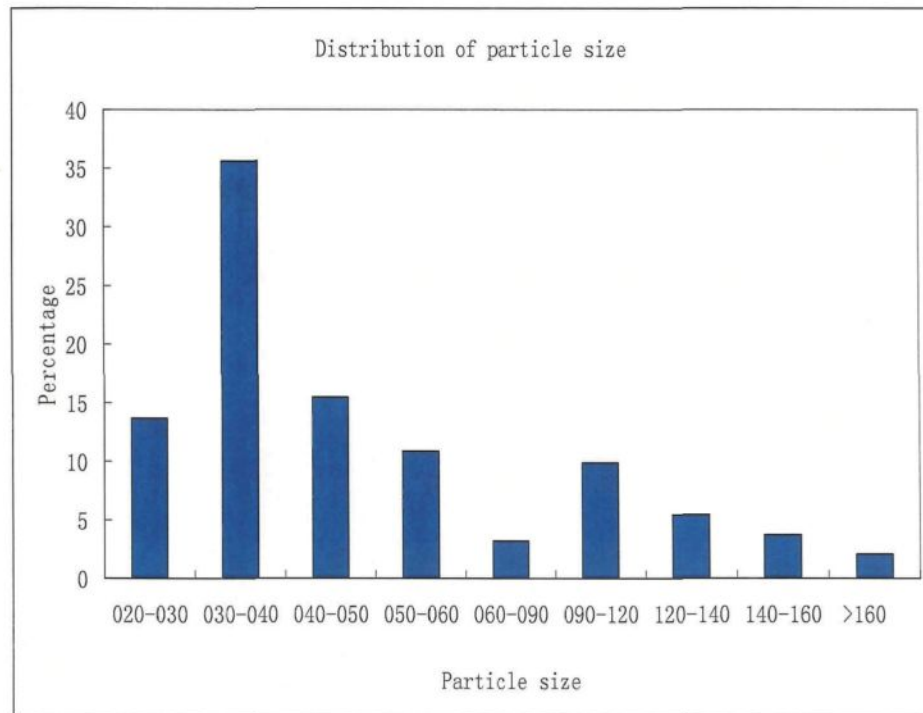


**Figure 53** Particle size distribution of  $\text{Al}_3\text{Ti}$  inclusions in commercial 356 alloy as a function of time (melt temperature  $680^\circ\text{C}$ ).

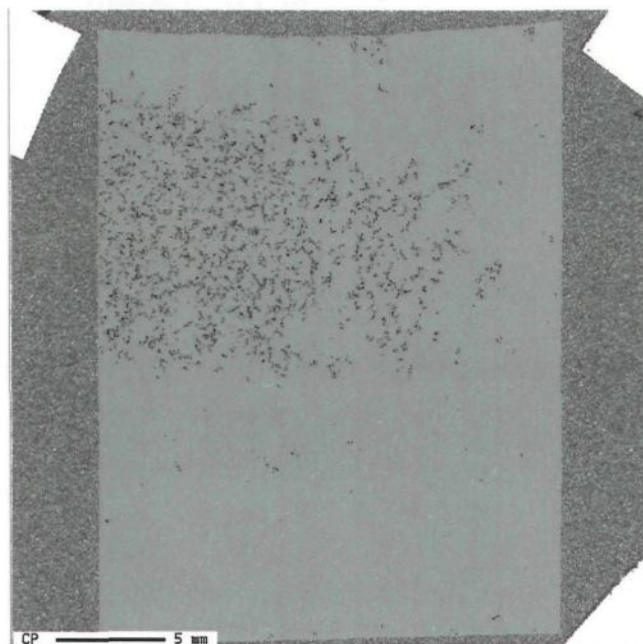


**Figure 54** The real condition of  $\text{Al}_3\text{Ti}$  inclusion in solidified sample obtained before the test (melt temperature  $680^\circ\text{C}$ ).

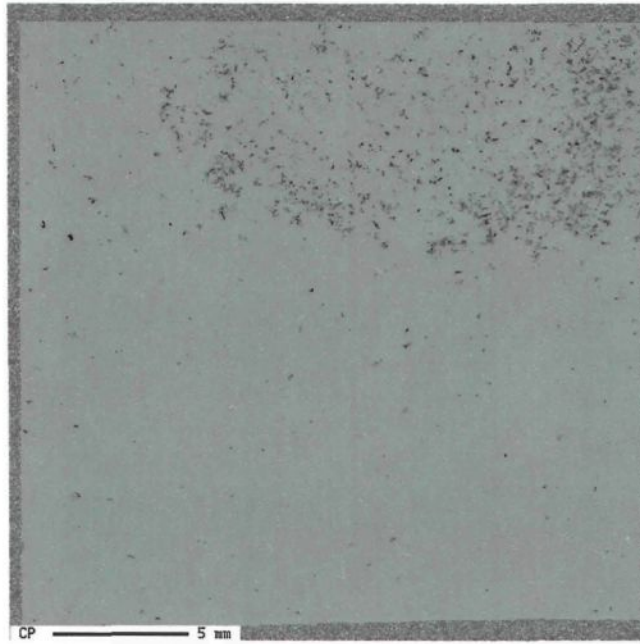


**Figure 55** The real condition of  $\text{Al}_3\text{Ti}$  inclusion in solidified sample obtained 0.5h after starting the test (melt temperature  $680^\circ\text{C}$ ).

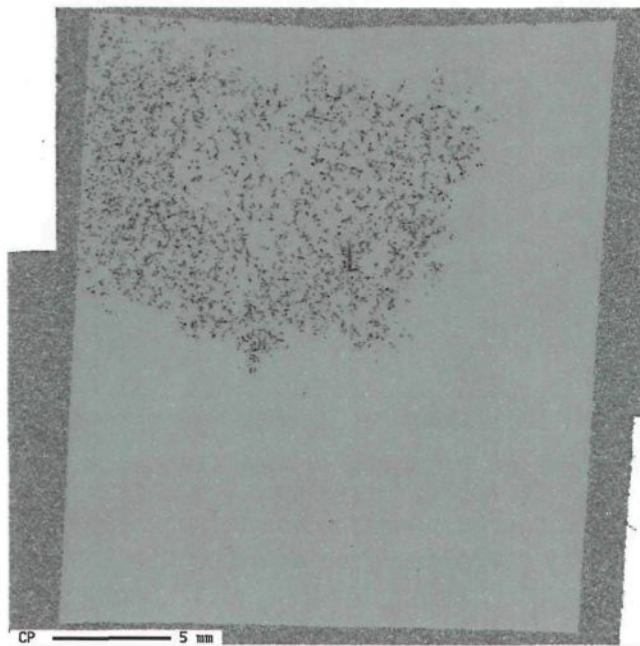


**Figure 56** The real condition of  $\text{Al}_3\text{Ti}$  inclusion in solidified sample obtained 5h after starting the test (melt temperature  $680^\circ\text{C}$ ).

**CHAPTER 5**

**CONCLUSIONS**

## **CHAPTER 5**

### **CONCLUSIONS**

The present study was undertaken to investigate the capacity of the ultrasonic technique for measuring different types of inclusions in commercial pure aluminum and 356 alloy at two different temperatures. The inclusion types studied include  $\text{TiB}_2$ ,  $\text{Al}_3\text{Ti}$ ,  $\text{AlSr}$  and  $\text{Al}_2\text{O}_3$ , representing inclusions typically found in aluminum castings. The former two types are of significance from the point of view of the grain refining treatments normally applied to aluminum alloys, using Al-Ti-B and Al-Ti type master alloys.

The data was obtained in the form of three charts which provide the cleanliness value, the average particle size and the distribution of particle size, respectively, as a function of time. Examination of the microstructure of solidified samples obtained from samplings of the melt was also carried out.

From an analysis of the ultrasonic data and their corresponding microstructures, the following may be concluded.

1. Melt cleanliness curves obtained from the ultrasonic machine are reliable and may be used as a guide for casting provided that the melt temperature and stirring conditions are properly adjusted.
2. Increasing the concentration of inclusions reduces the cleanliness level of the melt and is reflected by a corresponding decrease in the melt cleanliness curve of the ultrasonic machine, thus indicating its response to the change in inclusion level.
3. Superheating the melt may lead to a certain amount of sedimentation of inclusions causing an artificial increase in the melt cleanliness level as read by the machine. Thus, it is important to ensure that the melt is mechanically stirred while taking the measurements.
4. There is a significant difference between particle sizes measured by the ultrasonic machine and those obtained from polished surfaces of samples taken from the corresponding melt in the case of fine inclusions. The difference, however, is less significant when the inclusions exist in the form of short platelets.
5. The ultrasonic machine may be used as an on-line machine for determining the melt cleanliness for a long period of time (5 h in the present study), with proper mechanical stirring of the melt to minimize sedimentation of the inclusions.
6. In taking measurements of melt cleanliness, an initial period of 2~3 minutes should be disregarded, considering that the ultrasonic machine takes this amount of time to become stabilized with respect to the melt conditions.

7. Increasing the melt superheat accelerates the decomposition of the master alloy, hence increasing the number of inclusion particles in the melt and reducing the melt cleanliness value. It also accelerates the sedimentation kinetics, so that proper mechanical stirring is necessary to ensure that the machine reads the correct melt cleanliness value.



## **RECOMMENDATIONS**

Physical samplings for characterization of the microstructures should be taken on a regular basis to verify actual particle sizes compared to those read by the ultrasonic machine. It is of paramount importance that mechanical stirring of the melt be carried out so as to avoid the effects of sedimentation and thus maintain the same level of inclusions in the melt throughout the testing period of the machine.

## REFERENCES

## REFERENCES

- 1 D. Apelian and S. Shivkumar, "Molten Metal Filtration - Past, Present and Future Trends", Aluminum Casting Research Laboratory, Department of Materials Engineering, Drexel University, pp. 14-1 to 14-36.
- 2 S. Shivkumar, D. Apelian and H. Brucher, "Melt Cleanliness in Die Cast Aluminum Alloys", *Transactions of the 16<sup>th</sup> International Die Casting Congress and Exposition*, Detroit, Michigan, USA, 30 September-3 October, 1991, pp. 143-152.
- 3 Y. Ono, J. F. Moisan, Y. Zhang, C. K. Jen and C. Y. Su, "Ultrasonic Inclusion Detection and Cleanliness Measurement in Molten Aluminum and Magnesium", *Modeling, Control and Optimization in Ferrous and Nonferrous Industry*, 2003, pp. 193-207.
- 4 Yuu Ono, Jean-François Moisan and Cheng-Kuei Jen, "Ultrasonic Techniques for Imaging and Measurements in Molten Aluminum", *IEEE Transactions on Ultrasonics, Ferroelectrics and Frequency Control*, Vol. 50, No. 12, December 2003, pp.1711-1721.
- 5 Y. Ono, J.-F. Moisan, C.-K. Jen and D.R. França, "Development of Ultrasonic Techniques with Buffer Rod in Molten Aluminum", *IEEE Ultrasonics Symposium*, 2002, pp.805-810.
- 6 J.R. Davis, ASM Special Handbook: Aluminum and Aluminum Alloys, *ASM International*, The Materials Information Society, Materials Park, OH, 1994, pp. 1-30.
- 7 I. J. Polmear, "Metallurgy of the Light Metals", *Light Metals*, Monash University, Australia, pp. 27-65.
- 8 Jamshid Shirandasht, "Evaluation of the LiMCA II Technique for Inclusion Measurements in Pure Aluminum and Al-6%Si Cast Alloys: Role of Melt Temperature", Mémoire de thèse, Université du Québec à Chicoutimi, 2005.

9. J.E. Gruzleski and B.M. Closset, *The Treatment of Liquid Aluminum-Silicon Alloys*, American Foundry-men's Society, Inc., Des Plaines, IL, 1990, pp. 1.
10. C.J. Siemensen and G. Strand, *Z. Anal. Chem.*, Vol. 308, (1981), pp. 11-16.
11. D.P. Kanicki and W. M. Rasmussen, "Cleaning Up Your Metal", *Modern Casting*, February 1990, pp. 55-58.
12. M.J. Lessiter and W.M. Rasmussen, "To Pour or Not to Pour: The Dilemma of Assessing Your Aluminum Melt's Cleanliness", *Modern Casting*, March 1996, pp. 45-48.
13. H. Cong and X. Bian, "The Relationship of the Inclusions and Hydrogen Content in the Molten Aluminum Alloys", *Materials Science Forum*, Vol. 331-337, 2000, pp. 325-330.
14. S. Viswanathan, A.J. Duncan, Q. Han, W.D. Porter, and B.V. Rimmers, "Modeling of Solidification and Porosity in Aluminum Alloy Castings", *AFS Transactions*, Vol. 106, 1998, pp. 411-417.
15. C. J. Simensen and G. Berg, "A Survey of Inclusions in Aluminum", *Aluminum*, Vol. 56, 1980, pp. 335-340.
16. S. Makarov, D. Apelian and R. Ludwig, "Inclusion Removal and Detection in Molten Aluminum: Mechanical, Electromagnetic, and Acoustic Techniques", *AFS Transactions*, Vol. 107, 1999, pp. 725-735.
17. T. A. Zelinak, "Effective Degassing of Aluminum Alloys For Foundry Applications", Internal Report.
18. F. Frisvold, T. A. Engh, S. T. Johansen and T. Pedersen, "Removal of Inclusions – A Survey and Comparison of Principles", *Light Metals*, 1992, pp. 1125-1132.
19. C. Sztur, F. Balestreri, J.L. Meyer, B. Hannart, "Settling of Inclusions in Holding Furnaces: Modeling and Experimental Results", *Light Metals*, 1990, pp. 709-716.
20. S.L. Soo, "Fluid Dynamics of Multiphase Systems", Blaisdell Publishing Co, Massachusetts, 1967.

21. S. T. Johansen and S. Taniguchi, "Prediction of Agglomeration and Break Up of Inclusions during Metal Refining", *Light Metals*, 1998, pp. 855-861.
22. A. M. Samuel, "The Removal of Solid Inclusions from Aluminum Alloys Melts by Flotation – A Mathematical Model", 5<sup>th</sup> International AFS Conference Molten Aluminum Processing, Nov. 8-10, 1998, pp. 61-76.
23. Luiz C. B. Martins and Geoffrey K. Sigworth, "Inclusion Removal by Flotation and Stirring", 2<sup>nd</sup> International Conference on Molten Aluminum Processing, Nov. 6-7, 1989, American Foundry Society, pp. 16-1 to 16-28.
24. D.V. Neff and B.P. Cochran, "Chlorination Technology in Aluminum Recycling", *Light Metals*, 1993, pp. 1053-1060.
25. Y. Genma, Y. Tsunekawa, M. Okumiya, and N. Mohri, "Incorporation of Alumina Particles with Different Shapes and Sizes into Molten Aluminum Alloy by Melt Stirring with Ultrasonic Vibration", *Materials Transactions, JIM*, Vol. 38, 1997, pp. 232-239.
26. D. E. Groteke, "The Reduction of Inclusions in Aluminum by Filtration", *Modern Casting*, April 1983, pp. 25-27.
27. Dawid D. Smith, Leonard S. Aubrey and W. Chris Miller, "LiMCA II Evaluation of the Performance Characteristics of Single Element and Staged Ceramic Foam Filtration", *Light Metals*, 1998, pp. 893-915.
28. Michael M. Niedzinski, Edward M. Williams, Dawid D. Smith and Leonard S. Aubrey, "Staged Filtration Evaluation at An Aircraft Plate and Sheet Manufacturer", *Light Metals*, 1999, pp. 1019-1030.
29. James E. Dore, "A Practical Guide on How to Optimize Ceramic Foam Filter Performance", *Light Metals*, 1990, pp. 791-796.
30. M. Garnier, "Actual and Future Developments of Electromagnetic Processing of Materials", *Proceedings of The Julian Szekely Memorial Symposium on Material Processing*, 1997, pp. 313-322.
31. P. Sandford, "Getting the Junk out of the Molten Aluminum", *AFS Transactions*, Vol.

105, 1995, pp. 95-153.

32. S. King III and J. Reynolds, "Flux Injection/Rotary Degassing Process Provides Cleaner Aluminum", *Modern Casting*, April 1995, pp. 37-40.

33. L. Liu, F. H. Samuel, "Assessment of Melt Cleanliness in A356.2 Aluminum Casting Alloy Using The Porous Disc Filtration Apparatus Technique", *Journal of Materials Science*, vol. 32, 1997, pp. 5901-5918.

34. D. Doutre, B. Gariépy, J. P. Martin, G. Dubé, "Aluminum Cleanliness Monitoring: Methods and Application in Process Development and Quality Control", *Light Metals*, 1985, pp. 1179-1195.

35. S. A. Levy, "Applications of the Union Carbide Particulate Tester", *Light Metals 1981*, TMS, Warrendale, PA, 1981, pp. 723-733.

36. A. M. Samuel and F. H. Samuel, "Magnesium Metal Cleanliness: An Analysis of Inclusions, Their Measurement Techniques, and Removal Methods in Relation to Product Quality of Magnesium Alloys", *A Literature Review*, August 2000, pp. 24-25.

37. P. Bakke, J. A. Laurin, A. Provost and D. O. Karlsen, "Consistency of Inclusions in Pure Magnesium", *Light Metals 1997*, R. Huglen ( Ed.), The Minerals, Metals & Materials Society, Warrendale, PA, 1997, pp. 1019-1026.

38. F. H. Samuel, P. Ouellet and A. Simard, "Assessment of melt cleanliness and analysis of inclusions in Al-Si alloys using the Prefil pressure filtration technique", *Int. Journal of Cast Metals Research*, Vol. 12, 1999, pp. 17-33.

39. P. Bakke and D. O. Karlsen, "Inclusion Assessment in Magnesium and Magnesium Base Alloys", *Characteristics and Applications of Magnesium in Automotive Design*, SAE Technical Paper NO.970330, 1997, pp.61-73.

40. Nasser Habibi, "Évaluation des inclusions et des oxydes dans les alliages Al-Si en utilisant le technique prefil", Mémoire de thèse, Université du Québec à Chicoutimi, 2002, pp. 62-65.

41. Alain A. Simard, François Dallaire, Jasmin Proulx and Paul Rochette, "Cleanliness

- Measurement Benchmarks of Aluminum Alloys Obtained Directly At-Line Using the Prefil Footprinter Instrument”, *Light Metals*, 2000, pp. 739-744.
42. J.L. Roberge, M. Richard, “Qualiflash Apparatus for Testing the Inclusion Quality of Aluminum Alloy Baths”, Centre Technique des Industries de la Fonderie, 44 av. De la Division Leclerc 92312 SEVRES cedex FRANCE.
43. J.L. Roberge, M. Richard, “Instantaneous Evaluation of Inclusion Quantity of Liquid Aluminum Alloys”, *Materials Science Forum*, Vols. 217-222, 1996, pp. 135-140.
44. F. H. Samuel, P. Ouellet, and A. Simard, “Measurement of Oxide Films in Aluminum (6-17) wt% Si Foundry Alloys Using the Qualiflash Filtration Technique”, *Int. J. Cast Metals Res.*, Vol. 12, 1999, pp. 49-55.
45. C. N. Evans, W. Willmert, “Qualiflash as it Relates to Filtration and Degassing for Foundry and Extrusion Alloys”, 5<sup>th</sup> International AFS Conference on Molten Aluminum Processing, Nov. 8-10, 1998, pp. 349-364.
46. W. Rasmussen and C. Edward Eckert, “RPT Gauges Aluminum Porosity”, *Modern casting*, March 1992, pp. 29-31.
47. A. M. Samuel and F. H. Samuel, “The Reduced Pressure Test as a Measuring Tool in the Evaluation of Porosity/Hydrogen Content in Al-7 Wt pct Si-10 Vol. pct SiC(p) Metal Matrix Composite”, *Metallurgical Transactions A*, Vol. 24A, August 1993, 1857-1868.
48. W. La Orchan, M. H. Mulazimoglu and J. E. Gruzleski, “Quantification of the Reduced Pressure Test”, *AFS Transactions*, 1991, Vol. 99, pp. 653-659.
49. E. J. Asbjornsson, T. I. Sigfusson, D. G. McCartney, T. Gudmundsson and D. Bristow, “Studies on the Dissolution of Al-Ti-C Master Alloy Using LiMCA II”, *Light Metals*, 1999, pp. 705-710.
50. Roderick I. L. Guthrie and Mei Li, “In-Situ Detection of Inclusions in Liquid Metals: Part I. Mathematical Modeling of the Behavior of Particles Traversing the Electric Sensing Zone”, *Metallurgical and Materials Transactions B*, Vol. 32B, Dec. 2001, pp. 1067-1079.

51. J. P. Martin and François Painchaud, "On-Line Metal Cleanliness Determination in Molten Aluminum Alloys Using the LiMCA II Analyzer", *Light Metals* 1994, pp. 915-920.
52. Mei Li and Roderick I. L. Guthrie, "Liquid Metal Cleanliness Analyzer (LiMCA) in Molten Aluminum", *ISIJ International*, Vol. 41, 2001, No. 2, pp. 101-110.
53. Roderick I. L. Guthrie and Mei Li, "In-Situ Detection of Inclusions in Liquid Metals: Part II. Metallurgical Applications of LiMCA Systems", *Metallurgical and Materials Transactions B*, Vol. 32B, Dec. 2001, pp. 1081-1093.
54. I.D. Sommerville, N.D.G. Mountford and L.C.B. Martins, "Laboratory and Industrial Validation of An Ultrasonic Sensor for Cleanliness Measurement in Liquid Metals", *Light Metals*, 2000, pp.721-726.
55. M. Kurban, I.D. Sommerville, N.D.G. Mountford and P.H. Mountford, "An Ultrasonic Sensor for the Continuous Online Monitoring of the Cleanliness of Liquid Aluminum", *Light Metals*, 2005, pp.945-949.
56. F. Gazanion, X.G. Chen and C. Dupuis, "Studies on the Sedimentation and Agglomeration Behavior of Al-Ti-B and Al-Ti-C Grain Refiners", *Materials Science Forum*, Vol. 396-402, 2002, pp. 45-52.